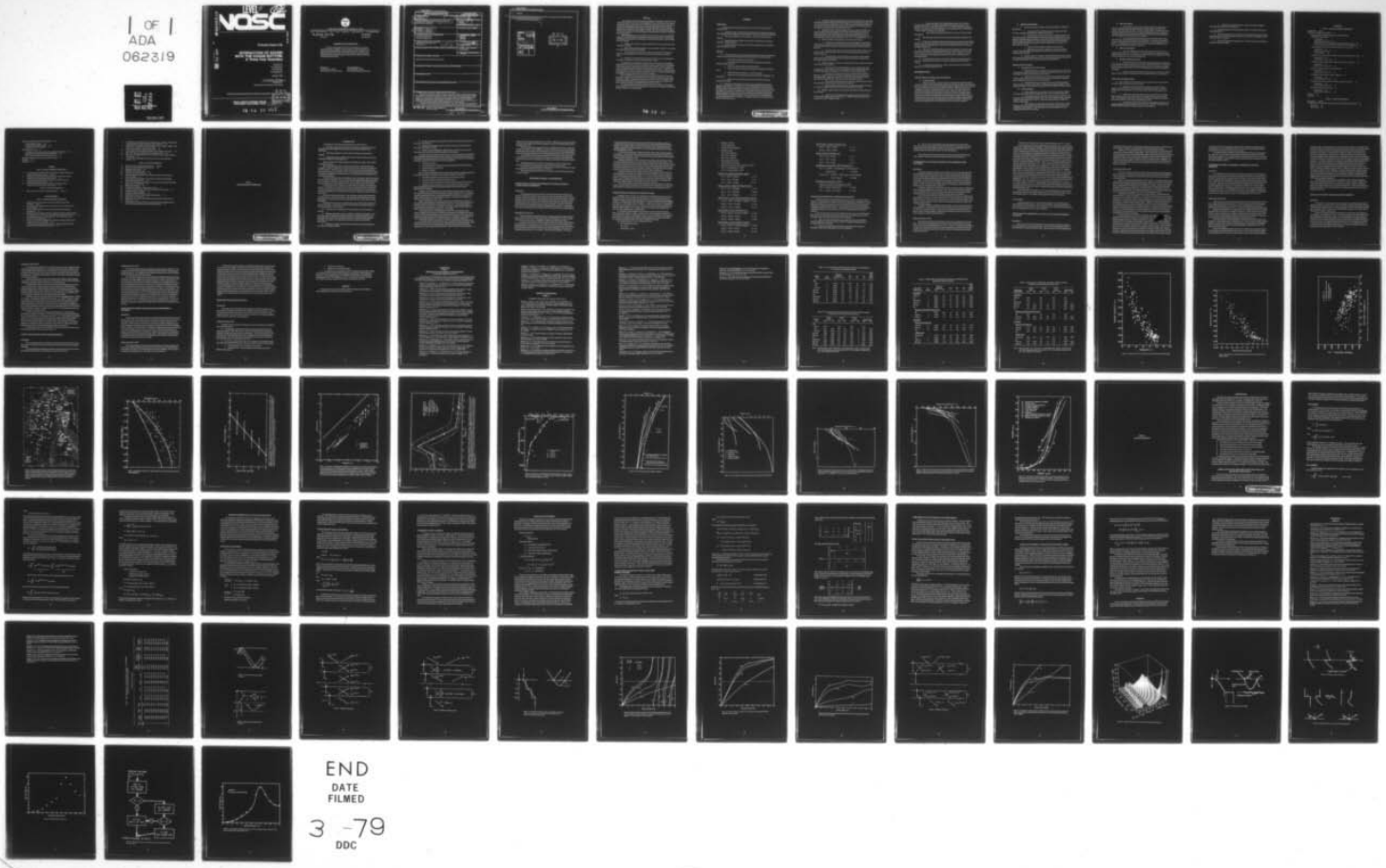
AD-A062 319 NAVAL OCEAN SYSTEMS CENTER SAN DIEGO CA F/G 20/1
INTERACTION OF SOUND WITH THE OCEAN BOTTOM: A THREE-YEAR SUMMAR--ETC(U)
APR 78 H E MORRIS, E L HAMILTON, H P BUCKER

UNCLASSIFIED NOSC/TR-242 NL

1 OF 1
ADA
062319



END
DATE FILMED
3 -79
DDC

LEVEL II

AD A062319

DDC FILE COPY

NOSC

NOSC TR 242

**Technical Report 242**

# INTERACTION OF SOUND WITH THE OCEAN BOTTOM: A Three-Year Summary

HE Morris
EL Hamilton
HP Bucker
RT Bachman

30 April 1978

Final Report: 1974-1977

Prepared for
Naval Electronic Systems Command

APPROVED FOR PUBLIC RELEASE; DISTRIBUTION UNLIMITED

DDC
RECEIVED
DEC 19 1978
D

NAVAL OCEAN SYSTEMS CENTER
SAN DIEGO, CALIFORNIA 92152

78 12 13 011

NAVAL OCEAN SYSTEMS CENTER, SAN DIEGO, CA 92152

AN ACTIVITY OF THE NAVAL MATERIAL COMMAND

RR GAVAZZI, CAPT, USN
Commander

HL BLOOD
Technical Director

## ADMINISTRATIVE INFORMATION

This three-year program (1974-1977) was sponsored by the Naval Electronic Systems Command, Code 320 (Task No. 70105): Interaction of Sound with the Ocean Bottom; by the Naval Sea Systems Command, Code 06H14 (Subproject 52-552-701, Task 16409): Sea Floor Studies For Sonar Performance, and Acoustic Properties of the Sea Floor; and by the Office of Naval Research (Code 480).

Released by
EB TUNSTALL, HEAD
Environmental Acoustics Division

Under Authority of
JD HIGHTOWER, HEAD
Environmental Sciences Department

UNCLASSIFIED

SECURITY CLASSIFICATION OF THIS PAGE *(When Data Entered)*

## REPORT DOCUMENTATION PAGE

READ INSTRUCTIONS BEFORE COMPLETING FORM

| | |
|---|---|
| 1. REPORT NUMBER: NOSC/TR-242 | 2. GOVT ACCESSION NO. |
| 3. RECIPIENT'S CATALOG NUMBER | |
| 4. TITLE (and Subtitle): INTERACTION OF SOUND WITH THE OCEAN BOTTOM: A THREE-YEAR SUMMARY | 5. TYPE OF REPORT & PERIOD COVERED: Final rept. 1974-1977 |
| 6. PERFORMING ORG. REPORT NUMBER | |
| 7. AUTHOR(s): H. E. Morris, E. L. Hamilton, H. P. Bucker R. T. Bachman | 8. CONTRACT OR GRANT NUMBER(s) |
| 9. PERFORMING ORGANIZATION NAME AND ADDRESS: Naval Ocean Systems Center, San Diego, California 92152 | 10. PROGRAM ELEMENT, PROJECT, TASK AREA & WORK UNIT NUMBERS: 70105 NESC, 16409 NSSC |
| 11. CONTROLLING OFFICE NAME AND ADDRESS: Naval Electronic Systems Command, Washington, D.C. | 12. REPORT DATE: 30 Apr 78 |
| (12) 88p. | 13. NUMBER OF PAGES: 83 |
| 14. MONITORING AGENCY NAME & ADDRESS *(if different from Controlling Office)* | 15. SECURITY CLASS. *(of this report)*: UNCLASSIFIED |
| | 15a. DECLASSIFICATION/DOWNGRADING SCHEDULE |

16. DISTRIBUTION STATEMENT *(of this Report)*

Approved for public release; distribution unlimited

17. DISTRIBUTION STATEMENT *(of the abstract entered in Block 20, if different from Report)*

18. SUPPLEMENTARY NOTES

19. KEY WORDS *(Continue on reverse side if necessary and identify by block number)*

20. ABSTRACT *(Continue on reverse side if necessary and identify by block number)*

This report documents the results of a three-year study of the interaction of sound with the sea floor. The investigation covered sea floor properties of interest in underwater acoustics, including velocity gradients in the sea floor, density, shear-wave velocities and other properties; research on acoustic propagation models, especially at low frequencies (2 to 200 Hz); and the development of accurate and efficient methods for coupling geoacoustic models to standard propagation models such as ray theory, normal mode theory and P. E. (a numerical method using the Parabolic Equation approximation to the wave equation).

During this period numerous reports were distributed to the acoustic community. Various predictions for the surveillance community have been calculated using the geoacoustic and acoustic models, support was

CONT'

DD FORM 1 JAN 73 1473 EDITION OF 1 NOV 65 IS OBSOLETE S/N 0102-014-6601 |



UNCLASSIFIED

SECURITY CLASSIFICATION OF THIS PAGE *(When Data Entered)*

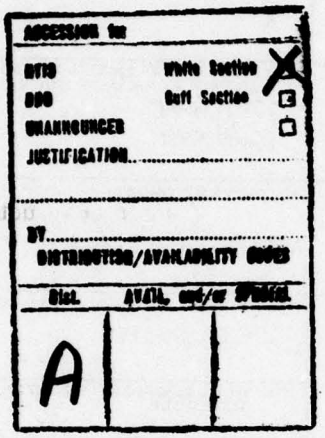
393 159

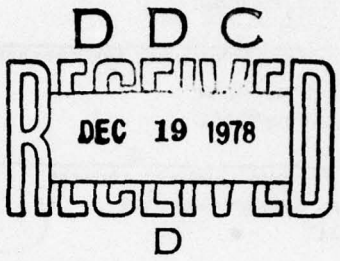
20. Continued

CONT'

provided to others developing models and support was provided on a continuous basis to surveillance programs including the Indian Ocean, MSS, SURTASS, and others.

An extensive list of references is included.



## PREFACE

The absorption of sound in the bottom sediments is the primary cause for a loss of energy when a sound wave interacts with the ocean bottom. This bottom interaction has an important effect on passive and active ASW systems. Knowledge of the ocean bottom can assist in understanding optimum array depths and degradation of signal coherence. Systems that are located near the bottom are strongly affected by bottom interaction. In addition, below 100 Hz the bottom begins to interact with long range sound propagation and thus has a direct effect on noise background (ambient noise) in which the surveillance systems must operate.

Because this parameter is so important, the Naval Ocean Systems Center (NOSC) (along with its predecessor the Naval Undersea Center) for several years has maintained a coordinated research program on interaction of sound with the sea floor. This work falls into four categories:

1. Studies of the acoustic and related properties of the sea floor and production of geoacoustic models

2. Basic studies in sound propagation theory, especially as related to the sea floor, and the development of bottom loss models

3. Use of geoacoustic models of the sea floor and theoretical, mathematical models of sound propagation and bottom loss to reconcile experiments at sea with theory

4. Prediction of both geoacoustic models and bottom loss versus grazing angle, or reflection coefficients, for areas not experimentally occupied

The objectives of the program for the past three years have been to investigate properties of the sea floor of interest in underwater acoustics, including velocity gradients in the sea floor, density, shear-wave velocities and other properties; conduct research on acoustic propagation models especially at low frequencies (from about 2 to 200 Hz); develop accurate and efficient methods for coupling geoacoustic models to standard propagation models such as ray theory, normal mode theory, and P. E. (a numerical method using the Parabolic Equation approximation to the wave equation).

We have published numerous reports that have been distributed to the acoustic community, calculated various predictions for the surveillance community using our geoacoustic and acoustic models and provided support to others who are developing models. We also have interfaced and supplied support on a continuous basis to surveillance programs including the Indian Ocean, MSS, SURTASS and other efforts.

The summary report gives a brief, general review of our research work during the three-year period, 1974-1977. This information, coupled with our referenced publications, provides a basis for more detailed study.

78 12 13 012

## SUMMARY

### OBJECTIVES

The general objectives during the past three years for the bottom-interaction program were to:

1. Determine, study, and predict those characteristics (or properties) of the sea floor affecting sound propagation and the prediction of sonar and surveillance performance
2. Place these properties in a form usable by underwater acousticians and engineers
3. Produce geoacoustic models of the sea floor as required for experimental, predictive, or theoretical work
4. Develop accurate and efficient methods for coupling geoacoustic models to standard propagation models.

### RESULTS

- It was determined that the following properties were required for geoacoustic models of the sea floor which are intended to support underwater acoustics studies:
  1. Thicknesses of sediment and rock layers
  2. Compressional wave (sound) velocity and attenuation profiles and gradients through the layers
  3. Density profiles and gradients through the layers
  4. Shear wave velocity and attenuation profiles and gradients through the layers
  5. Additional elastic properties (e.g., Lamé's constants)
  6. Bathymetry in any insonified area to get slope, relief, topography, and water depths
  7. Properties of the overlying water mass (as from Nansen casts and velocimeter lowerings)
- Laboratory measurements of sound velocity and associated properties in sediment cores continue to be valuable data. These measurements permit correction of laboratory sound velocity and density to in situ values and prediction of sound velocity and density due to interrelations between common proportion (e.g., sound velocity versus mean grain size or porosity). Revised tables of properties (and regression equations of their interrelations), separated into the main environments and sediment types, greatly facilitate predictions of various properties. New measurements in over 400 samples of calcareous sediments allow, for the first time, realistic predictions of sound velocity and density in this sediment type.



PRECEDING PAGE BLANK-NOT FILMED

- Continuous reflection profiling and associated measurements with expendable sonobuoys furnish data critical to underwater acoustics in two categories (for a given area or, in the general case, for prediction): (a) the form and true thicknesses of sediment and rock layers, and (b) the presence and values of velocity gradients. Specifically, data are furnished for several areas in the Northeast Indian Ocean.

- Statistical studies of velocity gradients in silt-clay sediments will allow prediction of sound velocity versus depth in the sea floor and the presence and values of velocity gradients in similar sediments in the world's oceans. Specifically, data in 17 areas of the world's oceans were averaged and a regression equation furnished for the velocity gradient, a, given one-way travel time, t ($a = 1.316 - 1.117t$)(see Figure 6, p. 34).

- Results of studies of the attenuation of sound were as follows:

1. Twenty-six new published values of the attenuation of compressional (sound) waves in marine sediments complement and supplement older data and support the conclusion that sound attenuation is approximately dependent on the first power of frequency.

2. New data support the conclusion that relations between sound attenuation and sediment properties allow prediction of attenuation when mean grain size or porosity are known.

3. A special study of sound attenuation versus depth in sands, silt-clays, sedimentary rocks, and basalts should allow generalized predictions of attenuation in these various layers in the sea floor.

- Results of studies of variations of sediment density and porosity versus depth in the sea floor were as follows:

1. Data from the Deep Sea Drilling Project were combined with other information to produce diagrams, curves, and regression equations of laboratory values of density and porosity versus depth in the sea floor for common sediment types.

2. The amount of volume increase (elastic rebound) from borehole to laboratory, caused by release from sediment overburden pressure, was estimated from soil mechanics tests. Maximum values of such rebound are about nine percent in silt-clays from depths of 600 meters. Rebound is less in other sediment types.

3. When percent rebound in porosity is deducted from laboratory porosity, an estimate of the in situ porosity (and density) is determined.

4. These data allow generalized curves and regression equations for density as a function of depth in the sea floor from which predictions can be made.

- Results of studies of shear wave velocities versus depth in marine sediments were as follows:

1. Twenty-nine in situ measurements of shear wave velocities in sands to 12 meter depths indicate (in these sands) that $V_S = 128D^{0.28}$; where $V_S$ is shear wave velocity in m/s, and D is depth in meters.

2. Forty-seven selected in situ measurements of shear wave velocity in silt-clays and turbidites to 650 meter depth yielded three regression equations. The equation for the 0 to 40 meter depth interval ($V_S = 116 + 4.65D$) indicates the gradient ($4.65\ sec^{-1}$) to be four to five times greater than for compressional waves in this interval. At greater depths the gradients are comparable.

3. These findings will facilitate prediction of shear wave velocity profiles and gradients.

- The attenuation of shear waves was studied and methods of prediction were outlined.

- Studies were completed which allowed construction of separate velocity versus density curves and equations for the common sediment and sedimentary rock types. This will allow prediction of density given a velocity from a sediment or rock layer (as from a sonobuoy measurement).

- There is now enough information on sediment properties to predict a reasonable geoacoustic model once an acoustic reflection survey is given for an area. This was done for several areas in the Indian, Pacific, and Atlantic Oceans. However, more work needs to be done in several categories to facilitate and improve such predictions (see Recommendations).

- A general purpose plane wave reflection model has been developed that can account for both liquid and/or solid layers. Computer calculations are efficient and accurate.

- A technique was developed to couple a bottom loss model to the Parabolic Equation (P.E.) sound propagation model.

## RECOMMENDATIONS

### Continuous Reflection Profiling and Associated Matters

- **General statement**

Measurements from continuous reflection profiling allow delineation of sediment and rock layers, their true thicknesses, their interval or mean velocities, and velocity gradients. Continuous acoustic reflection profiling was largely developed in Navy laboratories and in academic and research institutions supported by the Navy. When the utility of this technique for off-shore oil exploration became evident, there was a flash evolution to present-day techniques involving extremely expensive, multichannel, long-array equipment, and very expensive data processing at sea and ashore. The oceanographic institutions have entered this newer technology, but the costs inhibit progress. Ways need to be found to reduce costs (or acquire the money) and to simplify equipment and processing so that Navy-supported ships in the laboratories, academic and research institutions and the Naval Oceanographic Office (NAVOCEANO) can use the modern technology.

- **Specific recommendations**

1. Continue to support technology and data processing in the following general areas.

a. Acoustic reflection profiling (e.g., air gun, sparker), especially in the new techniques of multichannel, long-array technology.

b. Measurements of sediment and rock layer interval velocities, with expendable sonobuoys and multichannel, continuous reflection profiling using very long arrays and special laboratory processing of tape-recorded signals (as presently done in oil-industry geophysical exploration). Interval velocity measurements in the first tens of meters (to about 100 meters) using high-resolution, higher-frequency equipment (3.5 kHz) has shown promise.

c. Study of velocity gradients in sediment and rock layers.

d. Measurements of acoustic impedance of reflectors as seen by acoustic reflection profiling (some preliminary work has been done by Knott and his colleagues at Woods Hole).

2. Continue support of scientific expeditions that gather acoustic reflection and interval velocity information at sea. This has been a long-term program of the Office of Naval Research (ONR) and the National Science Foundation (NSF).

**Sediment and Rock Properties**

- **Compressional wave (sound) velocity**

1. Support laboratory and, especially, in situ measurements of sound velocity and associated properties (and their relationships) in sediments and rocks (as in cores, in boreholes, and with probes inserted into the sea floor).

2. Support in situ measurements of sound velocity gradients in the upper, surficial sediments (tens of meters), as with the special corer developed by Applied Research Laboratories, University of Texas, or in boreholes.

3. Although the Navy is not directly involved in the Deep Sea Drilling Project, the Navy should encourage NSF to strongly support downhole logging of sound velocity and density. These logs were recently started by the DSDP and should continue.

- **Sound attenuation**

1. Support laboratory and, especially, in situ measurements of compressional wave (sound) attenuation at frequencies from a few Hz to several hundred kHz.

2. Study relations between attenuation and frequency and between attenuation and common sediment properties in all of the common sediment types, especially in sands at low frequencies (a few Hz to 1 kHz); such studies facilitate and allow predictions of attenuation.

3. Sound attenuation measurements and studies should include, at lower frequencies, the whole sediment and sedimentary rock sections, and the surface of the underlying acoustic basement. This would result in profiles and gradients of sound attenuation with depth in the sea floor.

- **Shear wave velocity**

1. The introduction of shear wave velocity and velocity gradients into some, but not all, bottom-loss modeling requires accurate prediction of shear wave velocity versus depth in the sea floor. The shear modulus (which can be derived if shear velocity and density are known) is also an important engineering property of sediments. Accurate prediction of shear velocity versus depth in the full range of marine sediments and rocks requires much more data than now available.

2. It is recommended that laboratory and in situ measurements of shear wave velocity in marine sediments and rocks be supported. It is further recommended that at-sea measurements be emphasized with instruments, or probes, placed on or in the sea floor. A desirable final result is the profile of shear velocity with depth in the sea floor in the principal types of sediments and rocks.

- **Shear wave attenuation**

1. Very few studies have been made of the attenuation of shear waves in marine sediments and rocks. In this field, in situ studies should be emphasized with some supporting laboratory work. The profiles and gradient of shear wave attenuation in various common sediment and rock types also require study.

- **Densities of sediments and rocks**

1. Support laboratory and, especially, in situ measurements and studies of density and density profiles and gradients in sea floor sediments and rocks. In situ methods in the past have included measurements with nuclear probes and in boreholes by logging. Density logging in the boreholes of the Deep Sea Drilling Project should be supported and encouraged.

2. Results of the laboratory density measurements by the Deep Sea Drilling Project should be studied and supplemented with additional laboratory measurements.

**Atlases, Charts and Other Syntheses**

- The compilation of the following types of regional atlases, charts and other syntheses should be supported and/or encouraged.

1. Sediment types and properties (including mean grain size, density, porosity, and sound velocity) at the present-day water-sediment interface. Given only sediment type, or mean grain size, we can predict sound velocity and attenuation, and density.

2. Compilations of acoustic reflection data to show the form, true thicknesses, interval velocities, and velocity gradients of sediment and rock layers in a given region. This facilitates construction of geoacoustic models and extrapolation of models and experimental data within a region or geomorphic province.

3. A continued, intensive effort should be encouraged to produce the best possible topographic (bathymetric) charts of the sea floor. This is the overall province of NAVOCEANO and should be strongly supported by other agencies.

4. In all local and regional studies, the results of the Deep Sea Drilling Project should be considered or incorporated.

- Assess performance of current prediction models. Use Indian Ocean data to uncover deficiencies.

- Impact the development of surveillance systems especially tailored for bottom interaction areas by providing predicted performance as a function of configuration of the system and mode of operation.

- Evaluate the method for coupling bottom interaction into the P.E. (Parabolic Equation) propagation program.

## CONTENTS

### PART I: MARINE SEDIMENT PROPERTIES


Introduction . . . page 7
Programs in Geology and Geophysics . . . 9

- Sound velocity and related properties of marine sediments (laboratory measurements) . . . 9
  - Introduction . . . 9
  - Measurements to July 1975 . . . 9
  - Regression equations interrelating various sediment properties . . . 10
  - Recent and current measurements of sediment physical properties . . . 12
- Compressional-wave velocity profiles and gradients in the sea floor . . . 13
  - Introduction . . . 13
  - Studies from 1974 to 1977 . . . 13
  - Current studies . . . 14
- Attenuation of compressional (sound) waves in marine sediments and rocks . . . 14
  - Introduction . . . 14
  - Studies from 1974 to 1977 . . . 15
- Variations of density and porosity with depth in deep-sea sediments . . . 16
  - Introduction . . . 16
  - Studies from 1974 to 1977 . . . 16
- Shear wave velocity profiles in marine sediments . . . 17
  - Introduction . . . 17
  - Studies from 1974 to 1977 . . . 18
- Attenuation of shear waves in marine sediments . . . 18
  - Introduction . . . 18
  - Studies from 1974 to 1977 . . . 19
- Sound velocity-density relations in sea-floor sediments and rocks . . . 19
  - Introduction . . . 19
  - Studies from 1974 to 1977 . . . 19
- Production of geoacoustic models . . . 20
  - Introduction . . . 20
  - Studies from 1974 to 1977 . . . 20

Summary . . . 21
References . . . 22


### PART II: ACOUSTIC MODELING


Introduction . . . page 45
Formulation of the sound field using the plane wave reflection coefficient R . . . 45

- Ray theory . . . 46
- Wave theory . . . 46

Bottom loss models that account for gradients . . . 49

Liquid multilayer model . . . 49
Linear gradient multilayer model . . . 50
Comparison of the two models . . . 51

Solid multilayer model . . . 52

Calculation of R for many solid layers using Knopoff's method . . . 53
Comparison of multilayer solid and liquid models . . . 56
Effect of bottom interaction on the sound field . . . 56

Equivalent sediment layers for use with the P.E. model . . . 57
Summary . . . 58
References . . . 60

## TABLES

### PART I: MARINE SEDIMENT PROPERTIES

1a. Continental terrace (shelf and slope) environment; average sediment size analyses and bulk grain densities . . . page 26
1b. Continental terrace (shelf and slope) environment; sediment densities, porosities, sound velocities and velocity ratios . . . 26
2a. Abyssal plain and abyssal hill environments; average sediment size analyses and bulk grain densities . . . 27
2b. Abyssal plain and abyssal hill environments; sediment densities, porosities, sound velocities and velocity ratios . . . 28

### PART II: ACOUSTIC MODELING

3. Input parameters to the solid multilayer program . . . page 62

## ILLUSTRATIONS

### PART I: MARINE SEDIMENT PROPERTIES

1. Sediment porosity versus sound velocity, continental terrace (shelf and slope) . . . page 29
2. Mean diameter of mineral grains versus sound velocity, continental terrace (shelf and slope) . . . 30
3. Percent clay size versus sound velocity, abyssal hill and abyssal plain environments . . . 31
4. Sonobuoy station locations in the Bay of Bengal and adjacent areas as revised from Hamilton et al (1974) which contained only Antipode and Circe data . . . 32
5. Instantaneous velocity, V, and mean velocity, $\overline{V}$, versus one-way travel time in the Central Bengal Fan . . . 33
6. Average of linear velocity gradients, in meters per second per meter, versus one-way travel time, t, in seconds . . . 34
7. Attenuation of compressional (sound) waves versus frequency in natural, saturated sediments and sedimentary strata . . . 35

8. Attenuation of compressional waves (expressed as k in: $\alpha_{dB/m} = kf_{kHz}$) versus sediment porosity in natural, saturated surface sediments . . . 36
9. Attenuation of compressional waves (expressed as k in: $\alpha_{dB/m} = kf_{kHz}$) versus depth in the sea floor or in sedimentary strata . . . 37
10. Porosity versus depth in terrigenous sediments . . . 38
11. In situ density of various marine sediments versus depth in the sea floor . . . 39
12. Shear wave velocity versus depth in water-saturated sands . . . 40
13. Shear wave velocity measured in situ versus depth in water-saturated silt-clays and turbidites . . . 41
14. A summary of compressional wave velocity versus density in Hamilton (1977) . . . 42

PART II: ACOUSTIC MODELING

15. Ray theory representation (high frequency) . . . page 63
16. Wave theory representation (low frequency) . . . 63
17. Multilayer liquid model . . . 64
18. Multilayer linear liquid model . . . 65
19. Linear $K^2$ and constant K layers . . . 66
20. Phase comparison for linear $K^2$ and constant K models (zero attenuation for both models) . . . 67
21. Phase comparison for linear $K^2$ and constant K models using 0.05 dB/m attenuation for both models . . . 68
22. Bottom loss comparison for linear $K^2$ and constant K models using 0.05 dB/m attenuation for both models . . . 69
23. Multilayer solid model . . . 70
24. Comparison of multilayer solid and liquid models . . . 71
25. 3-D plot of bottom loss as a function of grazing angle and frequency . . . 72
26. Sound speeds and ray diagram . . . 73
27. Example of Gibb's oscillations . . . 74
28. Equivalent bottom for use with the Parabolic Equation . . . 74
29. Desired values of bottom loss . . . 75
30. Algorithm to generate an equivalent sediment model with smooth $K^2$ and bottom loss . . . 76
31. Good agreement between the bottom loss for the equivalent sediment mode (the line) and the desired bottom loss (the filled circles) . . . 77

# PART I:
# MARINE SEDIMENT PROPERTIES



PRECEDING PAGE BLANK-NOT FILMED

## INTRODUCTION

The objectives of the geology and geophysics part of the task are to:

1. Determine, study and predict those characteristics (or properties) of the sea floor affecting sound propagation and prediction of sonar and surveillance system performance

2. Place these properties in a form usable by underwater acousticians and engineers

3. Produce geoacoustic models of the sea floor for specific areas as required for experimental, predictive, or theoretical work.

The work thus involves marine geological and geophysical studies in direct support of underwater acoustics.

When sound interacts with the sea floor, the acoustician concerned with sound propagation, reflection coefficients, or bottom losses must have a full range of information about the sea floor. This information includes the basic physics of sound propagation in marine sediments and rocks, measured acoustic and related properties, properties determined by empirical relationships and outright estimates or extrapolations based on geological and geophysical probabilities.

At higher sound frequencies, the acoustician may be interested in only the first meters or tens of meters of sediments. At lower frequencies (and higher grazing angles) information must be provided on the whole sediment column and on properties of the underlying rock. This information should be provided in the form of geoacoustic models of the sea floor.

A "geoacoustic model" is defined as a model of the real sea floor with emphasis on measured, extrapolated, and predicted values of those properties important in underwater acoustics and those aspects of geophysics involving sound transmission. In general, a geoacoustic model details the true thicknesses and properties of the sediment and rock layers in the sea floor.

Geoacoustic models are important to the acoustician studying sound interactions with the sea floor in several critical aspects: they guide theoretical studies, help reconcile experiments at sea with theory, and aid in predicting the effects of the sea floor on sound propagation.

The information required for a complete geoacoustic model should include the following for each layer. In some cases, the state of the art allows only rough estimates, in others information may be non-existent.

- Properties of the overlying water mass from Nansen casts and velocimeter lowerings

- Sediment information (from cores, drilling, or geologic extrapolation): sediment types, grain-size distributions, densities, porosities, compressional and shear wave attenuations and velocities, and other elastic properties. Gradients of these properties with depth, for example, velocity gradients and interval velocities from sonobuoy measurements

- Thicknesses of sediment layers (in time) determined at various frequencies by continuous reflection profiling



PRECEDING PAGE BLANK-NOT FILMED

- Locations, thicknesses, and properties of reflectors within the sediment body as seen at various frequencies
- Properties of rock layers; those at or near the sea floor are of special importance to the underwater acoustician
- Details of bottom topography, roughness, relief, and slope as seen by underwater cameras, sea-surface echo sounders and deep-towed equipment

It has been shown by acousticians that the above types of information are essential to an understanding of sound interactions with the sea floor. Among the above properties and information, the following is the basic, minimum information on properties of the sediments and rocks required for most current work in sound propagation.

1. Thicknesses of layers
2. Compressional wave (sound) velocity profile and gradient through the layers
3. Sound attenuation in each layer
4. Density in each layer

Newer and more sophisticated mathematical models involving sound interaction with the sea floor, especially at lower frequencies, require (in addition to the above):

5. The profile and gradient of sound attenuation through the layers
6. The density profile and gradient through the layers
7. Shear wave velocity and attenuation profiles and gradients through the layers
8. Additional elastic properties (e.g., dynamic rigidity and Lamé's constant); given compressional and shear wave velocities and density, these and other elastic properties can be computed.

Examples of newer mathematical models involving sound interactions with the sea floor are given by Bucker (Part II of this report) and Bucker and Morris (1975). Additional examples are those models used at the Applied Research Laboratories of the University of Texas to study the effects of various sediment properties on bottom losses (Hawker and Foreman, 1976; Hawker et al, 1976, 1977).

Where sound penetrates the whole sediment layer (and sedimentary rock layers if they are present) and reflects from and refracts in the surface of the acoustic basement, it is necessary to know the properties of the basement surface (i.e., compressional and shear wave velocities and attenuations, and density). An example of this is in the Northcentral Pacific where 50 to 100 meters of pelagic clay overlies basalt.

A continuing project in the geology-geophysics group is improvement of geoacoustic modeling and acquisition and refinement of properties in coordination with acousticians to supply required information and to anticipate future needs. Except where specific geoacoustic models are required for experimental work, our emphasis is on the general case so that reasonable predictions can be made in the absence of specific measurements.

At the start of the three-year project in 1974, considerable work had been done by our laboratory (then NUC) in the acoustic and related properties of marine sediments. These studies were based on in situ measurements by divers and from submersibles and from measurements in cored sediments in the laboratory. Much of this work, with appropriate

references, was reviewed by Hamilton (1974a, 1974b). Additionally, work had commenced on studies of mean velocities and velocity gradients in the first, unlithified sediment layer (Hamilton et al, 1974).

During the three year program (1974-1977), NAVELEX, Code 320, has supported partially the continued work in sediment properties and layer sound velocities and velocity gradients and work concerned with the attenuation of shear waves and the relationship between sound velocity and density in the principal sediment and rock types of the sea floor.

In the gradients of some important properties, NAVELEX has also partially supported shear waves in marine sediments versus depth in the sea floor, sound attenuation versus depth in the sea floor, and density and porosity of sediments versus depth in the sea floor.

Additionally, geoacoustic models were furnished for a number of areas where acoustic experimental work was planned or where predictions were required.

The reports of these measurements and studies are included in our references under Work Supported by NAVELEX, Code 320: 1974-1977.

The work generally noted above will be summarized, with details and illustrations, in the next sections.

## PROGRAMS IN GEOLOGY AND GEOPHYSICS

## SOUND VELOCITY AND RELATED PROPERTIES OF MARINE SEDIMENTS (LABORATORY MEASUREMENTS)

### Introduction

The geology-geophysics group operates a sediment laboratory in which measurements are made of sound velocity, density, porosity, grain size and grain density of cored sediments. During the past three years, funds have not permitted a field program. However, through cooperative arrangements with Scripps Institution and others, the above measurements have been made on various suites of sediments from the Pacific and Indian Oceans. Specifically, there were sediments from six Scripps expeditions: four from the Central Pacific and two from the Indian Ocean (Bay of Bengal and Andaman Sea). Additionally, three suites of sediments from the Northeast Pacific were taken by Navy-sponsored groups.

### Measurements to July 1975

The measurements of physical properties of sediments and their empirical relationships (to about July 1975) have been studied and reviewed (Hamilton, 1975d). The data were presented in three forms: as diagrams, in regression equations and in tables.

One of the most useful and frequently used outputs of our work in physical properties of sediments is the production of a set of tables in which are listed the acoustic and related properties of various sediment types in the three main environments of the sea floor. The latest revision of the tables of sediment measurements (Hamilton, 1975d, 1976c) is reproduced here as Tables 1a, 1b, 2a and 2b. The earlier report (Hamilton, 1975d) also

contained tables (based on the same data) of computed values of impedance, reflection coefficients and bottom losses at normal incidence, and elastic properties (bulk modulus, Poisson's ratio, dynamic rigidity, and velocity of the shear wave). Reproduced here are regression equations for the more important and useful interrelationships between properties (from Hamilton, 1975d).

In the sections which follow, frequent references will be made to the three general environments: the continental terrace (shelf and slope), the abyssal hill environment, and the abyssal plain environment. These environments and associated sediments were discussed in greater detail by Hamilton (1971b).

Sediment nomenclature on the continental terrace follows that of Shepard (1954), except that within the sand sizes the various grades of sand follow the Wentworth scale. In the deep sea, pelagic clay contains less than 30 percent calcium carbonate or siliceous material. Calcareous ooze contains more than 30 percent calcium carbonate and siliceous ooze more than 30 percent silica in the form of Radiolaria or diatoms. The Shepard (1954) size grades are shown in these deep-sea sediment types to show the effects of grain size.

Examples of the many scatter diagrams of interrelationships are sound velocity (at one atmosphere and corrected to 23 degrees Celsius) versus sediment porosity, mean grain size, and percent clay-sized particles (Figures 1, 2, 3); these are three of the best indices to velocity. An advantage of using mean grain size or percent clay-sized materials as indices to sound velocity is that grain size and clay size tests can be made in dried or partially dried sediments in which porosity or sound velocity tests cannot be made.

These tables, diagrams, and regression equations are basic information on which predictions of sound velocity and density can be based given only a sediment type or grain size. The methods for such predictions were included in an earlier report (Hamilton, 1971b).

## Regression Equations Interrelating Various Sediment Properties

Regression lines and curves were computed for those illustrated sets of (x,y) data in Hamilton (1975d). These constitute the best indices (x) to obtain desired properties (y). Separate equations are listed, where appropriate, for each of the three general environments as follows: continental terrace (shelf and slope), (T); abyssal hill (pelagic), (H); abyssal plain (turbidite), (P). The Standard Errors of Estimate, $\sigma$, opposite each equation, are applicable only near the mean of the (x,y) values. Accuracy of the (y) values, given (x), falls off away from this region (Griffiths, 1967, p. 448). Grain sizes are shown in the logarithmic phi-scale ($\phi = -\log_2$ of grain diameter in millimeters).

It is important that the regression equations be used only between the limiting values of the index property (x values), as noted below. These equations are strictly empirical and apply only to the (x,y) data points involved. There was no attempt, for example, to force the curves expressed by the equations to pass through velocity values of minerals at zero porosity or the velocity value of sea water at 100 percent porosity.

The limiting values of (x), in the equations below, are:

1. Mean grain diameter, $M_Z$, $\phi$

   (T) 1 to 9 $\phi$

   (H) and (P) 7 to 10 $\phi$

2. Porosity, n, percent
   (T) 35 to 85 percent
   (H) and (P) 70 to 90 percent
3. Density, $\rho$, g/cm$^3$
   (T) 1.25 to 2.10 g/cm$^3$
   (H) 1.15 to 1.50 g/cm$^3$
   (P) 1.15 to 1.70 g/cm$^3$
4. Clay size grains, C, percent
   (H) and (P) 20 to 85 percent
5. Density X (Velocity)$^2$, $\rho V_p^2$, dynes/cm$^2$ X $10^{10}$
   (H) 2.7 to 3.4 dynes/cm$^2$ X $10^{10}$
   (P) 2.7 to 3.8 dynes/cm$^2$ X $10^{10}$

Porosity, n (%) vs Mean Grain Diameter, $M_z$ ($\phi$)

(T) $n = 30.95 + 5.50(M_z)$ $\sigma = 6.8$

(H) $n = 82.42 - 0.29(M_z)$ $\sigma = 4.7$

(P) $n = 45.43 + 3.93(M_z)$ $\sigma = 6.5$

Density, p (g/cm$^3$) vs Mean Grain Diameter, $M_z$ ($\phi$)

(T) $p = 2.191 - 0.095(M_z)$ $\sigma = 0.12$

(H) $p = 1.327 + 0.005(M_z)$ $\sigma = 0.09$

(P) $p = 1.879 - 0.06(M_z)$ $\sigma = 0.11$

Sound Velocity, $V_p$ (m/s) vs Mean Grain Diameter, $M_z$ ($\phi$)

(T) $V_p = 1924.9 - 74.18(M_z) + 3.04(M_z)^2$ $\sigma = 33.6$

(H) $V_p = 1594.4 - 10.2(M_z)$ $\sigma = 11.6$

(P) $V_p = 1631.8 - 13.3(M_z)$ $\sigma = 18.3$

Sound Velocity, $V_p$ (m/s) vs Porosity, n (%)

(T) $V_p = 2467.3 - 22.13(n) + 0.129(n)^2$ $\sigma = 33.7$

(H) $V_p = 1410.8 + 1.175(n)$ $\sigma = 13.3$

(P) $V_p = 1630.8 - 1.402(n)$ $\sigma = 20.6$

Sound Velocity, $V_p$ (m/s) vs Density, $\rho$ (g/cm$^3$)

(T) $V_p = 2263.0 - 1164.8(\rho) + 458.8(\rho)^2$ $\sigma = 34.2$

(H) $V_p = 1591.7 - 63.5(\rho)$ $\sigma = 13.2$

(P) $V_p = 1430.6 + 65.2(\rho)$ $\sigma = 21.7$

Sound Velocity, $V_p$ (m/s) vs Clay Size, C (%)

(H) $V_p = 1549.4 - 0.66(C)$ $\sigma = 9.9$

(P) $V_p = 1568.8 - 0.89(C)$ $\sigma = 18.3$

Density, $\rho$ (g/cm$^3$) vs Porosity, n (%)

(T) $n = 156.0 - 56.8(\rho)$ $\sigma = 2.7$

(H) $n = 150.1 - 51.2(\rho)$ $\sigma = 1.2$

(P) $n = 159.6 - 58.9(\rho)$ $\sigma = 1.4$

Bulk Modulus, $\kappa$ (dynes/cm$^2 \times 10^{10}$) vs Porosity, n (%)

(T) $\kappa = 215.09467 - 133.1006\ (\log_e n) + 28.2872\ (\log_e n)^2 - 2.0446\ (\log_e n)^3$ $\sigma = 0.01146$

(H) and (P) $\kappa = 128.9909 - 72.0478\ (\log_e n) + 13.8657\ (\log_e n)^2 - 0.9097\ (\log_e n)^3$ $\sigma = 0.0100$

Bulk Modulus, $\kappa$ (dynes/cm$^2 \times 10^{10}$) vs Density $\times$ (Velocity)$^2$, $\rho V_p^2$ (dynes/cm $\times 10^{10}$)

(H) $\kappa = 0.32039 + 0.862\ (\rho V_p^2)$ $\sigma = 0.049$

(P) $\kappa = 1.68823 + 0.134\ (\rho V_p^2)$ $\sigma = 0.069$

**Recent and Current Measurements of Sediment Physical Properties**

Calcareous sediments cover about 50 percent of the sea floor. In the past (and in Tables 2a, 2b), this important sediment type has been inadequately represented in our measurements. During the past two years and at the present time (September 1977) more than 400 samples of calcareous sediments from four expeditions have been obtained through cooperative work with Scripps Institution. Measurements in these samples should facilitate considerably prediction of sound velocity, density, and other properties of calcareous sediments.

A suite of 108 samples of calcareous sediments from box cores on the Ontong-Java Plateau in the western equatorial Pacific were examined in 1976 (Johnson et al, 1977a). Among the many conclusions of this study were the following:

- There is a continuous reduction of mean grain size with increasing water depth (probably due to winnowing of fine materials on topographic highs and solution of calcium carbonate with depth).

- Porosity and density bear little relation to sound velocity or grain size (probably because of the hollow shells or tests of Foraminifera).

- There is a good relationship between mean grain size and sound velocity and the velocity versus mean grain size regression equations for continental-terrace sands-silts-clays adequately describes these relations for these calcareous sediments. This is probably because the hollow shells interact as large, solid particles.

The continued measurements and studies in calcareous materials should furnish fairly definitive information on interrelationships between common properties.

## COMPRESSIONAL-WAVE VELOCITY PROFILES AND GRADIENTS IN THE SEA FLOOR

### Introduction

Continuous reflection profiling (as with a sparker or air gun) and wide-angle reflection measurements of sediment and rock layer interval velocities have become important sources of critical data in underwater acoustics. Continuous reflection profiling measures sound travel time between impedance mismatches within the sediment and rock layers of the sea floor. To derive the true thicknesses of these layers it is necessary to measure or predict the mean or interval layer velocity or use a sediment surface velocity and velocity gradient. At the present time, the simplest method of measuring layer interval velocities involves the use of expendable Navy sonobuoys.

Sonobuoy measurements of interval velocity also provide basic data for determining velocity profiles and gradients in the sea floor. When velocity measurements in sediment cores are available, these can be corrected to in situ values at the water-sediment interface and used with layer mean velocities to establish velocity profiles and gradients.

It has been shown by Morris (1970) and others that the presence of a positive velocity gradient in the sea floor is of critical importance in acoustic studies when sound interacts with the sea floor. In general, when a sediment layer has a positive velocity gradient, sound energy is refracted back into the water column at certain grazing angles and energy is lost over long refraction paths.

In summary, reflection profiling records yield data critical to underwater acoustics in two categories: the form and true thicknesses of sediment and rock layers and the presence and values of velocity gradients. These data, when examined statistically, yield regional velocity profiles and general, averaged velocity gradients that can be used to predict velocity gradients in similar sediments elsewhere.

### Studies From 1974 to 1977

During the three-year period of this project, three sets of sonobuoy data were analyzed. Two sets from the Northeast Indian Ocean have been analyzed, added to previous data in the area and reported (Hamilton et al, 1977). A suite of 17 sonobuoy measurements of interval velocity were made in the thick calcareous sediments and rocks in the Ontong-Java Plateau in the West Central Pacific. These records have been analyzed and reported (Johnson et al, 1978).

The abstract of the Indian Ocean report follows (Hamilton et al, 1977, p. 3003).

New measurements of interval compressional wave velocities were made in the first sediment layer, using the sonobuoy technique. These measurements were made during two expeditions in the Bay of Bengal, in the Andaman Sea and over the Nicobar Fan and Sunda Trench. Sediment interval velocities from these areas were added to those previously reported, and revised diagrams and regression equations of instantaneous and mean velocity versus one-way travel time are furnished for four areas of the Bengal Fan and for the Andaman Basin, Nicobar Fan, and Sunda Trench. The velocity gradients directly below the sea floor were used to separate the Bengal Fan into four geoacoustic provinces. In the north and west, the velocity gradients are 0.86 $s^{-1}$ and 1.28 $s^{-1}$, respectively; whereas in the central part of the fan, the gradient is 1.87 $s^{-1}$. These variations indicate lesser increases of velocity with depth in the sea floor in the north and west. They are due probably to more rapid deposition, less consolidation and less lithification near the riverine source areas of the sediments. The near-surface velocity gradients in the other areas are: the Andaman Basin, 1.53 $s^{-1}$; the Nicobar Fan, 1.63 $s^{-1}$; and the Sunda Trench, 1.41 $s^{-1}$. In a second part of the paper, the linear velocity gradients (from the sediment surface to a given travel time) in 17 areas of the Indian Ocean, Pacific area, Atlantic Ocean, and Gulf of Mexico were averaged at each 0.1 s from 0 to 0.5 s of one-way travel time. These averaged gradients ranged from 1.32 $s^{-1}$ at t = 0 to 0.76 $s^{-1}$ at t = 0.5 s. The regression equation for the velocity gradient, a, in $s^{-1}$ as a function of one-way travel time, t, in seconds is: $a = 1.316 - 1.117t$ (for use from t = 0 to 0.5 s). These average velocity gradients can be used with sediment surface velocities and one-way travel times (measured from reflection records) to compute sediment layer thicknesses in areas of turbidites lacking interval velocity measurements in the first sediment layer.

Three of the figures in Hamilton et al (1977) are reproduced here. Figure 4 shows the sonobuoy stations in the Northeast Indian Ocean; Figure 5 illustrates the type and scatter of the data; Figure 6, the averaged velocity gradients in these and other areas.

### Current Studies

At present (September 1977), sound velocity gradients in the principal types of marine sediments are being studied. These types include sands, terrigenous sediments (directly from land sources), calcareous ooze, and siliceous ooze. The emphasis in these studies will be on averaged values which can aid in predictions.

## ATTENUATION OF COMPRESSIONAL (SOUND) WAVES IN MARINE SEDIMENTS AND ROCKS

### Introduction

Some years ago it became apparent that sound propagated through the sea floor at certain frequencies and at certain grazing angles. In such cases quantitative knowledge of sound attenuation in marine sediments became a required property in understanding sound

interactions with the sea floor. Consequently, measurements and studies of sound attenuation have been a long-term, continuing project in the geology-geophysics group.

Hamilton (1972) reported the results of in situ measurements of sound velocity and attenuation in various sediments off San Diego. These measurements and others from the literature allowed analyses of the relationships between attenuation and frequency and other physical properties. It was concluded that attenuation in dB/unit length is approximately dependent on the first power of frequency and that velocity dispersion is negligible or absent in water-saturated sediments. The report also discussed the causes of attenuation, its prediction (given grain size or porosity), and appropriate viscoelastic models which can be applied to sediments.

**Studies From 1974 to 1977**

In 1975 and 1976 two reports were issued which revised data and two illustrations in the 1972 report. The first was a Naval Undersea Center report, NUC TP 482 (Hamilton, 1975c), followed by its publication in the Journal of the Acoustical Society of America (Hamilton, 1976b).

Figure 7 is reproduced from Hamilton (1976b, Figure 1). This figure illustrates the relations between attenuation in dB/m and frequency in kHz. The new data in this revised figure were given different symbols from the original (1972) figure. The new data complement and supplement the original data and strongly support an approximate first-power dependence of attenuation on frequency. The data in Figure 7 include sands, silt-clays and mixed-grained materials. The experimental evidence does not support any theory calling for a dependence of attenuation on $f^{1/2}$ or $f^2$ in either sands or silt-clays.

If attenuation is dependent on the first power of frequency, as indicated by the evidence in Figure 7, then in the equation $\alpha = kf^n$ (where the exponent n is one, $\alpha$ is attenuation in dB/m, f is frequency in kHz and k is a constant), the only variable is the constant k. This allows k to be related to common sediment properties such as mean grain size or porosity (Figure 8). Figure 8 (reproduced from Figure 2, Hamilton, 1976b) was revised from a similar figure in the 1972 report, with the addition of four new sets of measurements. These measurements did not alter the original conclusions. An important conclusion is that prediction of sound attenuation in the sediment surface can be based on mean grain size or porosity. To predict attenuation, we simply determine the constant k from its relations with porosity (or mean grain size in the 1972 report) and insert k into the above equation, which should be good at any frequency.

The main purpose of the 1975 and 1976 reports was to discus[illegible]iations of attenuation with depth in the sea floor. The sparse data were colle[illegible]uation and depth at various frequencies. These data were listed in a table a[illegible] Figure 3 of Hamilton (1976b) is reproduced here as Figure 9; these data ill[illegible]e sound attenuation (represented by the constant k) as a function of depth in the sea floor. It was concluded that attenuation decreases with about the −1/6 power of depth in sands. As a silt-clay sediment (mud), or turbidite, is placed under increasing overburden pressure, there may be a progressive increase in attenuation due to reduction in sediment porosity and a progressive decrease in attenuation due to increasing pressure on the sediment mineral frame. At some null point in the sediment (sparse evidence indicates about 200 meters), pressure becomes

the dominant effect and attenuation decreases smoothly thereafter with depth and overburden pressure. It was concluded that Figure 9 can be used to aid prediction of sound attenuation in sediment and rock layers in the sea floor.

The study of sound attenuation in marine sediments and rocks is a continuing project. Since the 1976 report new measurements have indicated the validity of the above approach and conclusions. The most important of these measurements were by Tyce (personal communication), using the Marine Physical Laboratory deep-tow equipment in both the Atlantic and Pacific Oceans.

## VARIATIONS OF DENSITY AND POROSITY WITH DEPTH IN DEEP-SEA SEDIMENTS

### Introduction

The values and variations of density and porosity with depth in marine sediments and rocks are of importance in both basic and applied studies of the earth. Specifically (in the field of sound interactions with the sea floor), density of various layers of the oceanic crust are important in the propagation of shear and compressional waves and other elastic waves. Values of density are required in all mathematical models of sound interacting with the sea floor. However, work at the Applied Research Laboratories of the University of Texas has indicated that, in many cases, the gradient of density may have only a small effect on bottom losses. At high grazing angles (above the shear wave critical angle), the effects amount to about 1 to 2 dB change in bottom loss. At low angles, very little effect is observed except in the vicinity of the low angle shear anomaly (discussed in a following section) where it can amount to as much as 2 to 8 dB (Hawker et al, 1976, p. 65).

### Studies From 1974 to 1977

Three reports were issued during the three-year period concerning variations of density and porosity with depth in the sea floor. The first was issued by the Naval Undersea Center as TP 459 (Hamilton, 1975a); this report was later published in the Journal of Sedimentary Petrology (Hamilton, 1976c). A resume with selected figures are noted below.

Bachman and Hamilton (1976) obtained a suite of samples from the Deep Sea Drilling Project Site 222 (Leg 23) in the northern Arabian Sea. At this site there was an unusually thick section of homogeneous, terrigenous sediment which was drilled to about 1300 meters. Density, porosity, and grain density were measured in the laboratory. These data were also included in the Hamilton and Bachman and Hamilton reports.

The critical question in relating laboratory measurements of sediment density and porosity to in situ measurements in a deep borehole is: how much has the sample expanded elastically as a result of removal from overburden pressure in the borehole to atmospheric pressure in the laboratory? This was the problem addressed in Hamilton (1976c). The abstract of this report follows.

Reduction of sediment porosity and increase in density under overburden pressure in the sea floor are important subjects in earth sciences. Data and samples from the Deep Sea Drilling Project allow a new look at these subjects, and are used to establish profiles of

laboratory values of density and porosity versus depth in the sea floor. To construct in situ profiles, the results of consolidation tests are used to estimate the amount of elastic rebound (increase in volume) which has occurred after removal of the samples from overburden pressure in the boreholes. In situ profiles of porosity and density versus depth are constructed for some important sediment types: calcareous ooze, siliceous oozes (diatomaceous and radiolarian oozes), pelagic clay, and terrigenous sediments. There is less reduction of porosity with depth in the first 100 meters in these deep-water sediments than previously supposed: 8 to 9 percent in pelagic clay, calcareous and terrigenous sediments and only 4 to 5 percent in the siliceous sediments. From depths of 300 meters the most rebound is in pelagic clay (about 7 percent) and the least in diatomaceous ooze (about 2 percent); calcareous ooze and terrigenous sediment should rebound from 300 meters about 4 to 5 percent. Terrigenous sediment, from the surface to 1000 meters depth, probably rebounds a maximum of about 9 percent. Methods are described and illustrated to predict density and porosity gradients in the sea floor and to compute the amounts of original sediments necessary to have been compressed to present thicknesses. Slightly over 2000 meters of original sediments would have been required for compression to a present-day thickness of 1000 meters of terrigenous sediments.

Two figures are reproduced here from Hamilton (1976c). Figure 10 illustrates laboratory measurements which have been corrected to in situ values and compared with data in shales (below 600 meters) from oil-industry explorations. Figure 11 illustrates density versus depth for the five most common sediment types. These data and tables and regression equations in the report should allow reasonable predictions of density at given depths in the sea floor.

## SHEAR WAVE VELOCITY PROFILES IN MARINE SEDIMENTS

### Introduction

The velocity of a compressional wave is dependent on the sediment bulk modulus, rigidity and density. Given shear wave velocity and density, rigidity can be easily computed. Given shear and compressional wave velocities and density, all of the other elastic properties can be computed. When a sound wave is reflected within a sediment or rock layer, part of the energy is converted to a shear wave.

Studies at the Applied Research Laboratories of the University of Texas (Hawker and Foreman, 1976; Hawker et al, 1976, 1977) found important effects when shear waves were introduced into bottom loss models. At low grazing angles in the case of clay and possibly silt (but not sand) overlying hard rock, it was found that a very large bottom loss can occur over a narrow angular range through the production of a Stoneley wave (closely related to the shear wave) along the sediment-rock interface. These dominant effects occurred between the shear velocity critical grazing angle of about 50 degrees and the compressional velocity grazing angle of about 70 degrees.

### Studies From 1974 to 1977

In an earlier report (Hamilton, 1971a), the presence and causes of rigidity and shear waves in marine sediments were reviewed. Hamilton with Bucker and his colleagues at the Naval Undersea Center (Hamilton et al, 1970) reported in situ measurements of compressional wave velocity, density, and velocities of Stoneley waves (from which shear waves can be determined). In these reports the variation of shear wave velocity with depth in the sediments was not considered.

A short study and review of shear wave velocity versus depth in marine sediments was issued by the Naval Undersea Center as TP 472 (Hamilton, 1975b), and later published in Geophysics (Hamilton, 1976e). The abstract of this report follows.

The objectives of this report are to review and study selected measurements of the velocity of shear waves at various depths in some principal types of unlithified, water-saturated sediments and to discuss probable variations of shear velocity as a function of pressure and depth in the sea floor. Because of the lack of data for the full range of marine sediments, data from measurements on land were used and the study was confined to the two "end-member" sediment types (sand and silt-clays) and turbidites.

The shear velocity data in sands included 29 selected, in situ measurements at depths to 12 meters. The regression equation for these data is: $V_S = 128D^{0.28}$, where $V_S$ is shear wave velocity in m/s and D is depth in meters. The data from field and laboratory studies indicate that shear wave velocity is proportional to the 1/3 to 1/6 power of pressure or depth in sands; that the 1/6 power is not reached until very high pressures are applied; and that in most sand bodies the velocity of shear waves is proportional to the 3/10 to 1/4 power of depth or pressure. The use of a depth exponent of 0.25 is recommended for prediction of shear velocity versus depth in sands.

The shear velocity data in silt-clays and turbidites include 47 selected, in situ measurements at depths to 650 meters. Three linear equations are used to characterize the data. The equation for the 0 to 40 meters interval ($V_S = 116 + 4.65D$) indicates the gradient (4.65 $sec^{-1}$) to be four to five times greater than is the compressional velocity gradient in this interval in comparable sediments. At deeper depths, shear velocity gradients are 1.28 $sec^{-1}$ from 40 to 120 meters and 0.58 $sec^{-1}$ from 120 to 650 meters. These deeper gradients are comparable to those of compressional wave velocities. These shear velocity gradients can be used as a basis for predicting shear velocity versus depth.

Two figures reproduced here from Hamilton (1976e) illustrate shear velocity versus depth in sands (Figure 12) and in silt-clays (Figure 13).

## ATTENUATION OF SHEAR WAVES IN MARINE SEDIMENTS

### Introduction

When a compressional wave is reflected at some impedance mismatch within the sea floor, some of the energy is converted to a shear wave and this converted energy is rapidly attenuated.

In some sophisticated mathematical models of sound interaction with the sea floor, the attenuation of shear waves is a required input (see Part II, this report).

### Studies From 1974 to 1977

Very little experimental data are available on the attenuation of shear waves. The available data are almost all in the fields of geotechnical (soil mechanics) engineering and earthquake research. The available data were collected, studied and reported by Hamilton (1976d) and the abstract of this report follows.

The objectives of this report are to review selected, published measurements of the attenuation, or energy damping, of low-strain shear waves in surficial water-saturated sands and silt-clays (mud) that might occur as marine sediments. In various computations, a linear viscoelastic model is favored in which velocity dispersion is negligible, linear attenuation is proportional to the first power of frequency and the specific dissipation function, 1/Q, and the logarithmic decrement are independent of frequency. The logarithmic decrement is favored as a measure of energy damping because of research in soil mechanics. The very sparse data indicate that in water-saturated sands and silt-clays, the logarithmic decrements are mostly between 0.1 and 0.6. If approximate values of shear wave energy losses are required for generalized computations, it is suggested that a value for the logarithmic decrement of $0.30 \pm 0.15$ be assumed for sands and $0.2 \pm 0.1$ for silt-clays. Measured logarithmic decrements of compressional waves in sands average about $0.10 \pm 0.03$; in silt-clays about $0.02 \pm 0.01$. The average values of the ratio of compressional- to shear-wave logarithmic decrements, using the above average values, would be 0.3 for sands and 0.1 for silt-clays.

## SOUND VELOCITY-DENSITY RELATIONS IN SEA-FLOOR SEDIMENTS AND ROCKS

### Introduction

Continuous acoustic reflection surveys are rapidly delineating the sediment and rock layers of the sea floor. Wide-angle reflection and refraction measurements (as with expendable sonobuoys) yield velocities in these layers. This allows true layer thicknesses to be computed. Further, the new velocity data frequently can be linked to sediment and rock types by geologic reasoning and by direct linkage to the boreholes of the Deep Sea Drilling Project. Therefore, it would be useful to establish relationships between velocity and density in the various sediment and rock types in the sea floor. This would allow prediction of density (a prime requirement) to correspond to measured sound velocities for purposes of modeling the sea floor for underwater acoustics studies. Additionally, density profiles can be constructed from these data or from densities derived from velocities computed from equations of velocity versus travel time or depth.

### Studies From 1974 to 1977

Naval Ocean Systems Center measurements of density and velocity in marine sediments were combined with information from the literature and a report published which relates density and velocity for common sediments and rocks (Hamilton, 1978). Figure 14 is a summary of individual curves. The abstract of the report follows.

In underwater acoustics, geophysics, and geologic studies, given a seismic measurement of velocity, the relations between sound velocity and density allow assignment of approximate values of density to sediment and rock layers of the earth's crust and mantle. In the past, single curves of velocity versus density represented all sediment and rock types. A large amount of recent data from the Deep Sea Drilling Project (DSDP) and reflection and refraction measurements of sound velocity, allow construction of separate velocity-density curves for the principal marine sediment and rock types. This report uses carefully-selected data from laboratory and in situ measurements to present empirical sound velocity-density relations (in the form of regression curves and equations) in terrigenous silt-clays, turbidites and shale, in calcareous materials (sediments, chalk, and limestone), and in siliceous materials (sediments, porcelanite and chert); a published curve for DSDP basalts is included. Speculative curves are presented for composite sections of basalt and sediments. These velocity-density relations, with seismic measurements of velocity, should be useful in assigning approximate densities to sea floor sediment and rock layers for studies in marine geophysics and in forming geoacoustic models of the sea floor for underwater acoustic studies.

## PRODUCTION OF GEOACOUSTIC MODELS

### Introduction

Geoacoustic models were defined and requirements for input information were noted briefly in the general introduction to Part I (Marine Sediment Properties). As noted in the general introduction, geoacoustic models of the sea floor are produced to guide theoretical studies, to reconcile experiments at sea with theory, and to predict the effects of the sea floor on underwater sound propagation.

### Studies From 1974 to 1977

During the three-year period of this project, geoacoustic models were furnished to various persons or groups.

- Two geoacoustic models were furnished to the Acoustic Environmental Support Detachment, ONR. One was for an area in the Northeast Pacific and was well founded on coring and acoustic reflection measurements. The second model was for the northern end of the Iberian Basin off the coast of Spain and was based on information in the literature. These data with accompanying bottom-loss curves were issued by the Naval Undersea Center TN 1470 (Morris et al, 1974).

- Geoacoustic models were furnished to investigators in the Undersea Surveillance Department, Naval Undersea Center, for areas or stations in the following localities.

    1. Continental slope west of the Strait of Juan de Fuca
    2. Northeast Pacific: Tufts Abyssal Plain, and another area south of Mendocino Escarpment

3. Off Point Sur, California

4. Ridge west of the Norwegian Basin

- In preparation for experimental work in the Arabian Sea, geoacoustic models were furnished for four stations to allow predictions of underwater sound propagation in the area. These models were part of the predictive study issued by the Naval Ocean Systems Center as TN 104 (Northrop et al, 1977). A portion of this report (Northrop et al, 1978) is in press as an article for the Journal of Underwater Acoustics.

## SUMMARY

The general summary of Part I (Marine Sediment Properties), with results and recommendations, is in the front section of this report.

## REFERENCES
## (PART I)

## REPORTS INVOLVING GEOLOGY AND GEOPHYSICS OF THE SEA FLOOR (1974-1977)

Partial support of NAVELEX, Code 320, was acknowledged in the following reports involving geology, geophysics, and acoustic properties of the sea floor during calendar years 1974-1977 (two reports in press in 1977 were published in January and February 1978).


Morris, H. E., Hamilton, E. L., and Bucker, H. P., 1974, Low frequency geoacoustic models and bottom loss curves for two areas in the Northeast Pacific and Iberian Basin, Naval Undersea Center TN 1470.

Hamilton, E. L., 1975a, Acoustic and related properties of the sea floor: density and porosity profiles and gradients, Naval Undersea Center TP 459.

Hamilton, E. L., 1975b, Acoustic and related properties of the sea floor: shear wave velocity profiles and gradients, Naval Undersea Center TP 472.

Hamilton, E. L., 1975c, Acoustic and related properties of the sea floor: sound attenuation as a function of depth, Naval Undersea Center TP 482.

Hamilton, E. L., 1975d, Acoustic properties of the sea floor: a review, in Proceedings of a Conference on Oceanic Acoustic Modelling (held at La Spezia, Italy, 8-11 September 1975), SACLANTCEN Conference Proceedings No. 17, Part 4 (Sea Bottom), Paper No. 18, 96 pp.

Hamilton, E. L., 1976a, Acoustic properties of shallow-water sediments: a review (U), Proceedings of Shallow Water Mobile Sonar Environmental Acoustic Modeling Symposium (U) (held at the Naval Research Laboratory, 23–25 September 1975), Vol. II (C), pp 361–433, SEA 06H1/036-EVA MOST-8, Naval Sea Systems Command, Washington, D.C.

Hamilton, E. L., 1976b, Sound attenuation as a function of depth in the sea floor, Journal of the Acoustical Society of America, Vol. 59, pp 528-535. Outside publication of Hamilton, 1975c.

Hamilton, E. L., 1976c, Variations of density and porosity with depth in deep-sea sediments, Journal of Sedimentary Petrology, Vol. 46, pp 280-300. Outside publication of Hamilton, 1975a.

Hamilton, E. L., 1976d, Attenuation of shear waves in marine sediments, Journal of the Acoustical Society of America, Vol. 60, pp 334-338.

Hamilton, E. L., 1976e, Shear-wave velocity versus depth in marine sediments: a review, Geophysics, Vol. 41, pp 985–996. Outside publication of Hamilton, 1975b.

Bachman, R. T., and Hamilton, E.L., 1976, Density, porosity, and grain density of samples from Deep Sea Drilling Project Site 222 (Leg 23) in the Arabian Sea, Journal of Sedimentary Petrology, Vol. 46, pp 654-658.

Hamilton, E. L., Bachman, R. T., Curray, J. R., and Moore, D. G., 1977, Sediment velocities from sonobuoys: Bengal Fan, Sunda Trench, Andaman Basin, and Nicobar Fan, Journal of Geophysical Research, Vol. 82, pp 3003-3012.

Johnson, T. C., Hamilton, E. L., and Berger, W. H., 1977, Physical properties of calcareous ooze: control by dissolution at depth, Marine Geology, Vol. 24, pp 259-277.

Northrop, J., Fabula, A. G., Colborn, J. G., Hamilton, E. L., Bachman, R. T., Solomon, L. P., Barnes, A. E., Bucker, H. P., and Wagstaff, R. A., 1977, Environmental acoustic predictions for the Northwestern Indian Ocean (U), Naval Ocean Systems Center TN 104 (C).

Johnson, T. C., Hamilton, E. L., Bachman, R. T., and Berger, W. H., 1978, Sound velocities in calcareous oozes and chalks from sonobuoy data: Ontong Java Plateau, Western Equatorial Pacific, Journal of Geophysical Research, Vol. 83, pp 283-288.

Hamilton, E. L., 1978, Sound velocity-density relations in sea floor sediments and rocks, Journal of the Acoustical Society of America, Vol. 63, pp 366-377.

Northrop, J., Colborn, J. G., Hamilton, E. L., and Bachman, R. T., 1978, Propagation loss predictions for the Northwestern Indian Ocean, Journal of Underwater Acoustics, in press.

## ADDITIONAL REFERENCES

## (PART 1)

(In addition to those above for the period 1974 to 1977)

Buchan, S., Dewes, F. C. D., Jones, A. S. G., McCann, D. M., and Smith, D. T., 1971, The Acoustic and Geotechnical Properties of North Atlantic Cores, Vols. 1 and 2, Marine Science Laboratories, University College of North Wales, Menai Bridge, North Wales, 22 pp and tables.

Bucker, H. P. and Morris, H. E., 1975, "Reflection of sound from a layered ocean bottom", Invited paper presented at Oceanic Acoustic Modelling Conference held at SACLANTCEN on 8-11 Sept. 1975, pp 19-1 to 19-35 in SACLANTCEN Conference Proceedings No. 17.

Christensen, N. I., and Salisbury, M. H., 1975, Structure and constitution of the lower oceanic crust, Reviews of Geophysics and Space Physics, Vol. 13, pp 57-86.

Dickinson, G., 1953, Geological aspects of abnormal reservoir pressures in Gulf Coast Louisiana, American Association of Petroleum Geologists, Vol. 37, pp 410-432.

Gardner, G. H. F., Gardner, L. W., and Gregory, A. R., 1974, Formation velocity and density – the diagnostic basics for stratigraphic traps, Geophysics, Vol. 39, pp 770-780.

Griffiths, J. C., 1967, Scientific Method in Analysis of Sediments, McGraw-Hill, New York, 508 pp.

Hamilton, E. L., 1971a, Elastic properties of marine sediments, Journal of Geophysical Research, Vol. 76, pp 579-604.

Hamilton, E. L., 1971b, Prediction of in situ acoustic and elastic properties of marine sediments, Geophysics, Vol. 36, pp 266-284.

Hamilton, E. L., 1972, Compressional wave attenuation in marine sediments, Geophysics, Vol. 37, pp 620-646.

Hamilton, E. L., 1974a, Prediction of deep-sea sediment properties: state of the art, in Deep-Sea Sediments, Physical and Mechanical Properties, pp 1-43, edited by A. L. Inderbitzen, Plenum Press, New York, 497 pp.

Hamilton, E. L., 1974b, Geoacoustic models of the sea floor, in Physics of Sound in Marine Sediments, pp 181–221, edited by L. Hampton, Plenum Press, New York, 567 pp.

Hamilton, E. L., Bucker, H. P., Keir, D. L., and Whitney, J. A., 1970, Velocities of compressional and shear waves in marine sediments determined in situ from a research submersible, Journal of Geophysical Research, Vol. 75, pp 4039-4049.

Hamilton, E. L., Moore, D. G., Buffington, E. C., Sherrer, P. L., and Curray, J. R., 1974, Sediment velocities from sonobuoys: Bay of Bengal, Bering Sea, Japan Sea, and North Pacific, Journal of Geophysical Research, Vol. 79, pp 2653-2668.

Hawker, K. E., and Foreman, T. L., 1976, A plane wave reflection coefficient model based on numerical integration; formulation, implementation, and application, Applied Research Laboratories, University of Texas at Austin, ARL-TR-76-23, 78 pp.

Hawker, K. E., Anderson, A. L., Focke, K. C., and Foreman, T. L., 1976, Initial phase of a study of bottom interaction of low frequency underwater sound, Applied Research Laboratories, University of Texas at Austin, ARL-TR-76-14, 180 pp.

Hawker, K. E., Focke, K. C., and Anderson, A. L., 1977, A sensitivity study of underwater sound propagation loss and bottom loss, Applied Research Laboratories, University of Texas at Austin, ARL-TR-77-17, 122 pp.

Houtz, R., Ewing, J., and LePichon, X., 1968, Velocity of deep-sea sediments from sonobuoy data, Journal of Geophysical Research, Vol. 73, pp 2615-2641.

Houtz, R., Ewing, J., and Buhl, P., 1970, Seismic data from sonobuoy stations in the northern and equatorial Pacific, Journal of Geophysical Research, Vol. 75, pp 5093-5111.

Igarashi, Y., 1973, In situ high-frequency acoustic propagation measurements in marine sediments in the Santa Barbara shelf, California, Naval Undersea Center TP 334, 40 pp.

Ludwig, W. J., Nafe, J. E., and Drake, C. L., 1970, Seismic refraction, in The Sea, Vol. 4, Part 1, pp 53-84, edited by A. E. Maxwell, John Wiley, New York.

Magara, K., 1968, Compaction and migration of fluids in Miocene mudstone, Nagaoka Plain, Japan, American Association of Petroleum Geologists Bulletin, Vol. 52, pp 2466-2501.

Moore, D. G., Curray, J. R., Raitt, R. W., and Emmel, F. J., 1974, Stratigraphic-seismic section correlations and implications to Bengal Fan history, in Initial Reports of the Deep Sea Drilling Project, Vol. 22, edited by C. C. von der Borch, J. G. Sclater et al., pp 403–412, U.S. Government Printing Office, Washington, D.C.

Morris, H. E., 1970, Bottom-reflection-loss model with a velocity gradient, Journal of Acoustical Society of America, Vol. 48, pp 1198-1202.

Muir, T. G., and Adair, R. S., 1972, Potential use of parametric sonar in marine archeology, Journal of the Acoustical Society of America, Vol. 52, p 122 (abstract); unpublished manuscript, Applied Research Laboratories, University of Texas at Austin.

Neprochnov, Yu. P., 1971, Seismic studies of the crustal structure beneath the seas and oceans, Oceanology (English translation), Vol. 11, pp 709-715.

Rieke, H. H., III, and Chilingarian, G. V., 1974, Compaction of Argillaceous Sediments, Elsevier Publishing Co., New York, 424 pp.

Shepard, F. P., 1954, Nomenclature based on sand-silt-clay ratios, Journal of Sedimentary Petrology, Vol. 24, pp 151-158.

Tyce, R. C., 1975, Near-bottom observations of 4 kHz acoustic reflectivity and attenuation, Geophysics, Vol. 41, pp 675-699.

Table 1a. Continental terrace (shelf and slope) environment; average sediment size analyses and bulk grain densities.

| Sediment Type | No. Samples | Mean Grain Diameter mm | Mean Grain Diameter $\phi$ | Sand, % | Silt, % | Clay, % | Bulk Grain Density, g/cm$^3$ |
|---|---|---|---|---|---|---|---|
| Sand | | | | | | | |
| Coarse | 2 | 0.5285 | 0.92 | 100.0 | 0.0 | 0.0 | 2.710 |
| Fine | 18 | 0.1638 | 2.61 | 92.4 | 4.2 | 3.4 | 2.708 |
| Very fine | 6 | 0.0915 | 3.45 | 84.2 | 10.1 | 5.7 | 2.693 |
| Silty sand | 14 | 0.0679 | 3.88 | 64.0 | 23.1 | 12.9 | 2.704 |
| Sandy silt | 17 | 0.0308 | 5.02 | 26.1 | 60.7 | 13.2 | 2.668 |
| Silt | 12 | 0.0213 | 5.55 | 6.3 | 80.6 | 13.1 | 2.645 |
| Sand-silt-clay | 20 | 0.0172 | 5.86 | 32.2 | 41.0 | 26.8 | 2.705 |
| Clayey silt | 60 | 0.0076 | 7.05 | 7.2 | 59.7 | 33.1 | 2.660 |
| Silty Clay | 19 | 0.0027 | 8.52 | 4.8 | 41.2 | 54.0 | 2.701 |

Table 1b. Continental terrace (shelf and slope) environment; sediment densities, porosities, sound velocities and velocity ratios.

| Sediment Type | Density, g/cm$^3$ Avg. | Density, g/cm$^3$ SE | Porosity, % Avg. | Porosity, % SE | Velocity, m/sec Avg. | Velocity, m/sec SE | Velocity Ratio Avg. | Velocity Ratio SE |
|---|---|---|---|---|---|---|---|---|
| Sand | | | | | | | | |
| Coarse | 2.034 | – | 38.6 | – | 1836 | – | 1.201 | – |
| Fine | 1.957 | 0.023 | 44.8 | 1.36 | 1753 | 11 | 1.147 | 0.007 |
| Very fine | 1.866 | 0.035 | 49.8 | 1.69 | 1697 | 32 | 1.111 | 0.021 |
| Silty sand | 1.806 | 0.026 | 53.8 | 1.60 | 1668 | 11 | 1.091 | 0.007 |
| Sandy silt | 1.787 | 0.044 | 52.5 | 2.44 | 1664 | 13 | 1.088 | 0.008 |
| Silt | 1.767 | 0.037 | 54.2 | 2.06 | 1623 | 8 | 1.062 | 0.005 |
| Sand-silt-clay | 1.590 | 0.026 | 66.8 | 1.46 | 1579 | 8 | 1.033 | 0.005 |
| Clayey silt | 1.488 | 0.016 | 71.6 | 0.87 | 1549 | 4 | 1.014 | 0.003 |
| Silty clay | 1.421 | 0.015 | 75.9 | 0.82 | 1520 | 3 | 0.994 | 0.002 |

Notes: Laboratory values: 23°C, 1 atm; density: saturated bulk density; porosity: salt free; velocity ratio: velocity in sediment/velocity in sea water at 23°C, 1 atm, and salinity of sediment pore water. SE: standard error of the mean.

Table 2a. Abyssal plain and abyssal hill environments; average sediment size analyses and bulk grain densities.

| Environment Sediment Type | No. Samples | Mean Grain Diameter mm | Mean Grain Diameter $\phi$ | Sand, % | Silt, % | Clay, % | Bulk Grain Density, g/cm$^3$ |
|---|---|---|---|---|---|---|---|
| **Abyssal Plain** | | | | | | | |
| Sandy silt | 1 | 0.0170 | 5.88 | 19.4 | 65.0 | 15.6 | 2.461 |
| Silt | 3 | 0.0092 | 6.77 | 3.2 | 78.0 | 18.8 | 2.606 |
| Sand-silt-clay | 2 | 0.0208 | 5.59 | 35.2 | 33.3 | 31.5 | 2.653 |
| Clayey silt | 22 | 0.0053 | 7.57 | 4.5 | 55.3 | 40.2 | 2.650 |
| Silty clay | 40 | 0.0021 | 8.90 | 2.5 | 36.0 | 61.5 | 2.660 |
| Clay | 6 | 0.0014 | 9.53 | 0.0 | 22.2 | 77.8 | 2.663 |
| Bering Sea and Okhotsk Sea (Diatomaceous) | | | | | | | |
| Silt | 1 | 0.0179 | 5.80 | 6.5 | 76.3 | 17.2 | 2.474 |
| Clayey silt | 5 | 0.0049 | 7.68 | 8.1 | 49.1 | 42.3 | 2.466 |
| Silty clay | 23 | 0.0024 | 8.71 | 3.0 | 37.4 | 59.6 | 2.454 |
| **Abyssal Hill** | | | | | | | |
| Deep-sea ("red") pelagic clay | | | | | | | |
| Clayey silt | 17 | 0.0056 | 7.49 | 3.9 | 58.7 | 37.4 | 2.678 |
| Silty clay | 60 | 0.0023 | 8.76 | 2.1 | 32.2 | 65.7 | 2.717 |
| Clay | 45 | 0.0015 | 9.43 | 0.1 | 19.0 | 80.9 | 2.781 |
| Calcareous ooze | | | | | | | |
| Sand-silt-clay | 5 | 0.0146 | 6.10 | 27.3 | 42.8 | 29.9 | 2.609 |
| Silt | 1 | 0.0169 | 5.89 | 16.3 | 75.6 | 8.1 | 2.625 |
| Clayey silt | 15 | 0.0069 | 7.17 | 3.4 | 60.7 | 35.9 | 2.678 |
| Silty clay | 4 | 0.0056 | 7.48 | 3.9 | 39.9 | 56.2 | 2.683 |

Table 2b. Abyssal plain and abyssal hill environments; sediment densities, porosities, sound velocities and velocity ratios.

| Environment / Sediment Type | Density, g/cm$^3$ Avg. | Density, g/cm$^3$ SE | Porosity, % Avg. | Porosity, % SE | Velocity, m/sec Avg. | Velocity, m/sec SE | Velocity Ratio Avg. | Velocity Ratio SE |
|---|---|---|---|---|---|---|---|---|
| **Abyssal Plain** | | | | | | | | |
| Sandy silt | 1.652 | – | 56.6 | – | 1622 | – | 1.061 | – |
| Silt | 1.604 | – | 63.6 | – | 1563 | – | 1.022 | – |
| Sand-silt-clay | 1.564 | – | 66.9 | – | 1536 | – | 1.004 | – |
| Clayey silt | 1.437 | 0.023 | 75.2 | 1.31 | 1526 | 3 | 0.998 | 0.002 |
| Silty clay | 1.333 | 0.019 | 81.4 | 1.03 | 1515 | 2 | 0.991 | 0.001 |
| Clay | 1.352 | 0.037 | 80.0 | 2.20 | 1503 | 2 | 0.983 | 0.001 |
| **Bering Sea and Okhotsk Sea (Diatomaceous)** | | | | | | | | |
| Silt | 1.447 | – | 70.8 | – | 1546 | – | 1.011 | – |
| Clayey silt | 1.228 | 0.019 | 85.8 | 0.86 | 1534 | 2 | 1.003 | 0.001 |
| Silty clay | 1.214 | 0.008 | 86.8 | 0.43 | 1525 | 2 | 0.997 | 0.001 |
| **Abyssal Hill** | | | | | | | | |
| **Deep-sea ("red") pelagic clay** | | | | | | | | |
| Clayey silt | 1.347 | 0.020 | 81.3 | 0.95 | 1522 | 3 | 0.995 | 0.002 |
| Silty clay | 1.344 | 0.011 | 81.2 | 0.60 | 1508 | 2 | 0.986 | 0.001 |
| Clay | 1.414 | 0.012 | 77.7 | 0.64 | 1493 | 1 | 0.976 | 0.001 |
| **Calcareous ooze** | | | | | | | | |
| Sand-silt-clay | 1.400 | 0.013 | 76.3 | 0.90 | 1581 | 8 | 1.034 | 0.005 |
| Silt | 1.725 | – | 56.2 | – | 1565 | – | 1.023 | – |
| Clayey silt | 1.573 | 0.020 | 66.8 | 1.22 | 1537 | 5 | 1.005 | 0.003 |
| Silty clay | 1.483 | 0.029 | 72.3 | 1.61 | 1524 | 7 | 0.996 | 0.005 |

Notes: Laboratory values: 23°C, 1 atm; density: saturated bulk density; porosity: salt free; velocity ratio: velocity in sediment/velocity in sea water at 23°C, 1 atm, and salinity of sediment pore water. SE: standard error of the mean.

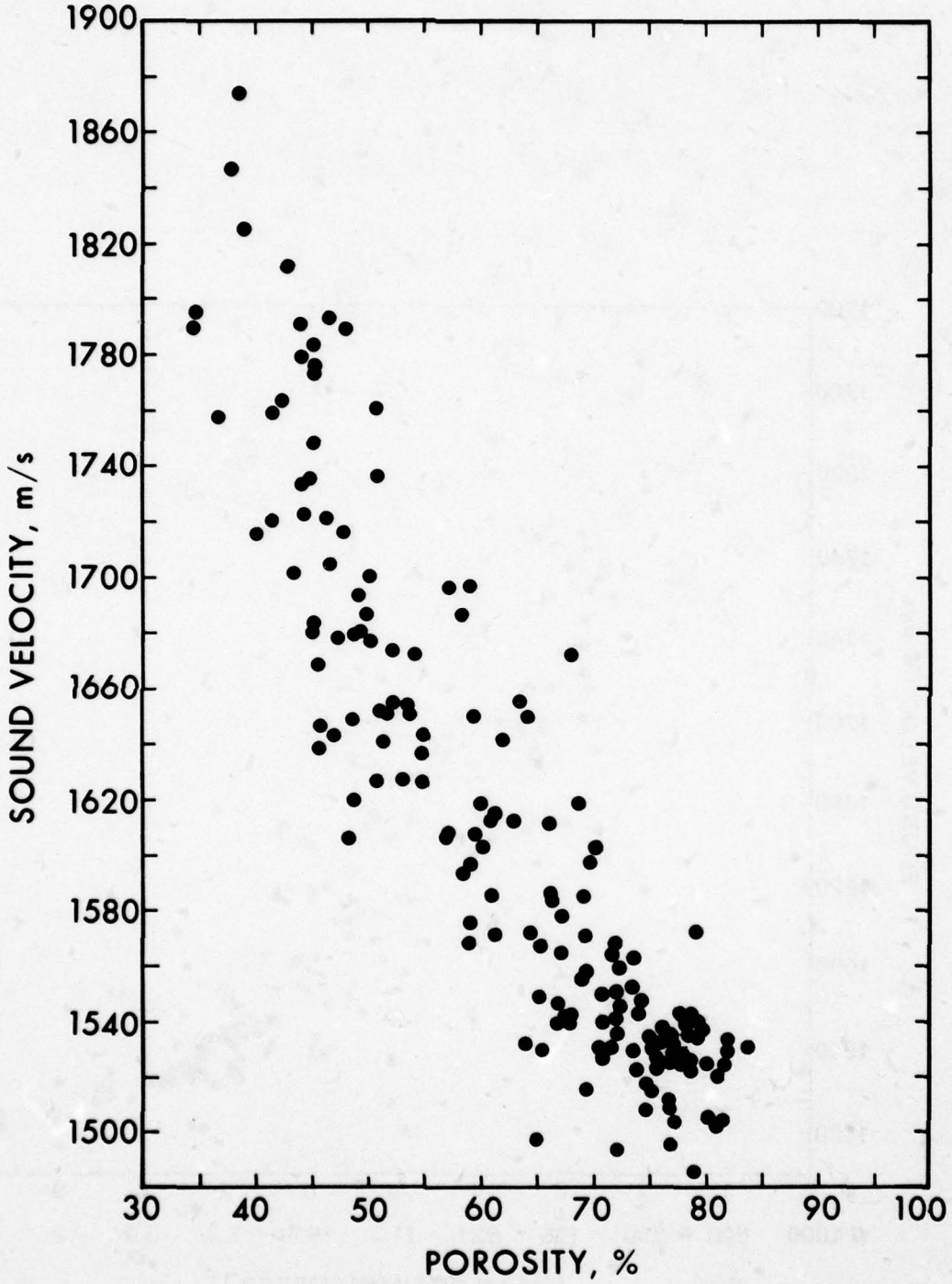



Figure 1. Sediment porosity versus sound velocity, continental terrace (shelf and slope).

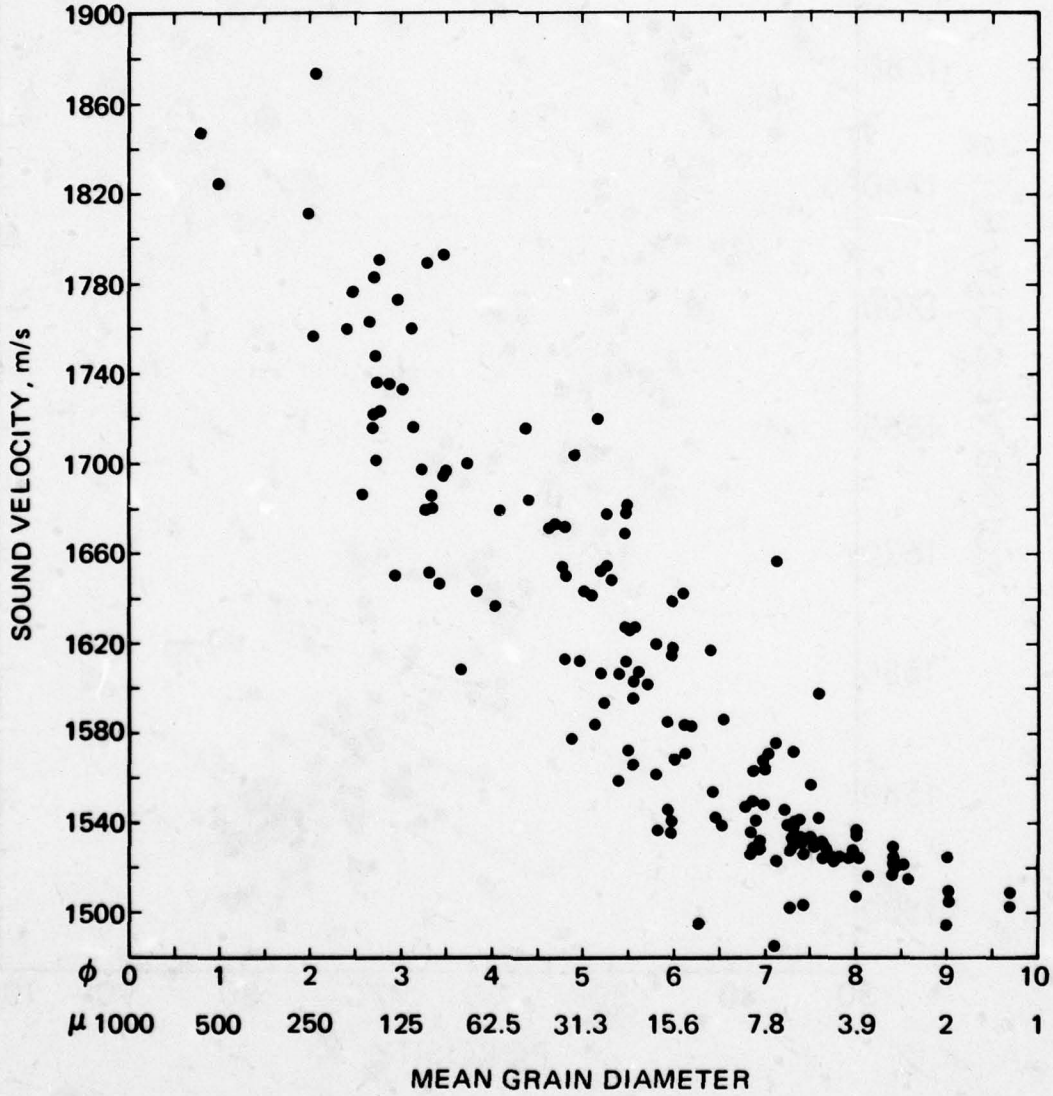



Figure 2. Mean diameter of mineral grains versus sound velocity, continental terrace (shelf and slope).

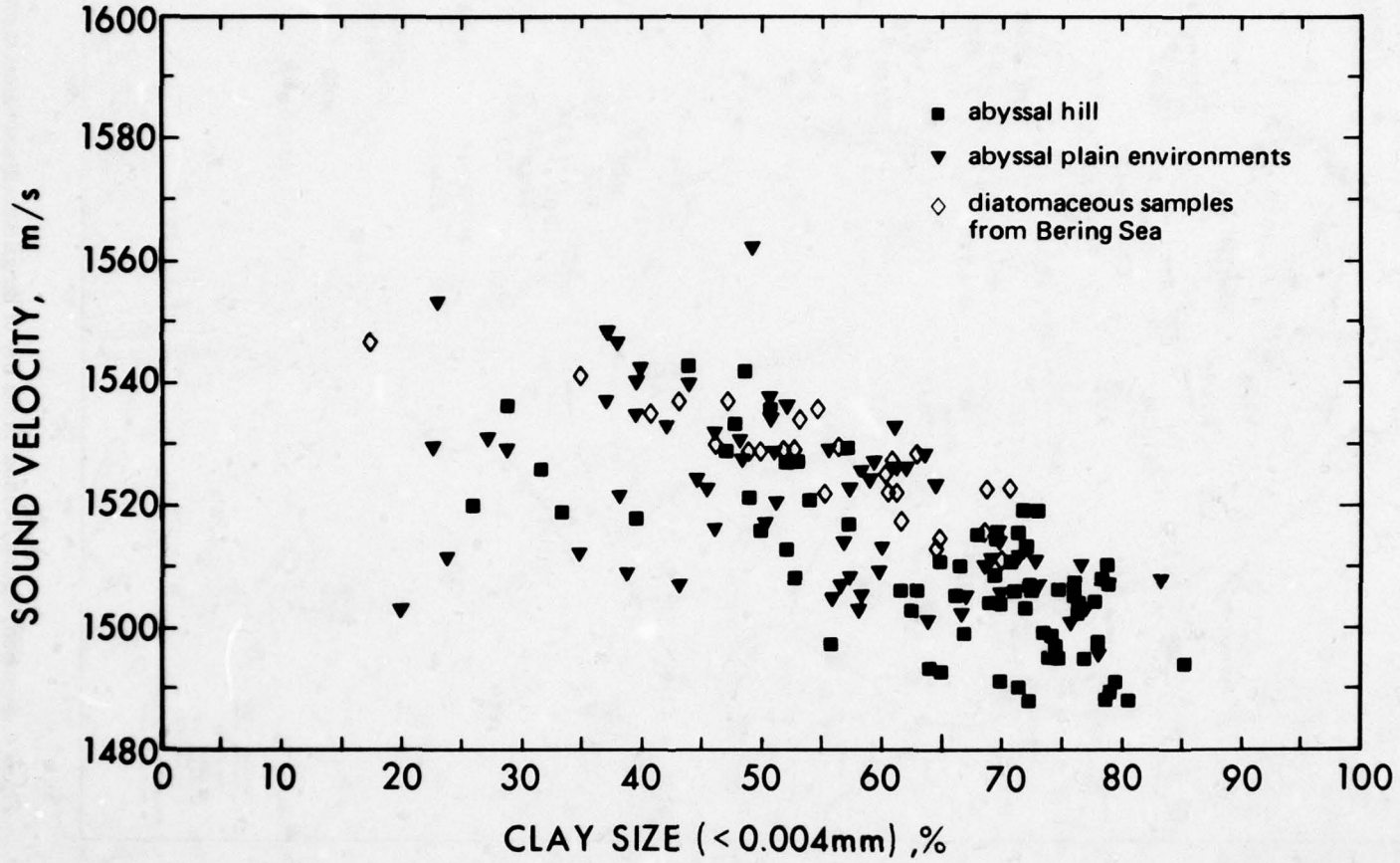



Figure 3. Percent clay size versus sound velocity, abyssal hill and abyssal plain environments.

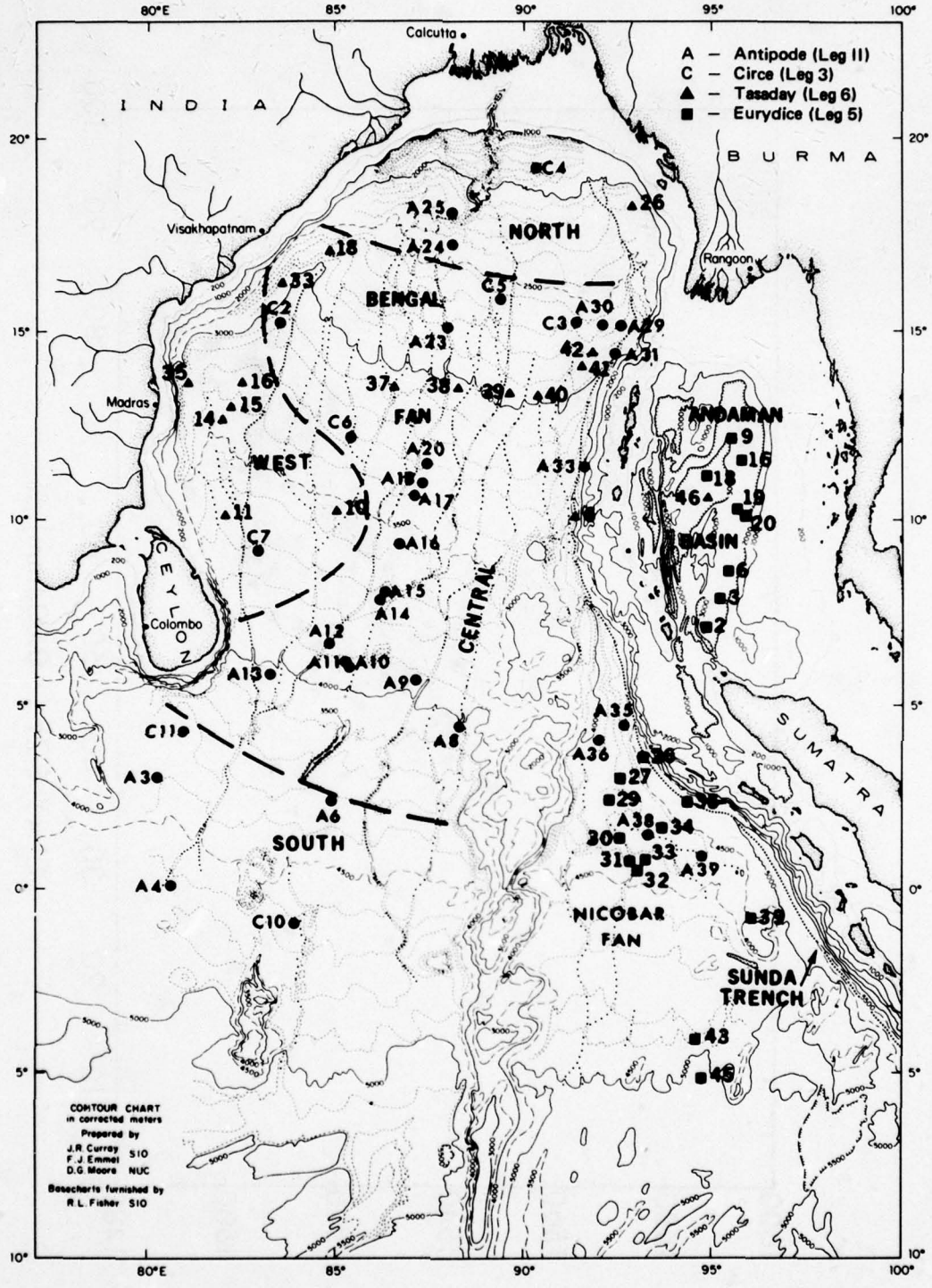



Figure 4. Sonobuoy station locations in the Bay of Bengal and adjacent areas as revised from Hamilton et al (1974) which contained only Antipode and Circe data. The base chart is from Moore et al (1974); contours are in meters, corrected for sound velocity. Station numbers are adjacent to symbols. Symbols refer to Scripps Institution of Oceanography expeditions. A number of closely-spaced sonobuoys (at a single, numbered station) are represented by a single dot.

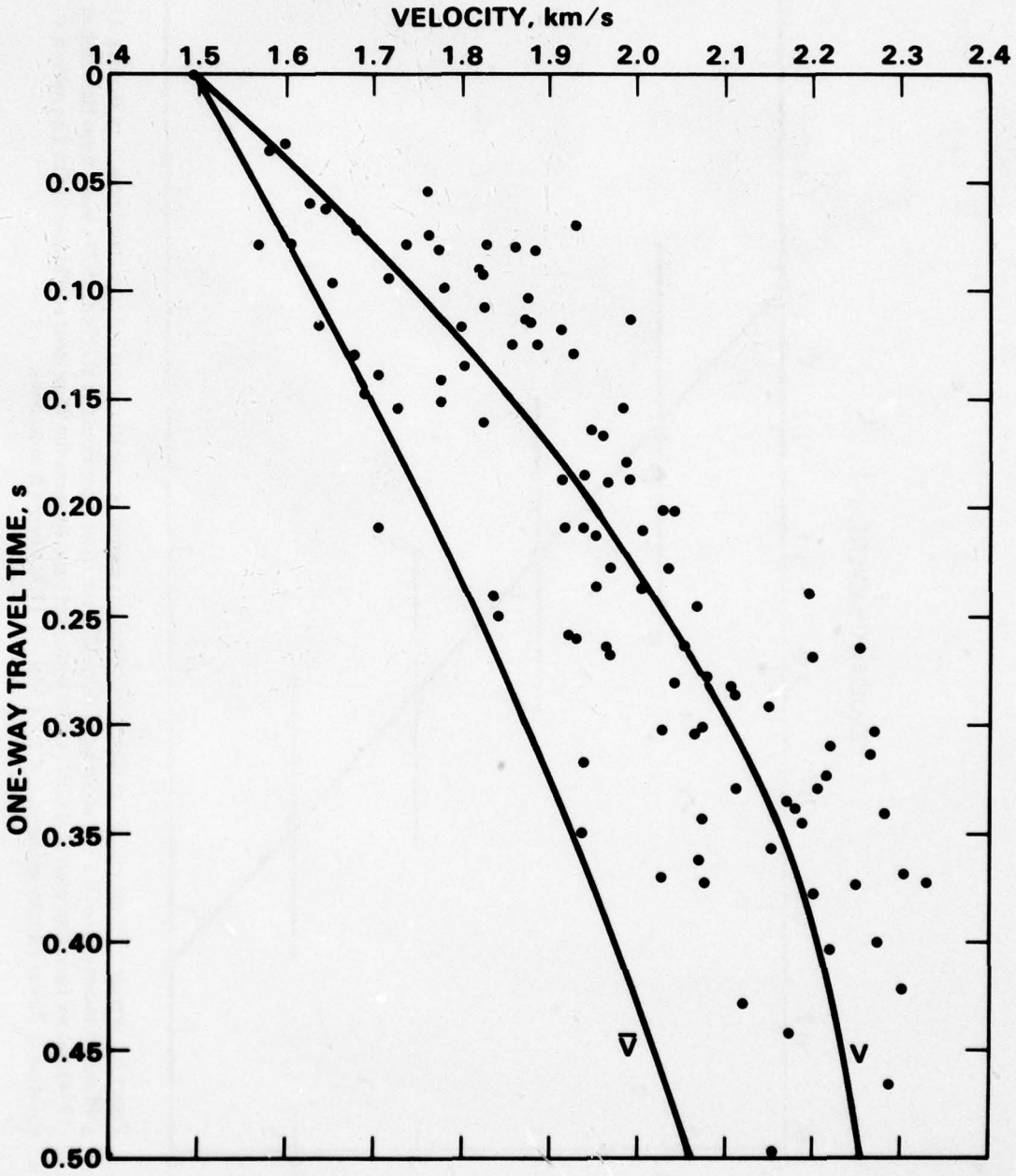



Figure 5. Instantaneous velocity, V, and mean velocity, $\overline{V}$, versus one-way travel time in the Central Bengal Fan.

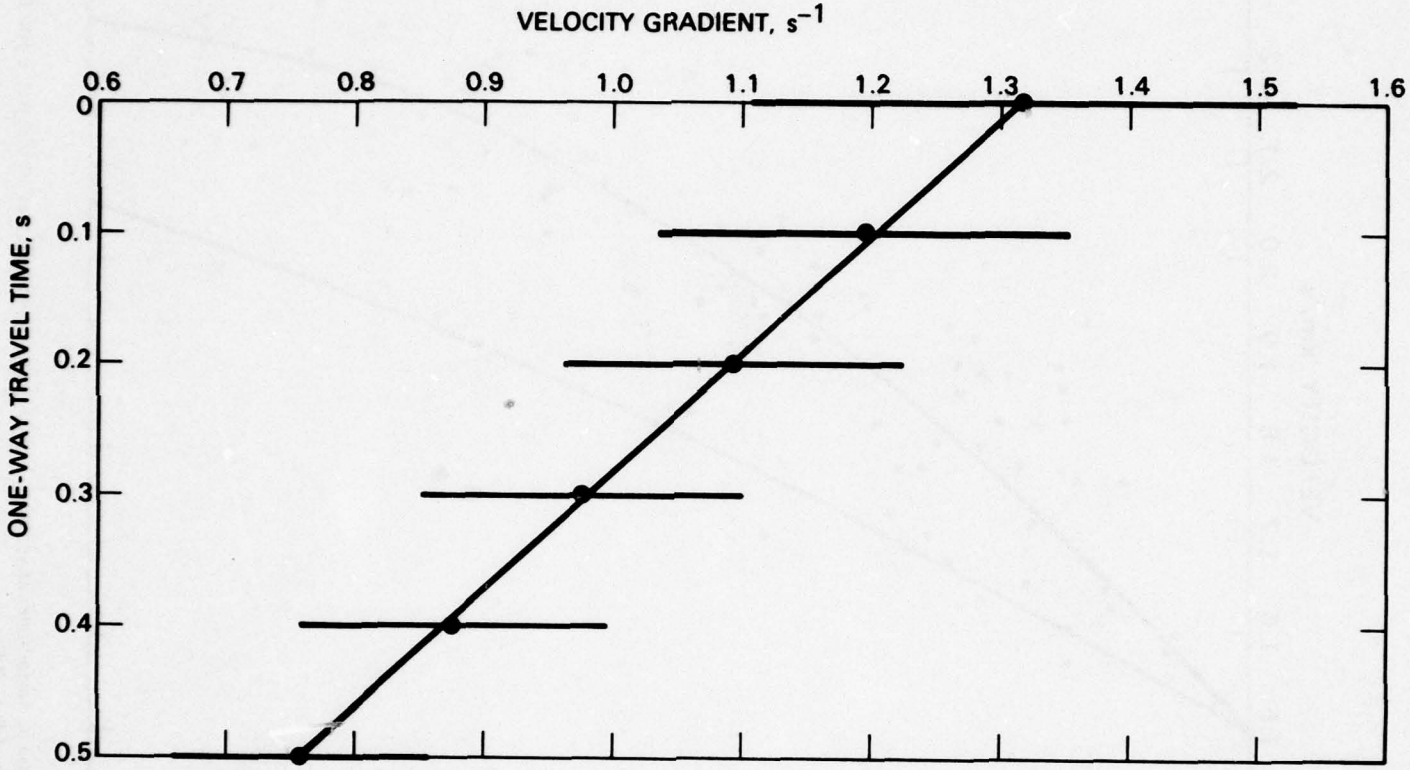



Figure 6. Average of linear velocity gradients, in meters per second per meter, versus one-way travel time, t, in seconds. Linear gradients at increments of 0.1 s were averaged from 17 areas: four from Houtz et al (1968, 1970), seven from Hamilton et al (1974) and six from Hamilton et al (1977). The horizontal bars represent the 95 percent confidence limits. The regression equation is: linear velocity gradient, a, $s^{-1} = 1.316 - 1.117t$, where t is in seconds.

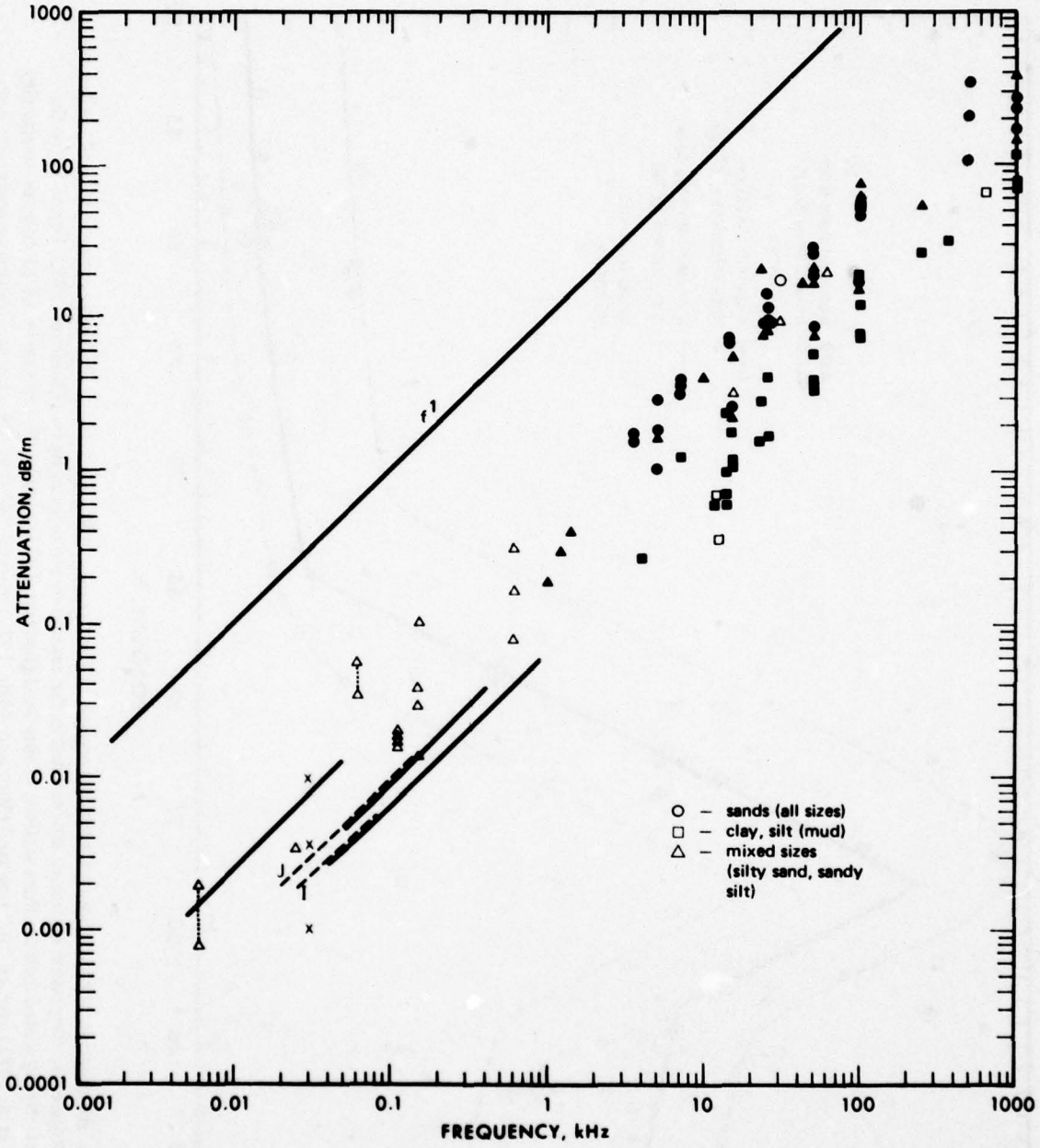



Figure 7. Attenuation of compressional (sound) waves versus frequency in natural, saturated sediments and sedimentary strata. The solid lines and symbols are from Hamilton (1972, Figure 2); the open symbols and dashed lines are newly-added data. The lines marked "J" and "I" represent general equations for the Japan Sea and Indian Ocean Central Basin (from Neprochnov, 1971). The vertical, dashed lines indicate a range of attenuation values at a single frequency. The line labelled "$f^1$" indicates the slope of any line having a dependence of attenuation on the first power of frequency.

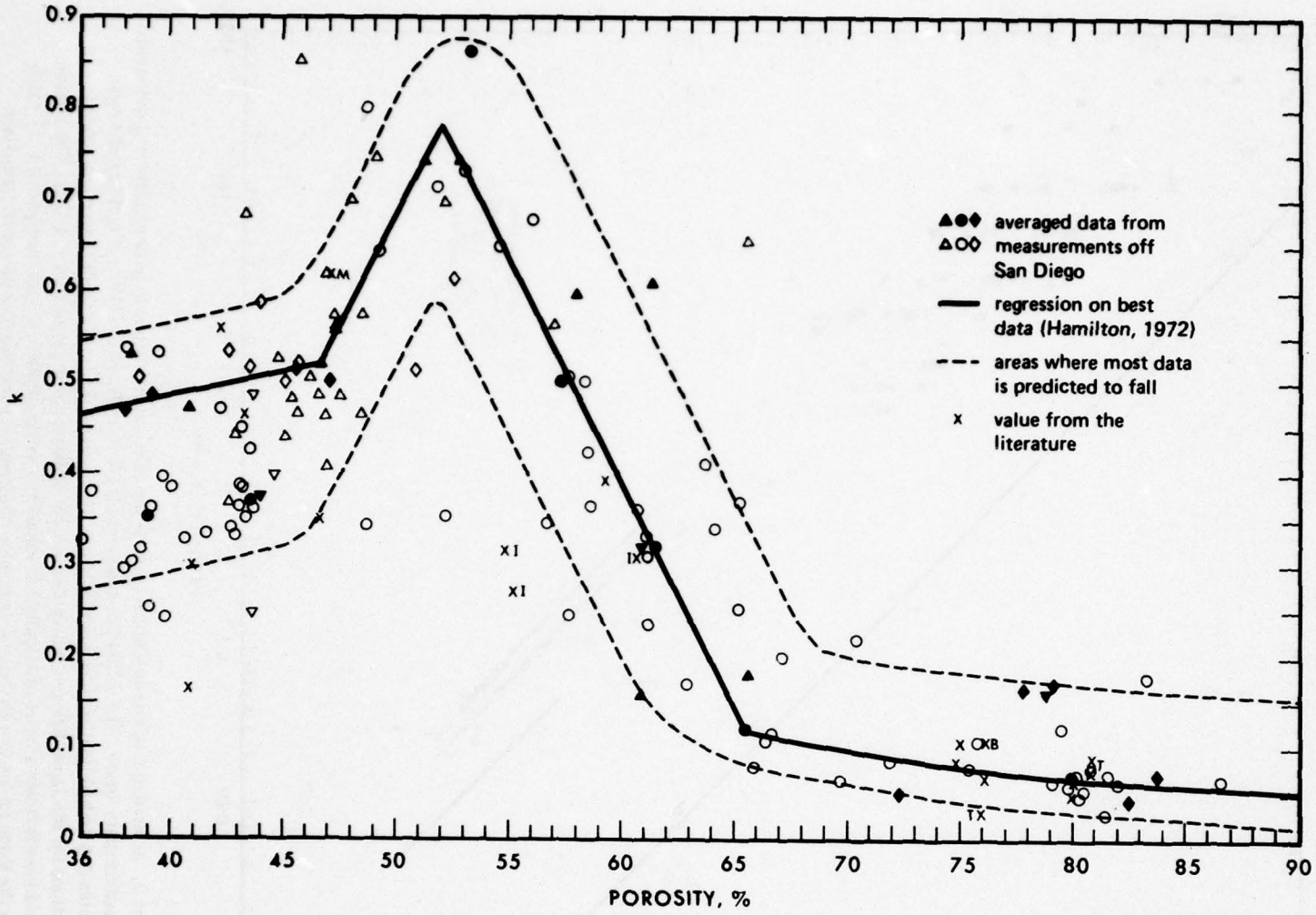



Figure 8. Attenuation of compressional waves (expressed as k in: $\alpha_{dB/m} = kf_{kHz}$) versus sediment porosity in natural, saturated surface sediments. Regression equations are included in the caption to the original figure (Hamilton, 1972, Figure 5) for the solid lines. Newly-added data are three stations in silty sand (Igarashi, 1973) marked "I," an average of 11 cores of pelagic clay (Buchan et al, 1971) marked "B," fine sand (Muir and Adair, 1972) marked "M" and silty clay and calcareous sediments from Tyce (1975) marked "T."

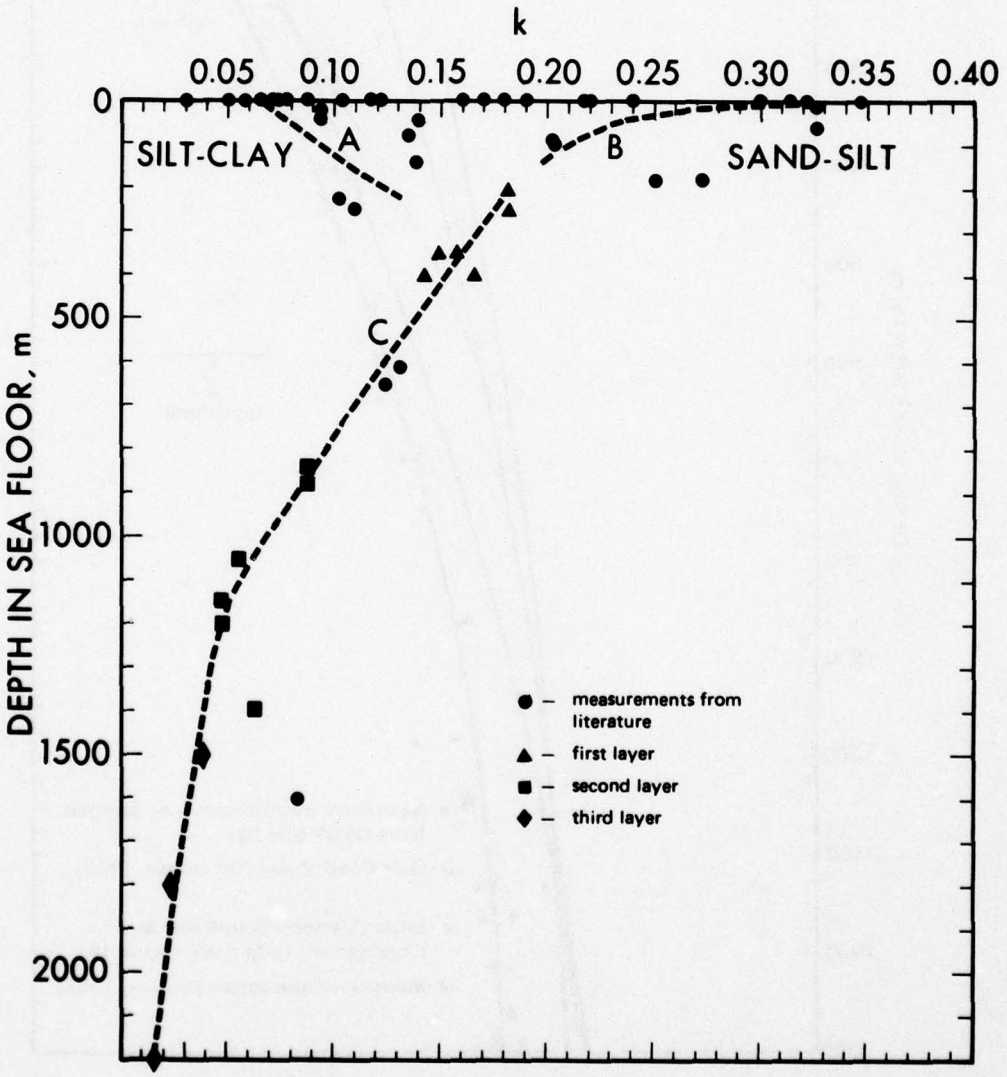



Figure 9. Attenuation of compressional waves (expressed as k in: $\alpha_{dB/m} = kf_{kHz}$) versus depth in the sea floor or in sedimentary strata. Symbols are layers in the sea floor in 7 areas (from Neprochnov, 1971).

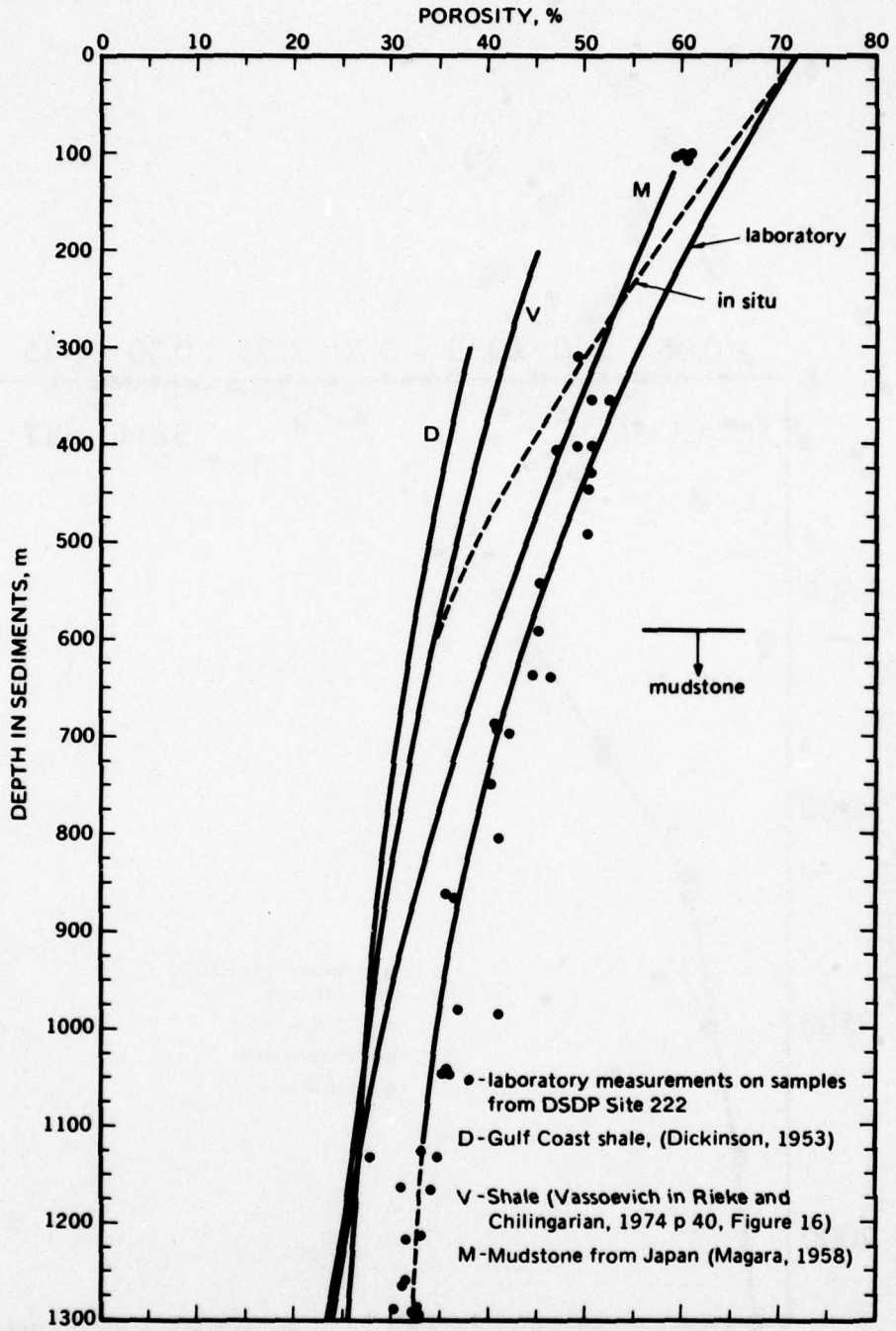



Figure 10. Porosity versus depth in terrigenous sediments.

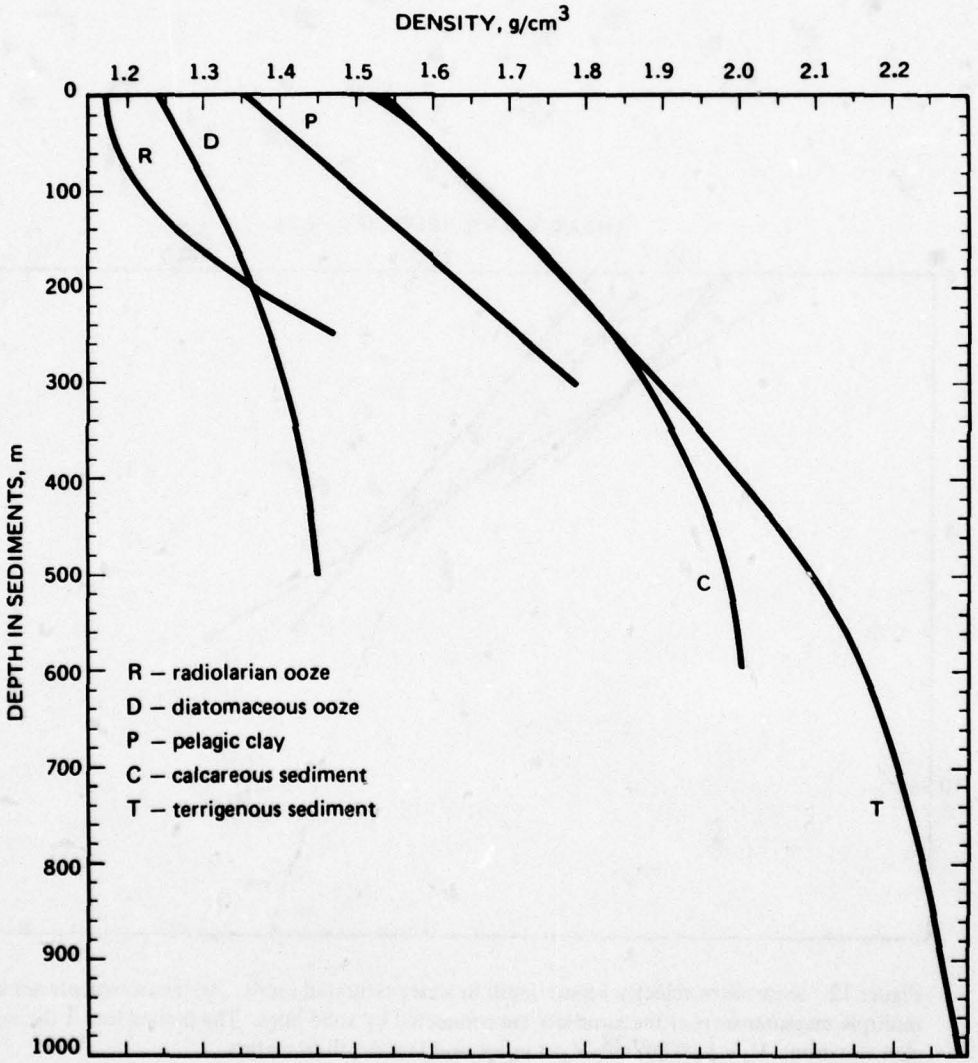



Figure 11. In situ density of various marine sediments versus depth in the sea floor.

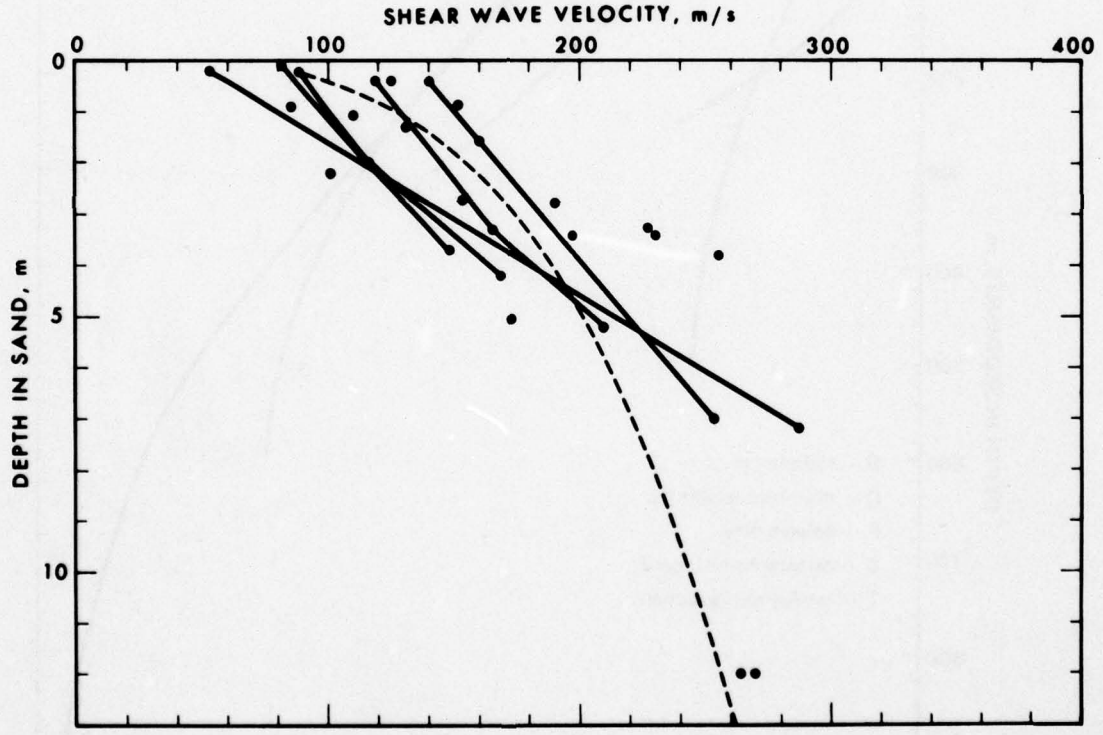



Figure 12. Shear wave velocity versus depth in water-saturated sands. All measurements are in situ; multiple measurements at the same site are connected by solid lines. The dashed line is the regression equation: $V_s = 128(D)^{0.28}$; $V_s$ in m/sec and D is depth in meters.

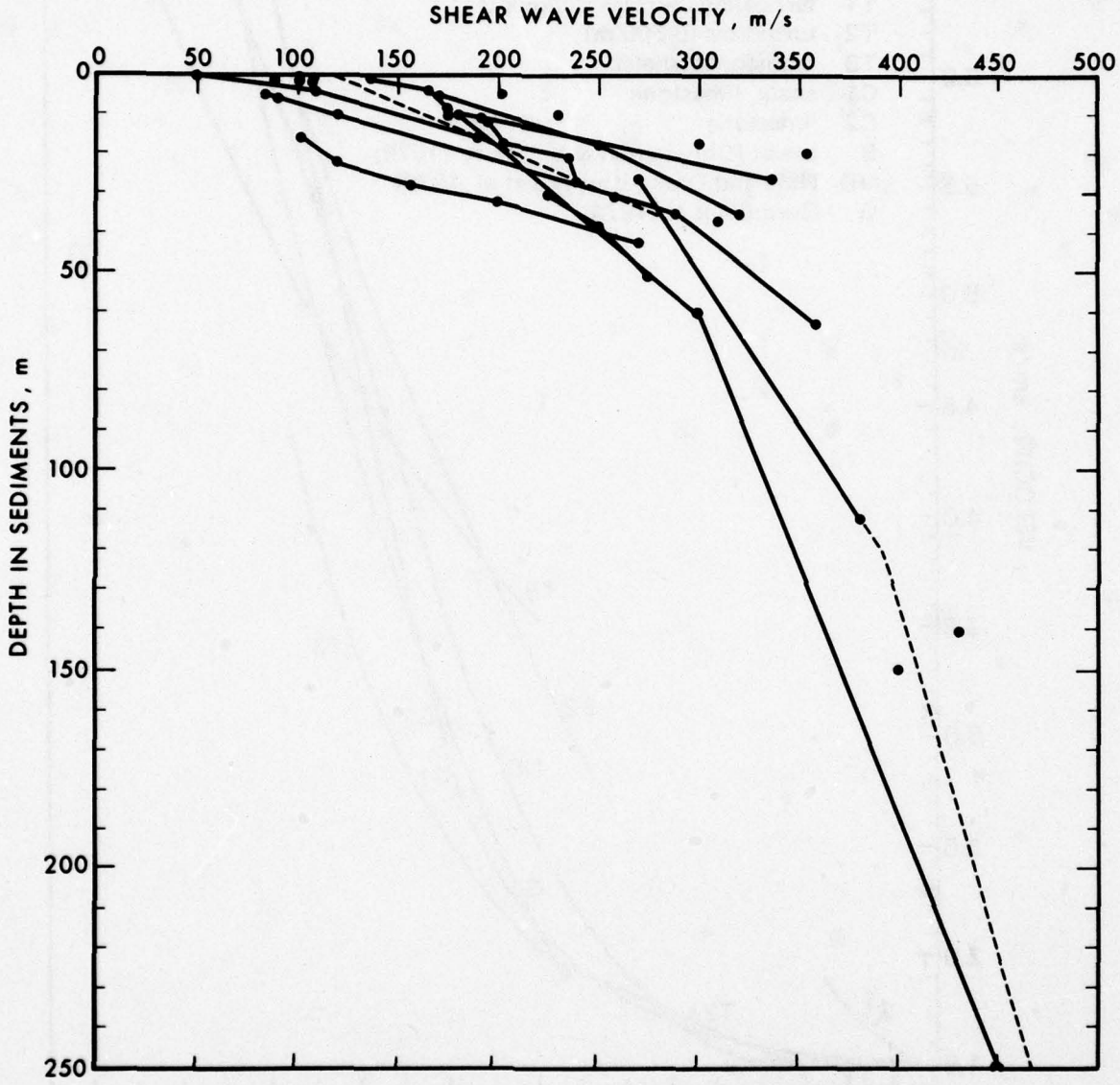



Figure 13. Shear wave velocity measured in situ versus depth in water-saturated silt-clays and turbidites. Multiple measurements at the same site are connected by solid lines. The dashed lines are three linear regressions. One measurement ($V_S$ = 700 m/sec at 650 meters) is not shown.

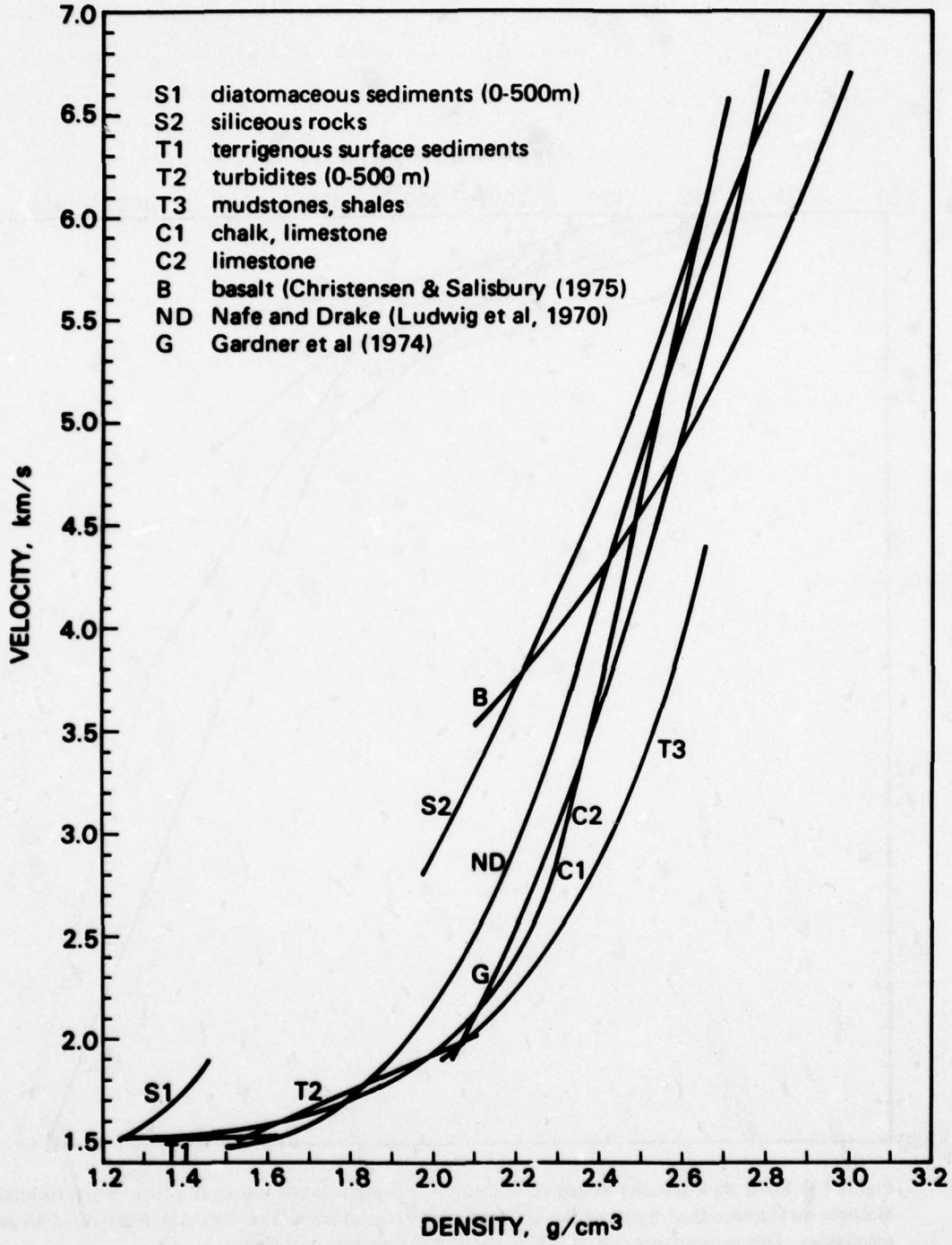



Figure 14. A summary of compressional wave velocity versus density in Hamilton (1977). The general curves of ND and G are included for comparisons. The equation for the curve of Gardner et al (1974, p 779) is $\rho = 0.23\ V_p^{0.25}$; where $\rho$ is density in g/cm$^3$ and $V_p$ is compressional wave velocity in feet per second.

# PART II:
# ACOUSTIC MODELING

## INTRODUCTION

This report describes the bottom loss models that comprise part of our effort in the Bottom Interaction Program for 1974-1977. Although some of these models were developed earlier, they continue to be modified and updated for current uses.

Our linear gradient multilayer model and our solid multilayer model were designed to study reflection of low frequency sound from the ocean bottom. Considerable depths (up to a kilometer) of ocean sediments are insonified at low frequencies. Consequently, sediment parameters can undergo considerable variation in the insonified region. This variation of sediment properties with depth must be taken into account if an accurate representation of bottom loss is to be attained. The liquid multilayer model can account for many layers of sediment in which the sound speeds are complex to account for absorption. The linear gradient model assumes complex sound speeds, also, but the sound speeds vary in a linear fashion in a particular sediment layer.

Our solid multilayer model is a general purpose plane wave reflection model that can account for both liquid and/or solid layers. We know that sediments have rigidity and, therefore, for more accurate model calculations we must take rigidity into account. Important parameters to the solid model are the speed and attenuation of both the compressional and shear waves that travel in the sediment. In our most recent programs we have chosen to model the variable sediment properties with many layers (up to 1000 layers or more, if necessary), and maintain the needed accuracy by use of Knopoff's formulation. We have taken the concept of many constant layers as in the liquid model (but for solid layers, i.e., sediments with rigidity) and made it possible to have the many constant layers approximate the results of a linear gradient concept.

The distinguishing features of the solid multilayer model are the following:

- All sediment layers can be realistically represented to have rigidity
- Both solid and liquid layers can be taken into account if required
- The Knopoff formulation provides fast and accurate computations
- Continuous density variations are accounted for
- The various outputs include bottom loss and/or R versus grazing angle
- The graphical forms include 3-dimensional representation

A so-called equivalent bottom concept has been developed for the Parabolic Equation (P.E.) propagation program. The Gibb's oscillations caused by a density discontinuity at the interface can be handled by calculating an equivalent reflection coefficient by assuming different sediment parameters. An example of the technique is included. This technique should enable the P.E. propagation program to be used for bottom limited areas.

## FORMULATION OF THE SOUND FIELD USING THE PLANE WAVE REFLECTION COEFFICIENT R

There are two types of solution to the wave equation which are of particular importance in sound transmission. One is the transformation of the wave equation to the eikonal equation and a solution in terms of wave surfaces and rays. The other is a development through specific boundary conditions into a solution in terms of normal modes. In



PRECEDING PAGE BLANK-NOT FILMED

some instances the physical conditions of the problem lead to a simpler solution in terms of rays. In others, a solution in terms of normal modes is more satisfactory. In any case, it is clear that the sediments that stratify the ocean bottom interact with the sound field through the bottom reflection coefficient, R, in the derived theoretical expressions which follow.

## RAY THEORY

In working with active sonar problems at frequencies of approximately 2.5 to 15 kHz usually we use ray theory. In ray theory, the sound field is made up of contributions of rays that travel from the source to the receiver as shown in Figure 15. On the right hand side of Figure 15 we show two neighboring rays that bracket the receiver at range r. Thus there is an eigenray somewhere between these that travels precisely from the source to the receiver. Call this the $n^{th}$ eigenray. The magnitude of the ray is $A_n$ and its phase is $\theta_n$ as expressed in the equation for the velocity potential, $\psi$

$$\psi = \sum_n A_n \exp(i\theta_n)$$

where

$$A_n = |R| \left[\cos \gamma_s \, \delta\gamma_s/(r\delta h)\right]^{1/2}$$

and

$$\theta_n = \int_o^r (\omega/c)\, d\ell + \arg(R) - m\pi/2 \ .$$

R is the reflection coefficient, $\omega$, the angular frequency, c, the sound speed, $d\ell$, a path length along the ray and m is the number of times the ray has touched a caustic.

The reflection coefficient R is defined for reflection of plane waves and is a complex number. The pressure carried by the ray is reduced by a factor equal to the modulus of R and the phase of the ray is advanced by the argument of R. In experimental work, $A_n$ can be measured and the |R| determined from the equation for $A_n$. At high frequencies, the plane and spherical coefficients essentially are equal. At low frequencies, the ray theory breaks down and the sound cannot be separated into packets that have a well defined trajectory. As shown in the following equations, the direct and bottom reflected sound field can be written at any frequency in terms of the plane wave reflection coefficient.

## WAVE THEORY

The general form of the sound field can be written as a sum of cylindrical waves in the form (Bucker, 1970)

$$\psi = \int_o^\infty -2\, U(z_o)\, V(z)\, W^{-1}\, J_o(kr)\, kdk \qquad (z_o \leq z \leq z_b)$$

where

$$W = U(z_o)\, V'(z_o) - U'(z_o)\, V(z_o) \ .$$

The zero depth, source depth, receiver depth and bottom depth are 0, $z_o$, z and $z_b$, respectively. The zero depth may be set at the air-water interface or at some other convenient point. It represents the depth above which no sound is refracted or reflected to the receiver. The horizontal wave number is k, r is the horizontal distance between the source and receiver, $J_o$ is the Bessel function of the first kind of order zero, U is a solution of the z-separated part of the wave equation, i.e., $U'' = (k^2 - \omega^2/v^2(z))U$, that satisfies the boundary condition at $z = 0$, and V is a solution of the z-separated part of the wave equation, i.e., $V'' = (k^2 - \omega^2/v^2(z))V$, that satisfies the boundary condition at $z = z_b$. Formally, our treatment will be restricted to $(z_o \leqslant z \leqslant z_b)$; however, a similar development for $(0 \leqslant z \leqslant z_o)$ is easily derived.

It is easy to show that dW/dz is zero so that W is independent of depth. Also, we are free to specify the value of U and V at a selected depth which we, for convenience, indicate by a bar and replace U and V by $\bar{U}$ and $\bar{V}$ where $\bar{U}(z_b) = \bar{V}(z_b) = 1$. It follows then that in the limit $z_p \to z_b$, $W = Wz_b = [i\,\ell_b(1-R) - (1+R)\,\bar{U}'(z_b)]/(1+R)$. Therefore, $\psi$ can be expressed as

$$\psi = -2\int_o^\infty \frac{(1+R)\,\bar{U}(z_o)\,\bar{V}(z)\,J_o(kr)\,kdk}{(i\ell_b - \bar{U}'(z_b)) - R(i\ell_b + \bar{U}'(z_b))} \ .$$

For the general sound speed profile it does not appear feasible to separate the direct sound paths from the bottom reflected paths. However, if the water has a constant sound speed then $\bar{U}(z) = \exp[i\ell(z_b - z)]$ and $\bar{V}(z) = [\exp - i\ell(z_b - z) + R \exp i\ell(z_b - z)]/(1+R)$. In this case it follows that

$$\psi = \underbrace{\int_o^\infty (i/\ell)e^{i\ell(z-z_o)}\,J_o(kr)\,kdk}_{\psi_D} + \underbrace{\int_o^\infty (i/\ell)Re^{i\ell(2z_b-z-z_o)}\,J_o(kr)\,kdk}_{\psi_R}$$

If the bottom reflected field $\psi_R$ can be measured directly then we have

$$\psi_R = \int_o^\infty (i/\ell)\,Re^{i\ell(2z_b-z-z_o)}\,J_o(kr)\,kdk$$

and R can be determined experimentally by use of the Hankel Transform

$$R = \int_o^\infty \psi_R\,J_o(kr)\,rdr/[(i/\ell)\exp i\ell(2z_b - z - z_o)] \ .$$

This is not a practical procedure, however, because quadrature sampling would be required to determine the real and imaginary parts of $\psi_R$. That is Real $(\psi_R) = p_R \cos\phi$ and

$\mathrm{Im}(\psi_R) = p_R \sin\phi$, where $p_R$ is 1/2 the peak to peak pressure of the bottom reflected signal and $\phi$ is the phase. In any event when realistic profiles are considered, it is not possible to separate the direct and bottom reflected paths at low frequencies.

The normal mode form of the wave theory representation, required for low frequency calculations, is shown in Figure 16 (Bucker, 1970). The source is at depth $z_o$ and range zero and the receiver is at depth z and range r. The potential function $\psi$ is given by

$$\psi = \left(\frac{2\pi}{r}\right)^{1/2} \sum_n U_n(z_o)\, U_n(z) \exp(ik_n r)$$

$$U = Af(z) + Bg(z) \ , \quad 0 \leq z \leq z_p$$

$$U = \exp(i\ell_b z) + R \exp[i\ell_b(2z_b - z)] \ , \quad z_p \leq z \leq z_b \ .$$

where

$$\ell_b^2 = (\omega/c_b)^2 - k^2 \ .$$

The depth function U is a sum of linearly independent solutions of the z-separated part of the wave equation and k is the horizontal wave number. The $k_n$ are those values of k for which U satisfies the boundary conditions. The plane wave coefficient R is introduced into the normal mode solution in the following manner. Assume that a "pseudo" isospeed layer, with sound speed $c_b$, extends from depth $z_p$ to $z_b$ as shown in Figure 16. Then the z-component solution for the layer can be written as a downgoing plane wave $\exp(i\ell_b z)$ and an upgoing plane wave $\exp(-i\ell_b z)$ multiplied by the plane wave reflection coefficient R. The vertical wave number is $\ell_b$. The values of the coefficients A and B can be determined by requiring the usual interface conditions at depth $z_p$. These conditions require that the pressure $(\rho\partial U/\partial t)$ and the vertical component of particle velocity $(\partial U/\partial z)$ must be continuous functions. Solve these two equations and take the limit $z_p \to z_b$ to obtain the values of A and B.

Interface Conditions:

continuity of pressure $(\rho U)$

continuity of vertical $(-\partial U/\partial z)$ component of particle velocity

Solve for A and B as $z_p \to z_b$.

$$A = \exp(i\ell_b z_b)\,[g'_b(1+R) - i\ell_b g_b(1-R)]/W \ .$$

$$B = \exp(i\ell_b z_b)\,[i\ell_b f_b(1-R) - f'_b(1+R)]/W \ .$$

where

$$W = f_b g'_b - f'_b g_b$$

$$f_b = f(z_b) \ , \ g_b = g(z_b) \ , \ f'_b = (df/dz)_{z=z_b} \ , \ g'_b = (dg/dz)_{z=z_b} \ .$$

Note that the isospeed layer has been removed from the problem as $z_p \to z_b$. However R remains in the solution in A and B.

## BOTTOM LOSS MODELS THAT ACCOUNT FOR GRADIENTS

The variation of sound speed in the ocean, configuration of the bottom, and bottom and subbottom properties are generally the most important environmental factors for the determination of underwater sound transmission. The bottom properties can vary considerably from one area to another. The more common types of sediments are sand, sand and mud, or mud. The areas of mud-size particles can vary in compactness from hard clay to a loose suspension. Not enough is known of the acoustic properties of the immediate bottom materials and the variation of these properties as a function of depth into the bottom as discussed in Part I. We do observe that the bottom characteristics have an important effect in some areas on sound transmission. In other areas the bottom has very little effect and the sound speed profile is the controlling factor. It is important to develop realistic models of the bottom which use sediment characteristics to predict the reflection coefficient R as a function of grazing angle for determining the acoustic transmission of an area.

### LIQUID MULTILAYER MODEL

We next want to consider multilayered sediment models that can be used either to represent actual layering (e.g., it is not uncommon to find alternating layers of sand and silt in shallow water) or to account for gradients. For the layered liquid case the solution is very simple. Figure 17 shows n sediment layers and a half-space labeled (n + 1). In each layer the potential function is the sum of an upgoing and a downgoing plane wave (e.g., $\psi_n = A_n \exp(i\ell_n z_n) + B_n \exp(-i\ell_n z_n)$) and in the halfspace the potential function represents a downgoing wave ($\psi_{n+1} = \exp(i\ell_{n+1} z_{n+1})$).

Let P represent the pressure and Q the vertical component of particle velocity. Then start at the interface between layer n and the half-space with the expressions for P and Q that follow. P and Q are easily evaluated at the n/(n+1) interface where $z_{n+1}$ is zero. Because P and Q are continuous functions they have the same values at the bottom of layer n (at $z_n = d_n$) that they have at the top of the half-space (at $z_{n+1} = 0$). Therefore, $A_n$ and $B_n$ can be calculated. From these calculate P and Q at the top of layer n (at $z_n = 0$). Continue working up the layers until $A_o$ and $B_o$ are calculated. The value of R is obtained from $R = B_o/A_o$.

Interface n/(n+1):

$$P = \rho\varphi = \rho_{n+1}\,, \quad Q = (d\varphi/dz) = i\ell_{n+1}$$

Layer n:

$$A_n = 1/2 \exp(-i\ell_n d_n)\,[P/\rho_n + Q/(i\ell_n)]$$

$$B_n = 1/2 \exp(i\ell_n d_n)\,[P/\rho_n - Q/(i\ell_n)]$$

Interface (n−1)/n:

$$P = \rho_n(A_n + B_n)$$

$$Q = i\ell_n(A_n - B_n)$$

Continue until $A_o$ and $B_o$ are calculated

Reflection coefficient: $R = B_o/A_o$

In ocean sediments it is common to find a series of layers of almost constant properties. This model will be a good representation of these cases. In other places thick layers (approximately one wave length) are found with continuous change of properties. This continuous change in this case can be represented by a large number of constant property layers. Later it will be shown there is good agreement between the gradient model and the multilayered model.

## LINEAR GRADIENT MULTILAYER MODEL

We developed another method for modeling the change of sediment properties with depth due to increasing compaction and temperature. In this approach changes in sound speed and density are accounted for by using single or multiple liquid layers where Airy functions can be used to represent the sound energy. This method was first used by Morris (1970) and the use and development of the model has continued (Morris, 1972, 1975). This model is used to explain low values of bottom loss at small grazing angles and low frequency. In this case we will use a somewhat different function $\chi$ so we can account for a density change in the layer. The general wave equation for the case where there is variation in both sound speed and density (Brekhovskikh, 1960) is

$$p = \sqrt{\rho}\chi$$

$$\text{Wave eq.} \qquad \nabla^2 \chi + K^2 \chi = 0$$

where

$$K^2 = (\omega/v)^2 + \frac{1}{2\rho}(d^2\rho/dz^2) - 3/4\left[\frac{1}{\rho}(d\rho/dz)\right]^2$$

If $K^2$ can be represented as a linear function of depth then the potential function $\chi$ can be written as the sum of the Airy functions Ai and Bi. The argument of the Airy functions is defined in terms of the horizontal wave number k, the profile parameters $K_o$ and $\beta$ and the depth z. To add the effect of absorption in the liquid an imaginary term $i\alpha/8.686$ is added to $K_o$.

If

$$K^2 = K_o^2(1+\beta z)$$

then

$$X = A \cdot A_i(\xi) + B \cdot B_i(\xi)$$

where

$$\xi = \frac{k^2 - K_o^2}{(K_o^2\beta)^{2/3}} - \left(K_o^2\beta\right)^{1/3} z$$

To add $\alpha$(dB/unit length) attenuation: $K_o \rightarrow K_o + i\frac{\alpha}{8.686}$

A multilayered model composed of linear $K^2$ and constant K (constant sound speed) layers is shown in Figure 18. We can start at the bottom and work up through the layers using the interface conditions of which the pressure and the vertical component of particle velocity are continuous functions. In this case p, equal to the pressure, is $\sqrt{\rho}\chi$ and Q, equal

to $-i\omega$ times the particle velocity, is $\rho^{-1}\, d(\sqrt{\rho\chi})/dz$. Note that in Figure 18 layer 2 is a constant K layer. The ability to mix linear and constant layers is necessary in a general program because, as the gradient, $\beta$, goes to zero, the argument of the Airy functions increases without limit. Thus, depending on frequency, layer thickness and computer word length, there is a minimum gradient that can be used. Layers with gradients smaller than this must be represented by constant K layers.

## COMPARISON OF THE TWO MODELS

It is instructive to see how these two models, the liquid multilayer and the linear gradient multilayer, compare. To do this, consider Figure 19. On the left hand side our linear model has a sound speed that increases from 1500 m/s at the water/sediment interface to 1800 m/s at a sediment depth of 300 meters, which corresponds to an average sound speed gradient equal to (1800 – 1500) m/s ÷ 300 m, or 1 $s^{-1}$. The constant K model is shown for two layers. The layers have the same thickness and the sound speed at the center of the layers (i.e., at 75 and 225 meters) is set equal to the sound speed of the linear layer at that depth.

On the right hand side of Figure 19 is a diagram that indicates the main physical events. Most of the energy either reflects at the surface or is refracted in the sediment because of the gradient. Morris (1973) has used a ray description to calculate the energy in each path and compare the ray description with the wave model. Of course there are second and higher order effects as indicated by the dashed arrows that are implicit in the wave model.

In Figure 20, the first comparison of the two models is shown. For the calculations we used a frequency of 100 Hz, a density ratio ($\rho$ in sediment)/($\rho$ in water) equal to 2.0 and zero attenuation. The reflection coefficient was calculated for grazing angles from 0 degree to 20 degrees which are of interest in sound propagation. With zero attenuation both models return all sound to the water for these grazing angles so the modulus of R is 1.0 or the bottom loss is zero. Figure 20 shows plots of phase, i.e., the argument of R, for different cases. The curve marked L is for the linear $K^2$ model, while the curves labeled 1, 3 or 10 correspond to 1, 3 or 10 constant K layers. The 10 layer case has a layer thickness of 30 meters, which is equal to 2 wavelengths in the water. For 30 layers (or a thickness of 0.67 $\lambda_w$) there is a maximum phase difference of 2.2 degrees at a grazing angle of 3.5 degrees which cannot be plotted on this scale. For 100 layers there is a maximum phase difference of 0.2 degrees.

In Figure 21 the same models are used except that there is an attenuation of 0.05 dB/m in both models. As in the previous case, the 10 layer model (thickness = 2 $\lambda_w$) has a maximum difference of ~10 degrees and the 30 layer model has essentially the phase as the linear model. It is interesting to note that the attenuation has slowed the phase change considerably. This will have a noticeable effect on the wave theory propagation models where a shift in phase of 360 degrees will add a new mode to the sound field (Bucker, 1964).

To complete the comparison of the linear and constant layers, the bottom loss curves are shown in Figure 22. The one layer case has much less bottom loss because the sound speed is equal to the sound speed of the linear model at 150 meter depth, which is 1629.6 m/s and corresponds to a critical angle greater than 20 degrees.

## SOLID MULTILAYER MODEL

Sediments have rigidity and for more accurate model calculations rigidity must be taken into account. An isotropic sediment layer can be described by three sediment parameters: the density $\rho$ and the two Lamé constants, $\lambda$ and $\mu$ (Ewing, Jardetsky, and Press, 1957). The density can be measured directly but $\lambda$ and $\mu$ are determined by the speed and attenuation of the compressional and shear waves that travel in the sediment. The sediment and acoustic parameters are related (Bucker et al, 1965) as follows

Sediment Parameters

$\rho$ , $\underbrace{\lambda , \mu}$

Lamé constants

Acoustic Parameters

$c_p$ = sound speed (compressional wave)

$c_s$ = sound speed (shear wave)

$a_p$ = attenuation, dB/unit length (compressional)

$a_s$ = attenuation, dB/unit length (shear)

Constitutive Equations

$$\lambda + 2\mu = \rho \left(x_p^2 - y_p^2 - i2x_p y_p\right) / \left(x_p^2 + y_p^2\right)^2$$

$$\mu = \rho \left(x_s^2 - y_s^2 - i2x_s y_s\right) / \left(x_s^2 + y_s^2\right)^2$$

where, $x_p = 1/c_p$ , $y_p = a_p/(8.686\omega)$

$x_s = 1/c_s$ , $y_s = a_s/(8.686\omega)$

There are several approaches to the problem of modeling the sediment layers when there are significant changes of the sediment properties with depth. Gupta (1966a, 1966b) has developed closed solutions for the case where the compressional and shear velocity varies linearly with depth while the density remains constant. More general variations can be treated with the propagator method developed by Gilbert and Backus (1966). One problem of the propagator method is loss of accuracy when sediment penetration of many wavelengths occurs. In our most recent programs we have chosen to model the variable sediment properties with many layers and to maintain accuracy by use of Knopoff's formulation (Knopoff, 1964).

The multilayer solid model is substantially more difficult than the multilayer liquid model for two reasons. First, there are twice as many waves (shear waves as well as compressional waves) and twice as many interface conditions (continuity of horizontal components of stress and strain, as well as continuity of vertical components of stress and strain). Second, you cannot start at the bottom and work to the top. All of the layers have to be considered as a group. The situation is shown in Figure 23. There are an upgoing and a downgoing compressional wave in the water, an upgoing and a downgoing

compressional wave and an upgoing and a downgoing shear wave in each solid layer and downgoing compressional and shear waves in the bottom half-space. We can arbitrarily set the coefficient $A_{n+1} = 1$, as shown, so that there are $4n + 3$ unknown coefficients $(A_0, B_0, A_1, B_1, C_1, \ldots, C_{n+1})$, where n is the number of layers. There are also $4n + 3$ interface conditions. Three conditions at the first interface (continuity of vertical components of stress and strain and zero horizontal stress) and four conditions at all other interfaces (continuity of vertical and horizontal stress and strain). Since the interface conditions can be written as a set of linear homogeneous algebraic equations, the solution can be done using standard matrix inversion algorithms. This is not a practical method of solution when n is large because it is necessary to invert a matrix of $(4n + 3)^2$ elements and because of loss of accuracy problems. The number of terms in the problem can be kept under control by using transfer matrices that move the stress and strain at one interface of a layer to the other interface. This method was developed by Thomson (1950). To solve the problem of sound transmission through plates, Bucker (Bucker et al, 1965) extended the method to include wave attenuation for the problem of bottom reflection. A serious drawback of the transfer matrix method is that it also suffers from loss of accuracy.

Fortunately, the accuracy problems can be solved using methods developed by the geophysicists for earthquake problems (Thrower, 1965; Dunkin, 1965; Watson, 1970; Schwab, 1970). For a layered structure of the same form that we have for the bottom reflection problem, there are natural vibrations at frequencies corresponding to zeroes of a determinant, $|\Delta_R|$, called the Rayleigh determinant. The geophysicists have developed very fast and accurate methods for calculating $|\Delta_R|$. We show that the reflection coefficient can be written as $R = (\rho_1 r_{\alpha 0} |\Delta_R| - \rho_0 |\Delta_S|)/(\rho_1 r_{\alpha 0} |\Delta_R| + \rho_0 |\Delta_S|)$, where $|\Delta_S|$ is the same as $|\Delta_R|$ except for row 1. Thus, the sophisticated methods of the geophysicists can be used to solve our problem. We do have to generalize the equations to account for attenuation which is neglected at earthquake frequencies.

## CALCULATION OF R FOR MANY SOLID LAYERS USING KNOPOFF'S METHOD

The standard methods of solution are not usable for the solid multilayer model because of accuracy, computer storage and computer run time problems. Fast and accurate methods developed in earth wave problems can be modified for calculation of R, in particular, the fast algorithm of Schwab (1970), which is based on Knopoff's formulation (Knopoff, 1964). The method has been adapted to our solid multilayer model by Bucker (Bucker and Morris, 1975). The notation used here is that of Haskell (1953).

The upgoing and downgoing compressional waves in a liquid layer or liquid half-space can be represented by the potential function

$$\phi_n = \frac{1}{\omega} [i A_n \cos p_n + B_n \sin p_n] \exp[i(\omega t - kx)] ,$$

where

$$p_n = k r_{\alpha n} z_n .$$

Also, choose the potential function representing the upgoing and downgoing shear waves in a solid layer or solid half-space to be

$$\psi_n = \frac{1}{\psi} [C_n \sin q_n + i D_n \cos q_n] \exp[i(\omega t - kx)] ,$$

where

$$q_n = k\, r_{\beta n}\, z_n .$$

The components of motion and stress in the $n^{th}$ layer are, therefore,

$$c\dot{U}_n = A_n \cos p_n - i B_n \sin p_n + r_{\beta n} C_n \cos q_n - i r_{\beta n} D_n \sin q_n ,$$

$$c\dot{W}_n = -i r_{\alpha n} A_n \sin p_n + r_{\alpha n} B_n \cos p_n + i C_n \sin q_n - D_n \cos q_n ,$$

$$\sigma_n = \rho_n(\gamma_n - 1) A_n \cos p_n - i \rho_n(\gamma_n - 1) B_n \sin p_n$$

$$+ \rho_n \gamma_n r_{\beta n} C_n \cos q_n - i \rho_n \gamma_n r_{\beta n} D_n \sin q_n ,$$

$$\tau_n = i \rho_n \gamma_n r_{\alpha n} A_n \sin p_n - \rho_n \gamma_n r_{\alpha n} B_n \cos p_n$$

$$- i \rho_n(\gamma_n - 1) C_n \sin q_n + \rho_n(\gamma_n - 1) D_n \cos q_n .$$

In the above, c is the horizontal phase velocity ($c = \omega/k$), $\dot{U}_n$ and $\dot{W}_n$ are the horizontal and vertical components of particle velocity, $\sigma_n$ is the normal (vertical) stress and $\tau_n$ is the tangential (horizontal) stress.

By separating $\phi_0$ into an incident and reflected wave it is easy to show that the plane wave reflection coefficient R is given by

$$R = (A_0 - B_0)/A_0 + B_0) .$$

For convenience set the value of $A_0 \equiv 1$. The three interface conditions at the water/sediment layer 1 interface can be written as

$$r_{\alpha 0} B_0 = r_{\alpha 1} B_1 - D_1 \qquad \text{(continuation of } \dot{W}\text{)}$$

$$-\rho_0 = \rho_1(\gamma_1 - 1) A_1 + \rho_1 \gamma_1 r_{\beta 1} C_1 \qquad \text{(continuation of } \sigma\text{)}$$

$$0 = -\rho_1 \gamma_1 r_{\alpha 1} B_1 + \rho_1(\gamma_1 - 1) D_1 \qquad \text{(continuation of } \tau\text{)}$$

Divide the last two above equations by $\rho_1$ and form the matrix of coefficients of $B_0$, $A_1$, $B_1$, $C_1$, $D_1$

| $B_0$ | $A_1$ | $B_1$ | $C_1$ | $D_1$ | |
|---|---|---|---|---|---|
| $r_{\alpha 0}$ | 0 | $-r_{\alpha 1}$ | 0 | 1 | = 0 |
| 0 | $(\gamma_1 - 1)$ | 0 | $\gamma_1 r_{\beta 1}$ | 0 | $= -\rho_0/\rho_1$ |
| 0 | 0 | $-\gamma_1 r_{\alpha 1}$ | 0 | $(\gamma_1 - 1)$ | = 0 |

Now modify the basis vectors so that the interface conditions can be within in the following matrix form

$$\begin{bmatrix} 1 & 0 & -1 & 0 & +1 \\ 0 & (\gamma_1-1) & 0 & \gamma_1 & 0 \\ 0 & 0 & -\gamma_1 & 0 & (\gamma_1-1) \end{bmatrix} \times \begin{bmatrix} B_0\, r_{\alpha 0} \\ A_1 \\ B_1\, r_{\alpha 1} \\ C_1\, r_{\beta 1} \\ D_1 \\ A_2 \end{bmatrix} = \begin{bmatrix} 0 \\ -\rho_0/\rho_1 \\ 0 \\ 0 \\ 0 \\ 0 \end{bmatrix}$$

Now solve for $B_0$ using Cramer's Rule

$$B_0\, r_{\alpha 0} = \frac{\begin{vmatrix} 0 & 0 & -1 & 0 & +1 \\ -\rho_0/\rho_1 & & & & \\ 0 & & \Delta_R & & \\ 0 & & & & \end{vmatrix}}{\begin{vmatrix} 1 & 0 & -1 & 0 & +1 \\ 0 & & & & \\ 0 & & \Delta_R & & \\ 0 & & & & \end{vmatrix}}$$

The elements inside the dashed areas designated $\Delta_R$ are the elements of the Rayleigh determinant. Fast and accurate methods are finding $|\Delta_R|$ have been developed (as mentioned before) because the zeroes of $|\Delta_R|$ determine the phase velocity of earthquake waves. Finally, we can write

$$\frac{B_0\, r_{\alpha 0}}{(\rho_0/\rho_1)} = \frac{\begin{vmatrix} 0 & -1 & 0 & 1 \\ 0 & -\gamma_1 & 0 & (\gamma_1-1) \end{vmatrix}}{\begin{vmatrix} \gamma_1-1 & 0 & \gamma_1 & 0 \\ 0 & -\gamma_1 & 0 & (\gamma_1-1) \end{vmatrix}} = \frac{|\Delta_S|}{|\Delta_R|}$$

In the above $|\Delta_R|$ is the Rayleigh determinant and $|\Delta_S|$ is the same except for the first row. The fast methods developed for calculation of $|\Delta_R|$ can be used to evaluate $|\Delta_S|$. It follows then that the plane wave reflection coefficient can be written as

$$R = (\rho_1\, r_{\alpha 0}\, |\Delta_R| - \rho_0\, |\Delta_S|)/(\rho_1\, r_{\alpha 0}\, |\Delta_R| + \rho_0\, |\Delta_S|) \ .$$

## COMPARISON OF MULTILAYER SOLID AND LIQUID MODELS

In Figure 24 is a plot of bottom loss for a model of 100 layers. The curve labeled L is for the liquid layer model (it is also the bottom loss curve for the linear model). The other curves are for a 100 layer solid model with different values of rigidity. For r = 0 the curve is quite similar to the liquid model except that there is slightly more loss due to some conversion of compressional waves into shear waves. As the rigidity increases there are lower losses than the liquid model at very small grazing angles and higher losses than the liquid model at larger grazing angles. Most likely the propagation to long ranges would be better for the r = 0.1 curve than for the liquid model.

## EFFECT OF BOTTOM INTERACTION ON THE SOUND FIELD

In this section, a sample case is analyzed where the bottom affects the sound field. The first step is a ray theory calculation in which the most significant (i.e., with the least propagation loss) eigenrays are identified. An eigenray is a ray that travels from the source to the receiver. If the significant eigenrays do not reflect from the bottom then there is no bottom interaction problem unless the frequencies are very low, e.g., $< 20$ Hz. In many cases the significant eigenrays do have bottom reflections and the ray tracing program can be used to determine the grazing angle of the rays when they reflect at the bottom, $\gamma_b$.

The next step in the analysis is the calculation of a three-dimensional bottom loss surface as shown in Figure 25. Table 3 lists the parameters used for this particular calculation. The values are typical of the deep ocean and are representative of properties provided by E. L. Hamilton's geoacoustic models. Bottom loss is plotted as a function of grazing angle of the ray on the bottom, $\gamma_b$, and frequency. To understand Figure 25, it is useful to consider Figure 26. On the left several sound speeds are plotted as a function of depth. Here $c_w$ is the sound speed in water, $c_1$ and $c_2$ are the sound speeds at the top and bottom of the upper sediment layers, and $c_s$ and $c_p$ are the shear speed and the compressional speed in the basement.

A typical ray path is shown on the right side of the figure. We can follow the path of a ray using Snell's law,

$$\frac{c(z)}{\cos(\gamma)} = c_h = \text{constant} .$$

In Snell's law (c(z) is the sound speed at depth z, $\gamma$ is the grazing angle of the ray at depth z and $c_h$) the horizontal phase speed of the ray is a constant for any given ray. Using Snell's law, $c_h$ can be determined by $c_h = c_w/\cos\gamma_b$ and the depth at which the refracted ray becomes horizontal, i.e., at the depth at which $c(z) = c_h$. Figure 26 shows the refracted ray turning over in the upper sediment layers so $c_h < c_2$ because the ray with $c_h = c_2$ will become horizontal at the interface between the upper sediment layers and the basement. The Stoneley wave can exist at the interface between the upper sediment layers and the basement when excited by waves which have a certain relationship between frequency and horizontal phase speed. This relation is called a dispersion equation. The high losses at low frequency and low grazing angles are caused by a coupling of energy from

the refracted ray into the Stoneley wave. This effect has been previously described by Hawker, Focke and Anderson (1977).

There is almost no loss when $c_h = c_s$ (i.e. $\gamma_b \approx 54°$) and when $c_h = c_p$ (i.e., $\gamma_b \approx 74°$) (see Figure 25). Between these two angles the loss increases because of shear wave generation in the basement. Otherwise the bottom loss is mostly due to absorption of energy from the refracted ray. This loss increases, in general, with frequency. This effect is apparent in Figure 25 at frequencies above 50 Hz. There is also an interference effect that causes the bottom loss surface to be wavy. This is caused by the coherent addition of the refracted and reflected rays.

It is clear that bottom interaction is somewhat complicated at low frequencies. However, by considering the fundamental physical processes that are responsible for the bottom interaction the total sound propagation field can be determined.

## EQUIVALENT SEDIMENT LAYERS FOR USE WITH THE P.E. MODEL

In previous sections it is shown how the bottom reflection coefficient R is incorporated in the propagation models. In the normal mode formalism, the use of R results in an exact solution. In the case of ray theory, a slight error is introduced by the use of a plane wave coefficient when a spherical coefficient is called for. However, the error is negligible at frequencies above ~ 100 Hz. When there are appreciable horizontal changes in the sound speed or bathymetry we must use either perturbation solutions of wave theory or the P.E. (Parabolic Equation) model. At the present time almost all efforts in model development center around the P.E. model. This is due probably to the simplicity of the P.E. method and the early development work by the Acoustic Environmental Support Detachment (AESD).

As do most acoustic propagation algorithms, the P.E. model starts with the reduced wave equation

$$\nabla^2 \psi + K^2 \psi = 0 \ ,$$

where $K^2$ has been defined before and $\psi$ is the potential function. The first step in the solution is to assume a product form for $\psi$ in which one term contains the range variation that would occur if there were no horizontal changes and the other term represents the depth (z) dependence of $\psi$ plus a small range dependence due mostly to horizontal changes. That is,

$$\psi(r,z) = U(r,z)\, H_o^{\,1}\,(k_o r) \ ,$$

where $H_o^{\,1}(k_o r)$ is a Hankel function of the first type and order zero and $k_o$ is a separation constant. Substitution of the above form of $\psi$ into the wave equation results in the following second order partial differential equation.

$$\frac{\partial^2 U}{\partial r^2} - i\,2\,k_o \frac{\partial U}{\partial r} + \frac{\partial^2 U}{\partial z^2} + \left(K^2 - k_o^{\,2}\right) U = 0 \ .$$

Leontovich and Fock (1946) have shown that if the term $\partial^2 U/\partial r^2$ can be neglected, a marching solution to the resulting Parabolic Equation can be written in the following form

$$U(r+\Delta r,z) = \exp\left[-i\,\Delta r\left(K^2 - k_o^2\right)/2\right]$$

$$\left\{\exp\left[(i\,\Delta r/2\,k_o)\,\partial^2/\partial z^2\right]\right\}_{op} U(r,z) \ .$$

Using results that they had developed for electromagnetic propagation problems associated with the SAFEGUARD ABM program, Tappert (1977) was able to show that the exponential operator acting on U could be calculated using a discrete Fourier transform F.

$$\left\{\ \right\}_{op} U(r,z) = F^{-1}\left\{\exp\left[-i\,\Delta r s^2/(2\,k_o)\right]\ F\,U(r,z)\right\} \ ,$$

where s is an index of F, and $F^{-1}$ is the inverse transform. Because there are fast forms of the discrete Fourier transform available, the P.E. model has proved to be a reasonably efficient method for calculating the sound field for non-bottom limited cases.

In bottom limited cases the P.E. method runs into serious difficulties. The sound pressure is continuous across the interface between the water and the sediment. However, the density is discontinuous since the sediment density usually is at 20 to 100 percent greater than that of water. Since $U = \rho^{1/2}\,p$, where $\rho$ is the density and p is the pressure, U is discontinuous. This leads to the well known Gibb's phenomenon in which oscillations are generated by taking the Fourier transform of a discontinuous function (Figure 27). To avoid Gibb's phenomenon it is necessary to replace an accurate representation of the bottom sediments by one in which $K^2$ and $\rho$ have minimum variation with z but which also is consistent with the value of bottom loss that is calculated for the realistic sediment model, Figure 28. The filled circles in Figure 29 represent the correct values of $|R|$. We want to generate an equivalent sediment model that has smooth $K^2$ and also has the bottom loss shown in Figure 29.

This is done with a simple algorithm as shown in Figure 30. The symbol x represents either the real part of $K^2$, the imaginary part of $K^2$ or the density. A change $\Delta x$ is made and the least mean square error of the difference, E, between the desired curve and the calculated bottom loss curve is calculated. If E is reduced by a change in $+\Delta x$ or $-\Delta x$ then $\pm\Delta x$ is increased. If the calculated E is larger, then x and E remain the same but $\Delta x$ is reduced for the next iteration.

The final results are shown in Figure 31 where there is good agreement between the the bottom loss for the equivalent sediment mode (the line) and the desired bottom loss (the filled circles).

## SUMMARY

We have developed a general purpose plane wave reflection model that can account for both liquid and/or solid layers. Earlier models which we developed, such as the solid model and the linear gradient model, contributed and laid the basis for our most recent

work. The present solid multilayer program models the variable sediment properties with many layers (up to 1000 layers or more, if necessary) and maintains the accuracy needed for efficient computer calculation. Important physical parameters used in the model are the speed and attenuation of both the compressional and shear waves that travel in the sediment. The many constant layers are used to approximate the results of a linear gradient concept.

The solid multilayer model should be satisfactory as the coupling mechanism between the sediment parameters and the calculations of the acoustic field. The model includes all physical factors except for roughness which usually is not important at low frequencies. This model, based on wave theory, is interfaced very easily with most sound propagation normal mode programs.

In addition, a so-called equivalent bottom concept has been developed for the Parabolic Equation propagation program. This technique should enable the P.E. program to be used for bottom limited areas.

The geoacoustic model discussed in Part I, which presents sediment properties, is an essential input to the bottom loss model. We recommend that when geoacoustic information is available, the principal method of analyzing bottom interaction and making predictions should be through the sediment models. The predictions should be supplemented when possible by careful direct measurements of bottom loss.

## REFERENCES

## (PART II)


Brekhovskikh, L. M., 1960, Waves in Layered Media, English translation, Academic Press, New York, p 171.

Bucker, H. P., 1964, Normal mode propagation in shallow water, Journal of the Acoustical Society of America, Vol. 36, pp 251-258.

Bucker, H. P., Whitney, J. A., Yee, G. S., and Gardner, R. R., 1965, Reflection of low frequency sonar signals from a smooth ocean bottom, Journal of the Acoustical Society of America, Vol. 37, pp 1037-1051.

Bucker, H. P., 1970, Sound propagation in a channel with lossy boundaries, Journal of the Acoustical Society of America, Vol. 48, pp 1187-1194.

Bucker, H. P. and Morris, H. E., 1975, Reflection of sound from a layered ocean bottom, invited paper presented at Oceanic Acoustic Modelling Conference at SACLANTCEN on 8-11 September 1975, pp 19-1 to 19-35 in SACLANTCEN Conference Proceedings No. 17, 15 October 1975.

Dunkin, J. W., 1965, Computation of modal solutions in layered elastic media at high frequencies, Bulletin of the Seismological Society of America, Vol. 55, pp 335-358.

Ewing, W. M., Jardetsky, W. S., and Press, Frank, 1957, Elastic Waves in Layered Media, pp 79-83, McGraw-Hill Book Company, New York.

Gilbert, Freeman and Backus, G. E., 1966, Propagator matrices in elastic wave and vibration problems, Geophysics, Vol. 31, pp 326-332.

Gupta, R. N., 1966a, Reflection of sound waves from transition layers, Journal of the Acoustical Society of America, Vol. 39, pp 255-260.

Gupta, R. N., 1966b, Reflection of elastic waves from a linear transition layer, Bulletin of the Seismological Society of America, Vol. 56, pp 511-526.

Haskell, N. A., 1953, The dispersion of surface waves in multilayered media, Bulletin of the Seismological Society of America, Vol. 43, p 17.

Hawker, K. E., Focke, K. C., and Anderson, A. L., 1977, A sensitivity study of underwater sound propagation loss and bottom loss. ARL-TR-77-17.

Leontovich, M. A. and Fock, V. A., 1946, Journal of Physics (USSR), Vol. 10, pp 13-24.

Knopoff, L., 1964, A matrix method for elastic wave problems, Bulletin of the Seismological Society of America, Vol. 54, pp 431-438.

Morris, H. E., 1970, Bottom reflection loss model with a velocity gradient, Journal of the Acoustical Society of America, Vol. 48, pp 1198-1202.

Morris, H. E., 1972, Comparison of calculated and experimental bottom reflection losses in the North Pacific, Naval Undersea Center TP 327.

Morris, H. E., 1973, Ray and wave solutions for bottom reflection for linear sediment layers, Journal of the Acoustical Society of America, Vol. 53, p 323 (A).

Morris, H. E., 1975, Bottom reflection model validation with measured data from FASOR III stations in the Pacific and Indian oceans, Naval Undersea Center TP 460.

Schwab, Fred, 1970, Surface-wave dispersion computations: Knopoff's method, Bulletin of the Seismological Society of America, Vol. 60, pp 1491-1520.

Tappert, F., 1973, Unpublished notes and abstracts of talks given at 8th International Congress on Acoustics 1974 and SIAM meeting, SIAM Review, Vol. 15, pp 423.

Tappert, F. D., 1977, The parabolic approximation method, in Lecture Notes in Physics, No. 71, edited by J. B. Keller and J. Papadakis, Springer-Verlag, New York.

Thomson, W. T., 1950, Transmission of elastic waves through a stratified solid medium, Journal of Applied Physics, Vol. 21, pp 89-93.

Thrower, E. N., 1965, The computation of dispersion of elastic waves in layered media, Journal of Sound and Vibration, Vol. 2, pp 210-226.

Watson, T. H., 1970, A note on fast computation of Rayleigh wave dispersion in the multilayered half-space, Bulletin of Seismological Society of America, Vol. 60, pp 161-166.

Table 3. Input parameters to the solid multilayer program. Corresponding bottom loss values are shown in figure 25.

(Units in meters, m/s, g/cm$^3$)

| Layer N | Layer Thickness | Depth $Z_b$ | Density $\rho$ | Re ($\lambda$) | Im ($\lambda$) | Rigidity | Im ($\mu$) | Sound Speed Compressional Wave | Attenuation Compressional Wave | Sound Speed Shear | Attenuation Shear |
|---|---|---|---|---|---|---|---|---|---|---|---|
| Water | | | 1.053 | | | | | 1540.0 | | | |
| 1 | 10.00 | 10.00 | 1.270 | .2983 + 07 | -.1173 + 05 | .0000 | .1759 + 05 | 1532.60 | .1400 - 02 | 166.44 | .3279 + 01 |
| 2 | 10.00 | 20.00 | 1.270 | .3030 + 07 | -.1201 + 05 | .0000 | .1801 + 05 | 1544.60 | .1400 - 02 | 168.40 | .3241 + 01 |
| 3 | 10.00 | 30.00 | 1.270 | .3077 + 07 | -.1229 + 05 | .0000 | .1843 + 05 | 1556.60 | .1400 - 02 | 170.37 | .3203 + 01 |
| 4 | 10.00 | 40.00 | 1.270 | .3125 + 07 | -.1257 + 05 | .0000 | .1886 + 05 | 1568.60 | .1400 - 02 | 172.34 | .3167 + 01 |
| 5 | 10.00 | 50.00 | 1.270 | .3173 + 07 | -.1286 + 05 | .0000 | .1930 + 05 | 1580.60 | .1400 - 02 | 174.32 | .3131 + 01 |
| 6 | 10.00 | 60.00 | 1.270 | .3221 + 07 | -.1316 + 05 | .0000 | .1974 + 05 | 1592.60 | .1400 - 02 | 176.31 | .3095 + 01 |
| 7 | 10.00 | 70.00 | 1.270 | .3270 + 07 | -.1346 + 05 | .0000 | .2019 + 05 | 1604.60 | .1400 - 02 | 178.31 | .3061 + 01 |
| 8 | 10.00 | 80.00 | 1.270 | .3319 + 07 | -.1376 + 05 | .0000 | .2065 + 05 | 1616.60 | .1400 - 02 | 180.31 | .3027 + 01 |
| 9 | 10.00 | 90.00 | 1.270 | .3368 + 07 | -.1407 + 05 | .0000 | .2111 + 05 | 1628.60 | .1400 - 02 | 182.32 | .2993 + 01 |
| 10 | 10.00 | 100.00 | 1.270 | .3418 + 07 | -.1439 + 05 | .0000 | .2158 + 05 | 1640.60 | .1400 - 02 | 184.34 | .2961 + 01 |
| 11 | .00 | 100.00 | 2.600 | .4673 + 08 | .0000 | .4039 | .0000 | 5700.00 | .0000 | 2694.24 | .0000 |

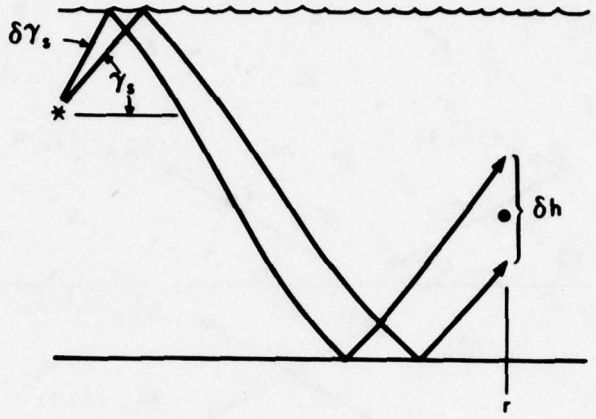



Figure 15. Ray theory representation (high frequency).

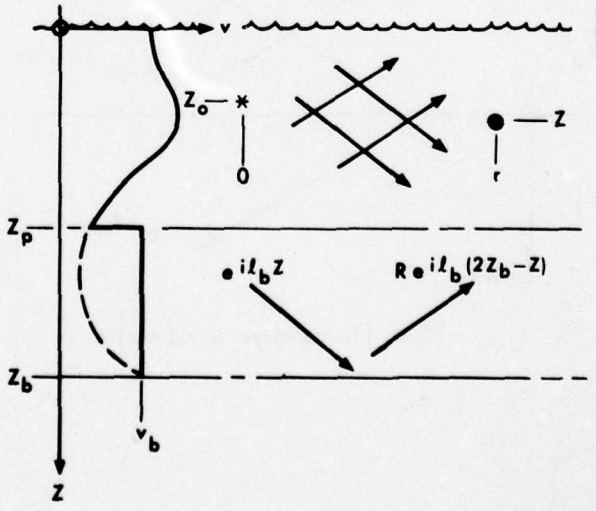



Figure 16. Wave theory representation (low frequency).

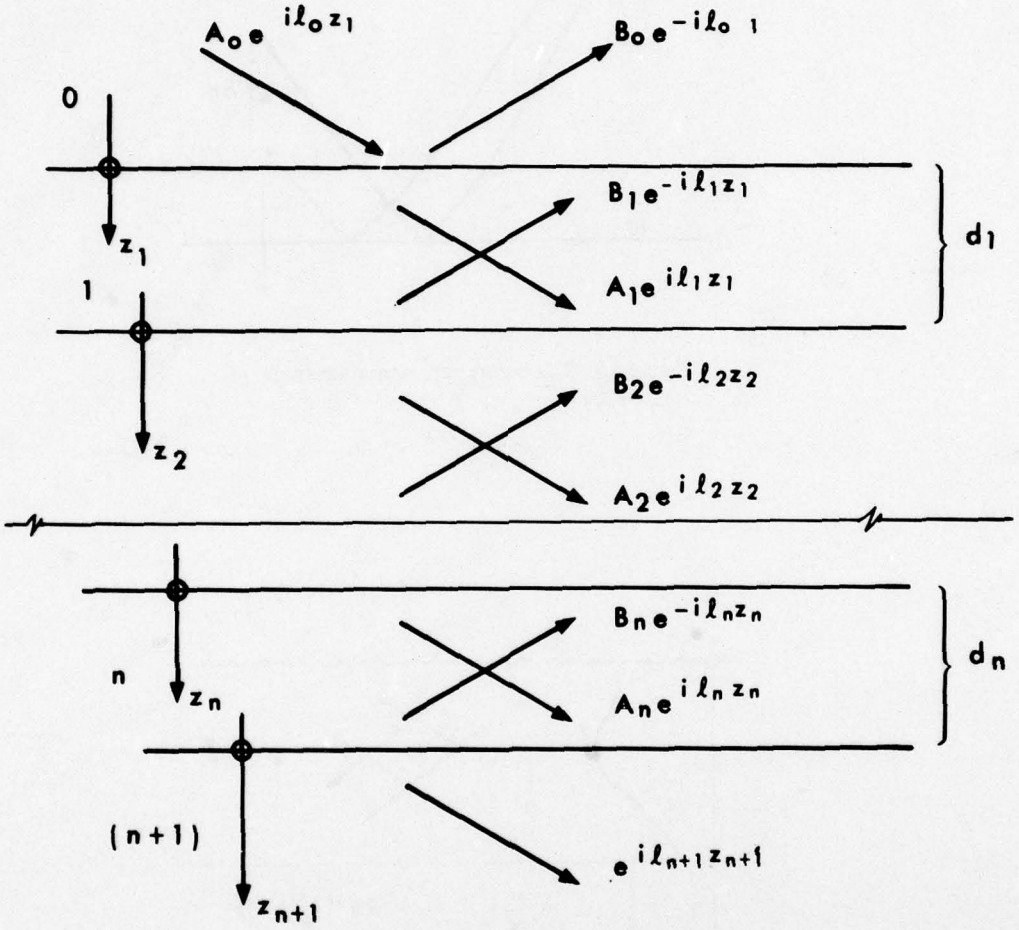



Figure 17. Multilayer liquid model.

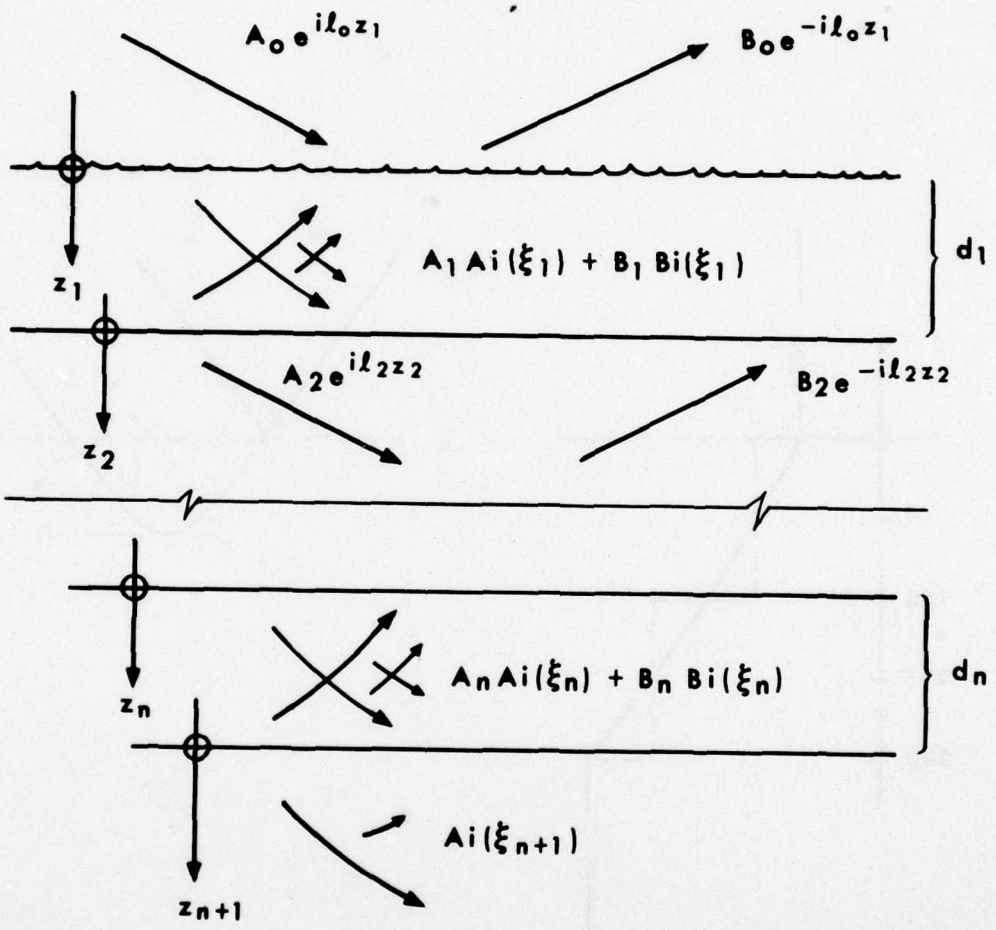



Figure 18. Multilayer linear liquid model.

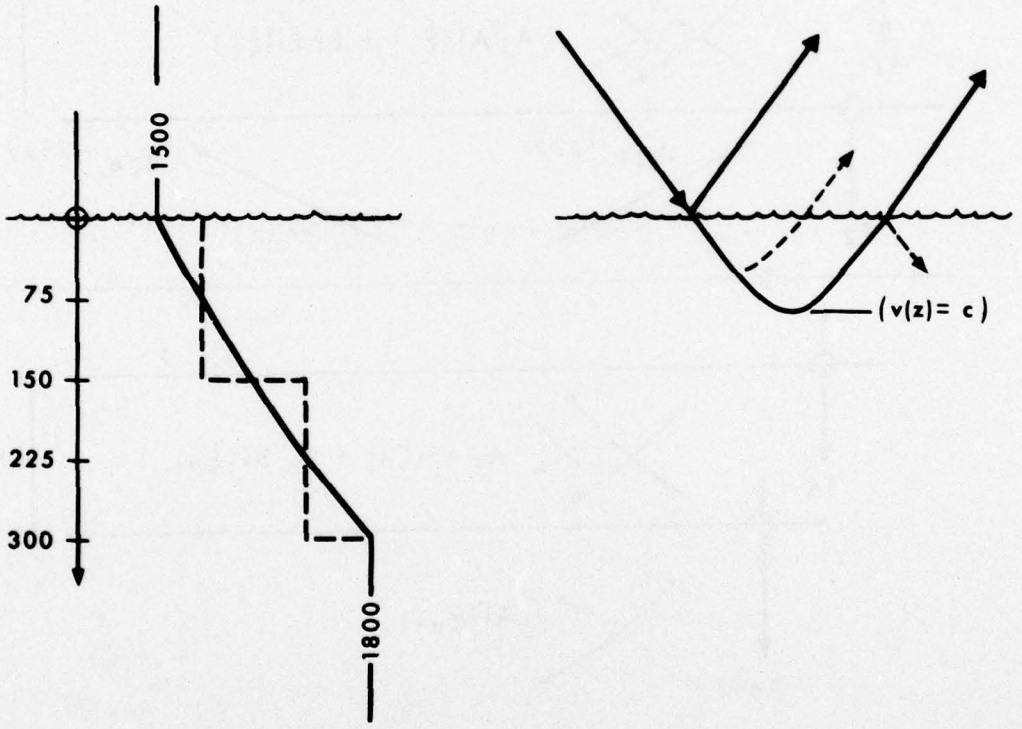



Figure 19. Linear $K^2$ and constant K layers. The diagram on the right indicates the main physical events where the energy reflects at the surface or is refracted in the sediment.

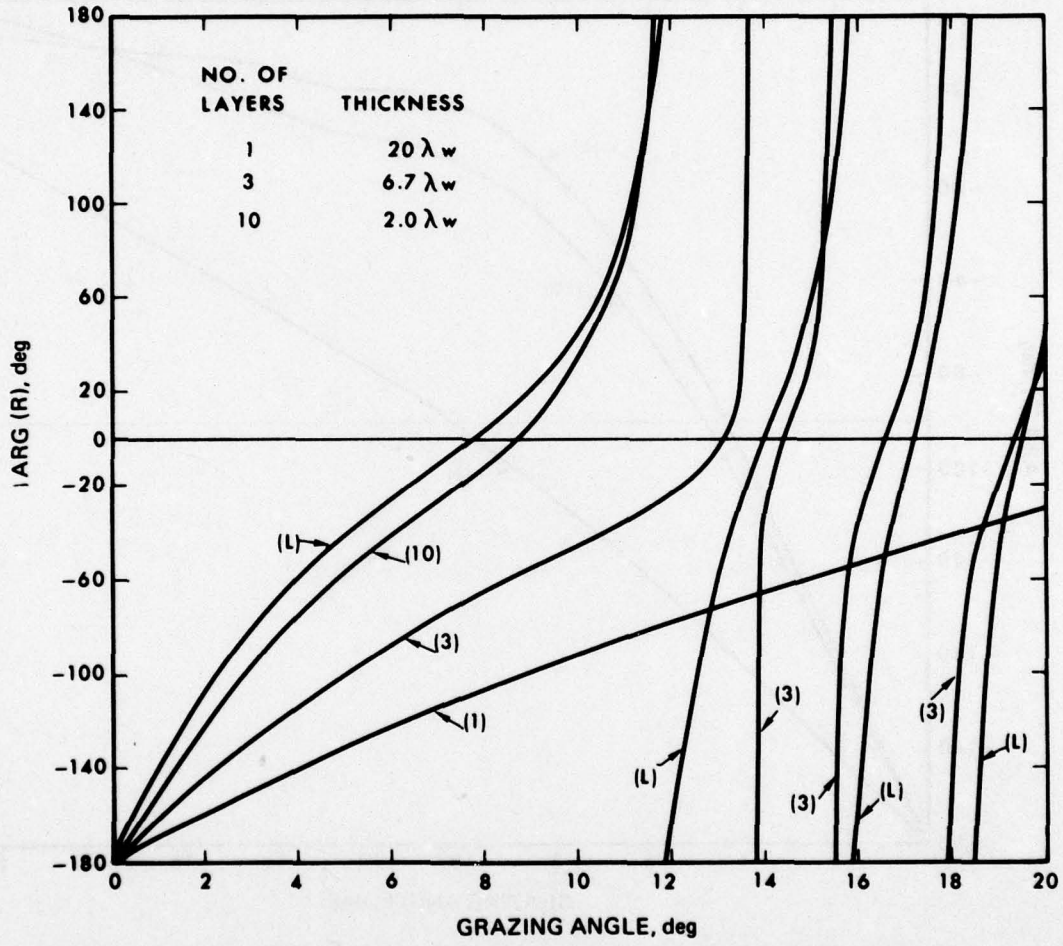



Figure 20. Phase comparison for linear $K^2$ and constant K models (zero attenuation for both models). The curve marked L is for the linear $K^2$ model, while the curves labeled 1, 3 or 10 correspond to constant K layers.

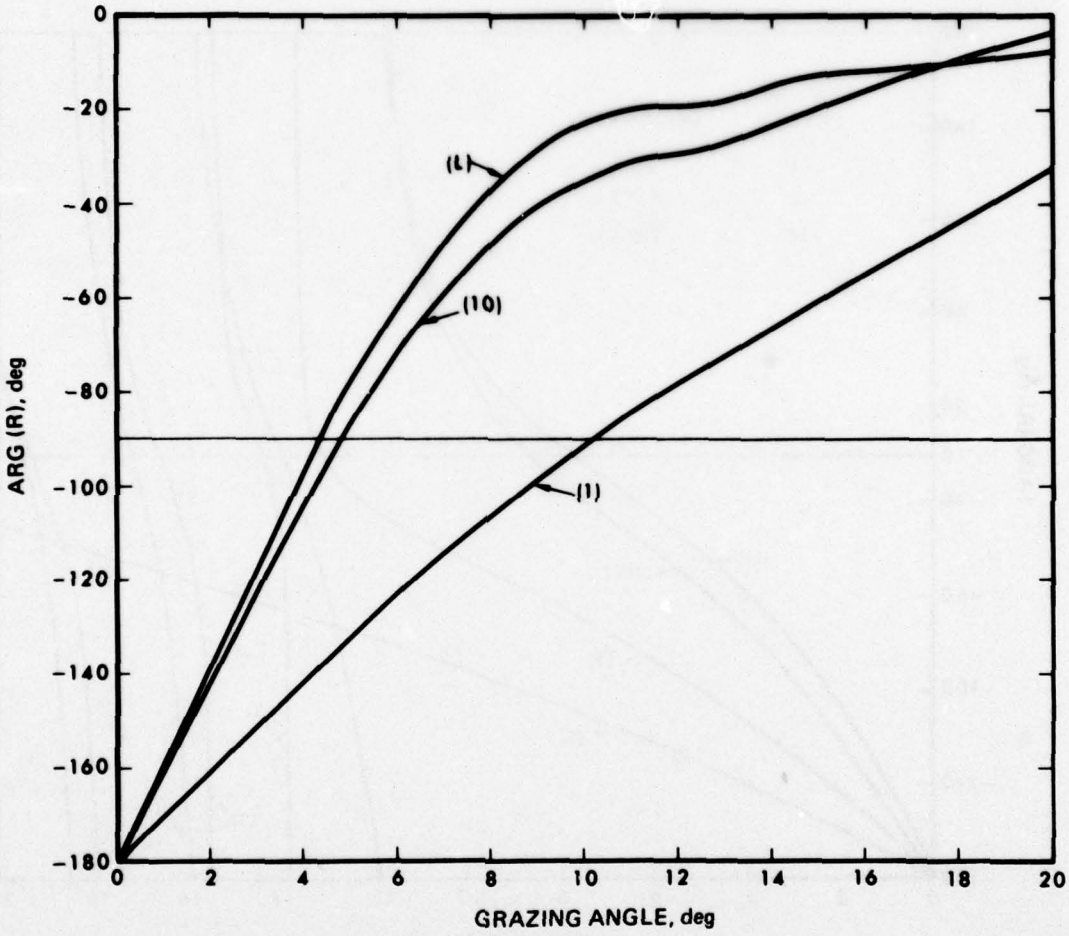



Figure 21. Phase comparison for linear $K^2$ and constant K models using 0.05 dB/m attenuation for both models.

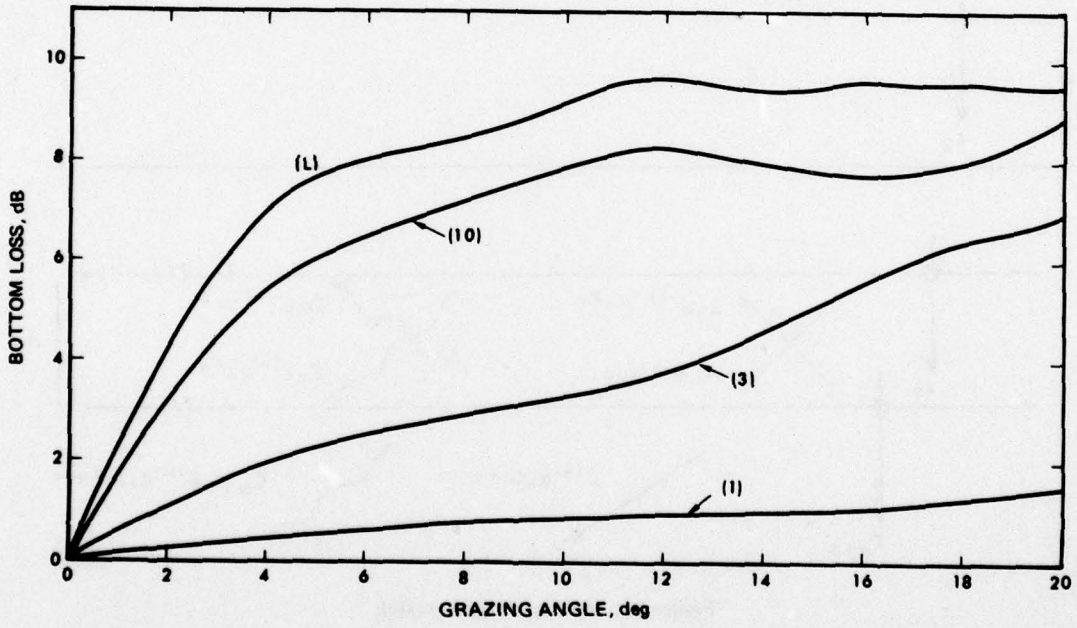



Figure 22. Bottom loss comparison for linear $K^2$ and constant K models using 0.05 dB/m attenuation for both models.

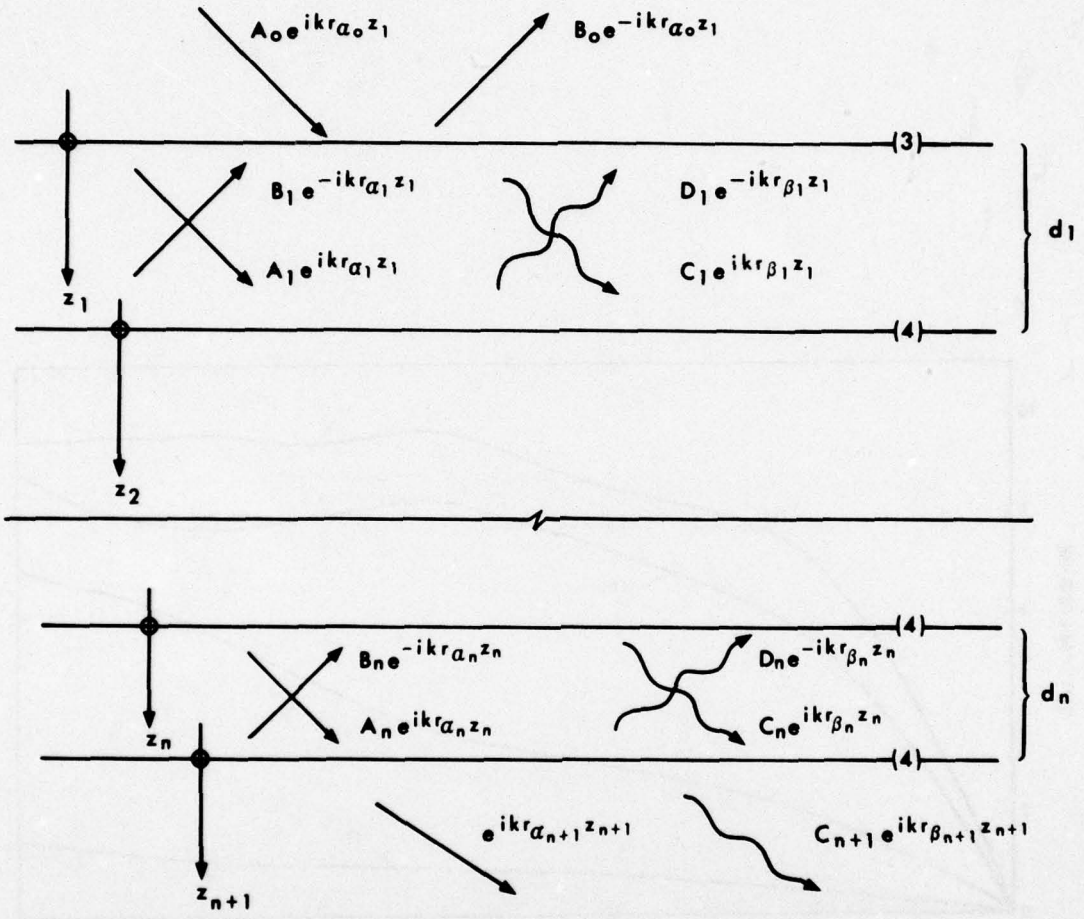



Figure 23. Multilayer solid model.

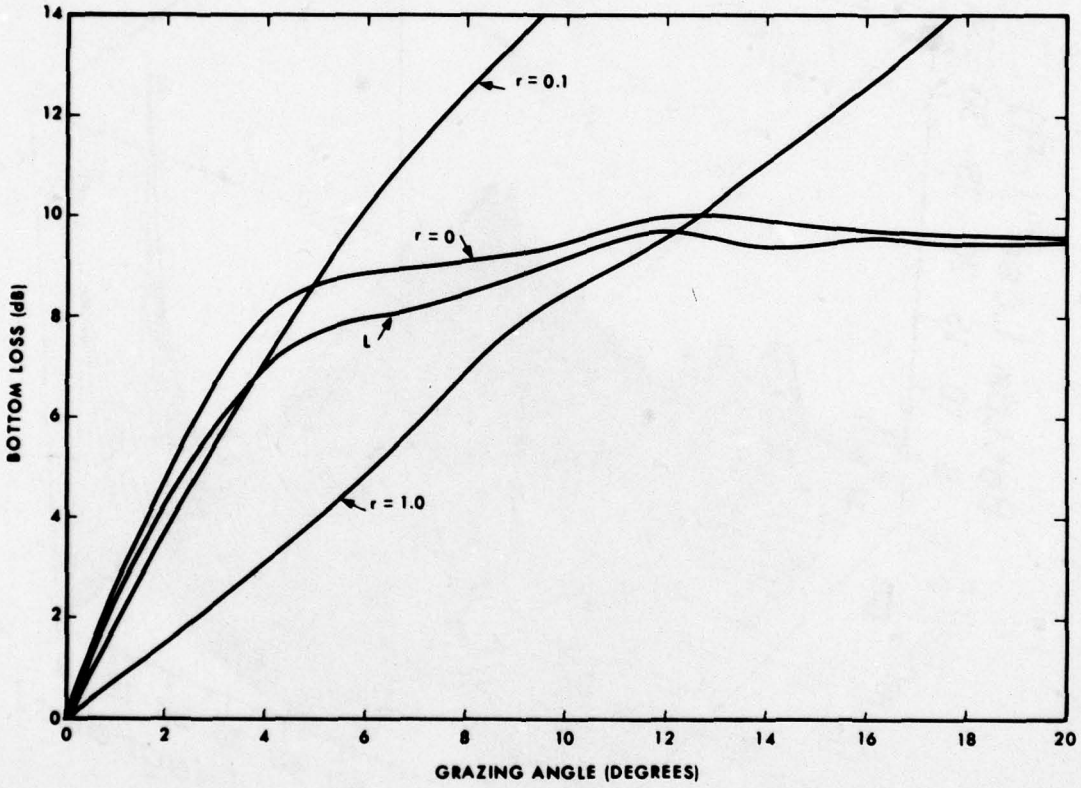



Figure 24. Comparison of multilayer solid and liquid models. L represents the bottom loss for the linear and its liquid layer models. The other curves are for a 100 layer solid model with different values of rigidity, r.

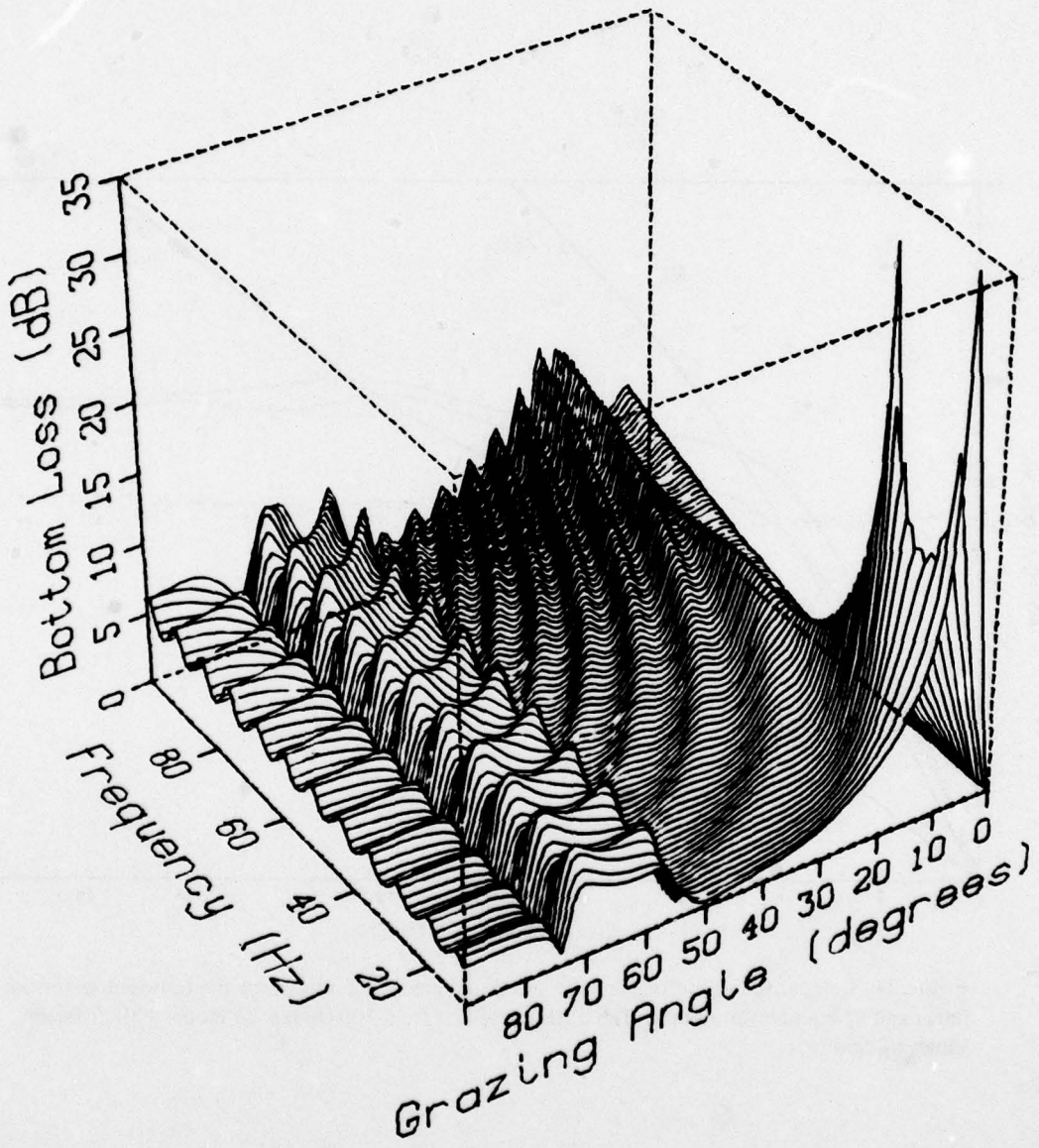



Figure 25. 3-D plot of bottom loss as a function of grazing angle and frequency.

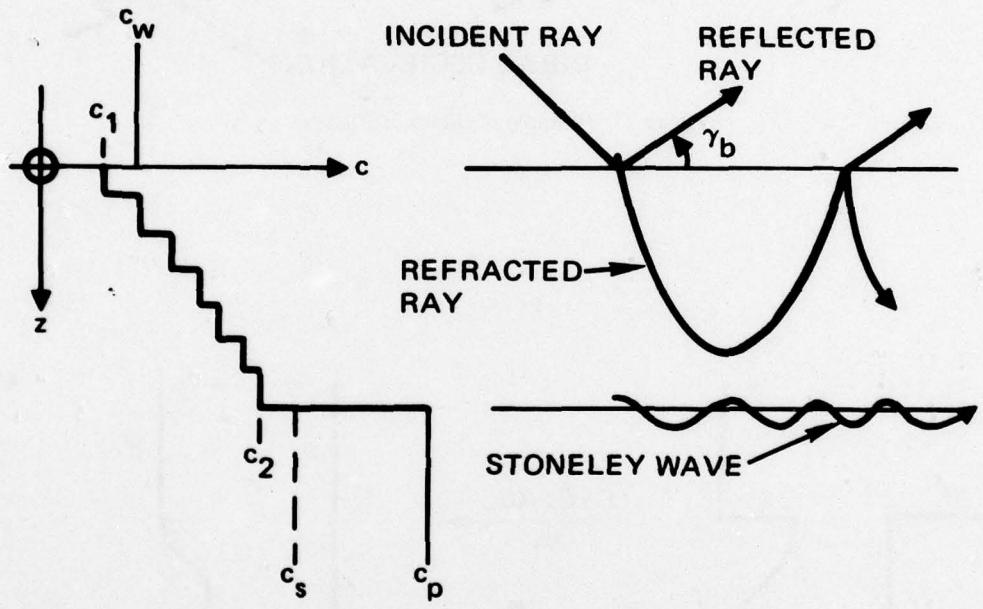



Figure 26. Sound speeds and ray diagram.

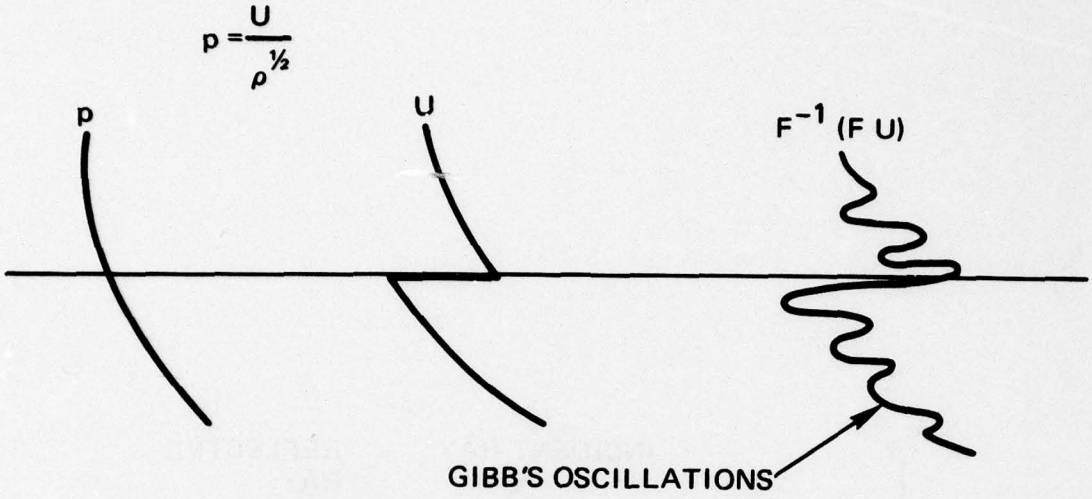



Figure 27. Example of Gibb's oscillations.

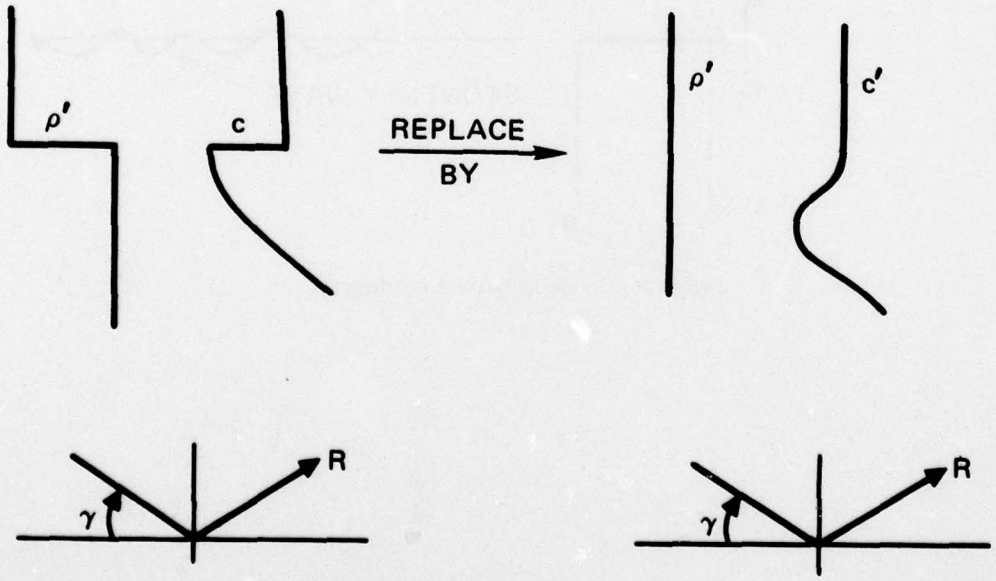



Figure 28. Equivalent bottom for use with the Parabolic Equation.

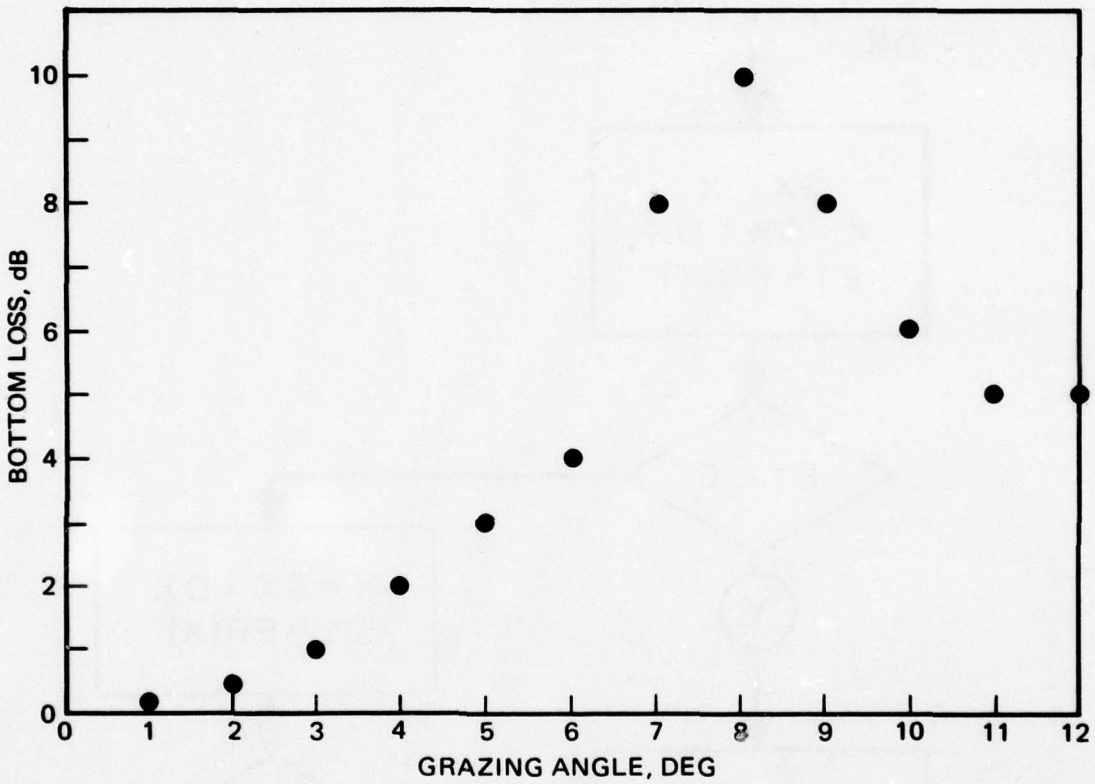



Figure 29. Desired values of bottom loss.

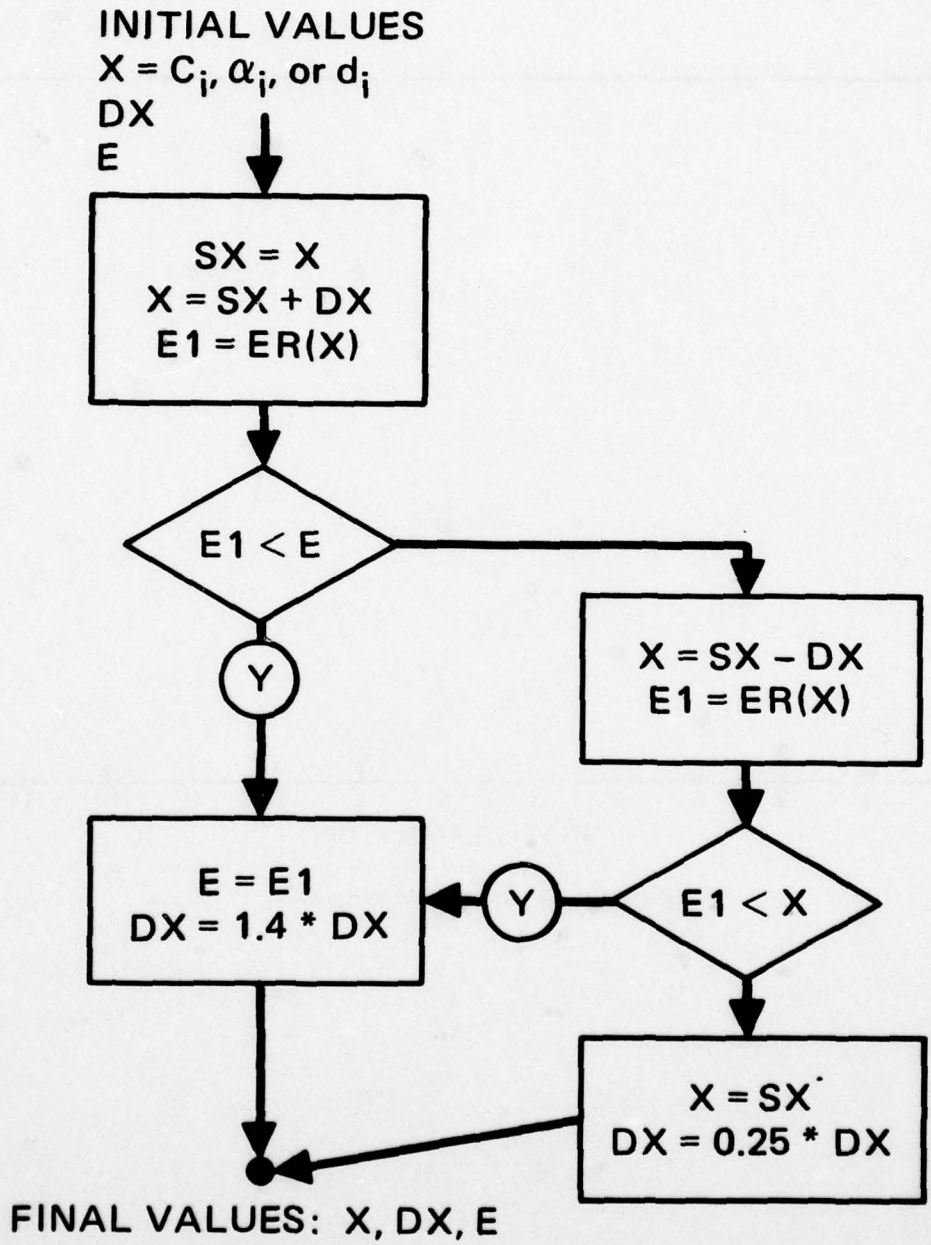



Figure 30. Algorithm to generate an equivalent sediment model with smooth $K^2$ and bottom loss.

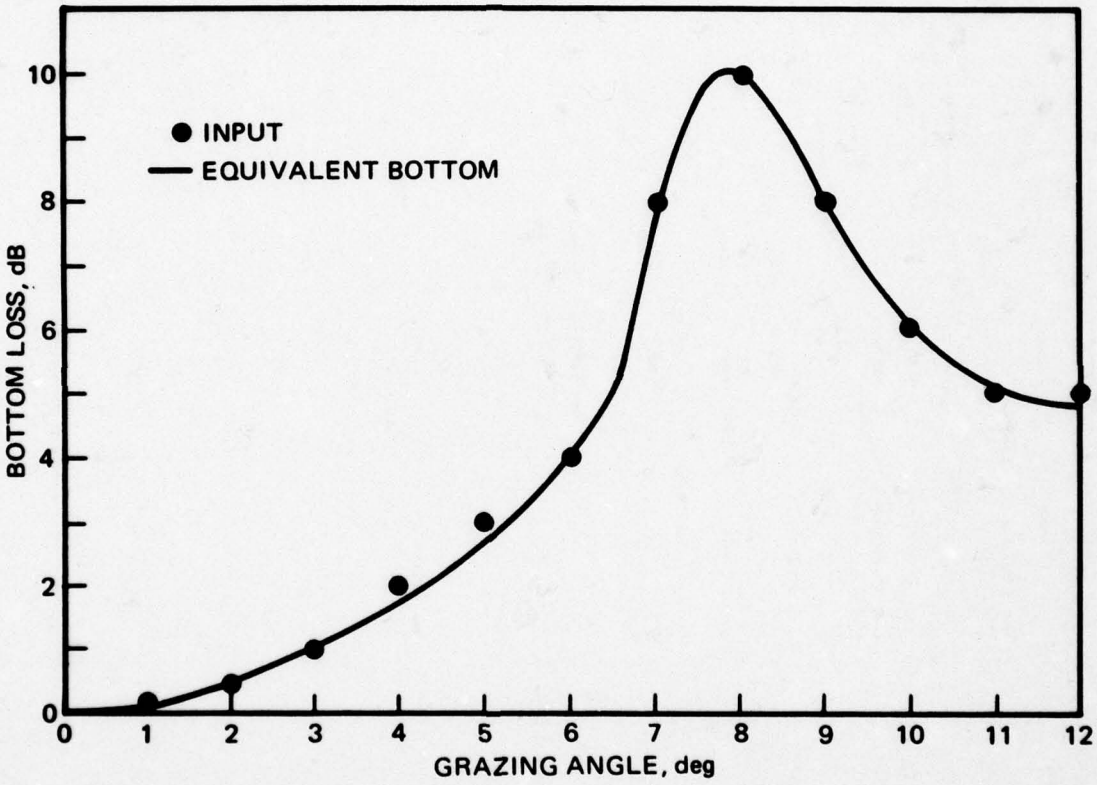



Figure 31. Good agreement between the bottom loss for the equivalent sediment mode (the line) and the desired bottom loss (the filled circles).